Reliability-based assessment procedures for existing concrete structures

Jeppsson, Joakim

2003

Report: TVBK-1026
ISSN: 0349-4969
ISRN: LUTVDG/TVBK-03/1026-SE (198)

RELIABILITY-BASED ASSESSMENT PROCEDURES FOR EXISTING CONCRETE STRUCTURES

JOAKIM JEPPSSON

DOCTORAL THESIS

Lund University
Division of Structural Engineering
P.O. Box 118
SE 221 00 LUND
SWEDEN

Telephone: +46 46 222 00 00
Telefax: +46 46 222 42 12
WWW: http://www.kstr.lth.se/

PREFACE

"Ah, this is obviously some strange usage of the word 'safe' that I wasn't previously aware of."

The quotation above is by Arthur Dent in Douglas Adam's book "The Hitchhiker's Guide to the Galaxy" a trilogy in five parts, and was a good description of my knowledge base regarding safety when I started to work on the reliability of structures and probability-based safety assessment. When I was later able to could incorporate some findings of Bayesian statistics into my knowledge it was possible for me to disagree with Oscar Wilde, who said:

"It is a very sad thing that nowadays there is so little useless information."

It is not a sad thing that there is so little useless information, on the contrary, is it a sad thing that there is so little useful information. At the end of my work on this thesis it crossed my mind that it's never too late to give up; this was when I once again had to agree with Mr Adams

"I love deadlines. I like the whooshing sound they make as they fly by."

But finally I was finished.

For the fact that I finally completed this work I would like to express my gratitude to all my colleagues at the Division of Structural Engineering here at Lund University, and to acknowledge my supervisor, Professor Sven Thelandersson, for introducing me to the concept of "consistent degree of crudeness". This concept has been my guiding star during the work on this thesis.

All of my colleagues at the Division of Structural Engineering have been very helpful, they are: Professor Jan Alemo, Patrick Anderson, Fredrik Carlson, Robert Danewid, Christina Foley, Eva Frühwald, Tomas Gustavsson, Martin Hansson, Pål Hansson, Tord Isaksson, Johan Jönsson, Ingbritt Larsson, Miklos Molnar, Annika Mårtensson, Agnes Nagy, Clary Nykvist-Person, Stefan Persson, Dan Pettersson, Per-Olof Rosenkvist and Staffan Svensson.

Special thanks are directed to Sverker for being a good friend during our deportation to the third floor, Martin for being a resourceful computer wizard in times of emergency, Tord for being both a computer and statistical wizard and for helping me with proof reading and Staffan for being who he is. The silence in the corridor during Staffan's year in Canada was loud.

I would like to express my gratitude to Professor Göran Fagerlund at the Division of Building Materials at Lund University for his support and advice in a variety of questions regarding service life assessment of concrete. From the same division, I have also had some help from Professor Kyösti Tuutti, who is also head of the Skanska Research and Development. Skanska, together with the Division of Structural Engineering, and VINNOVA (the Swedish Agency for Innovation Systems) financed this project. Besides VINNOVA support has been provided for the project in the form of information and test results from Banverket (the Swedish National Railroad Administration) in Malmö by Lars Lindeberg. In the same manner Vattenfall Utveckling AB has supported the project by

providing information through Christian Bernstone. Apart from all of my colleagues here at the University, I would like to express my gratitude to my colleagues at Skanska Teknik AB for their support.

Thanks to the time I spent on the third floor I have had the privilege to get to know many helpful friends at the Division of Building Materials. Mårten Janz, Björn Johannesson, Tomas Ekström, Katja Fridh and Manoucher Hassanzadeh have all been helpful on different occasions. Other divisions that have involuntarily have become involved in my project are the Division of Structural Mechanics, where I received useful help from Erik Serrano and the Division of Geo Technology, where Christian Bernstone, Peter Jonsson, Per Lind, and Nils Rydén provided assistance. Christian has been helpful with regard to our common dam assessment, and Tomas Ekström has answered questions regarding dam design. Peter Jonsson had a hard job teaching me what to touch and not to touch on the computer, and Nils tried out his measuring equipment on the railway bridge.

During the final stages of this project Jan Lanke, Professor emeritus in statistical medicine helped me with the problem of introducing new information into a system for the purpose of improving the predictions of the future states of the structure. Outside Lund, Lennart Elfgren, Professor in Structural Engineering at Luleå University of Technology, was the person who suggested that I should start working on this research project. I will always be grateful to him for this.

ABSTRACT

A feasibility study of reliability theory as a tool for the assessment of present safety and residual service life of damaged concrete structures has been performed in order to find a transparent methodology for the assessment procedure.

It is concluded that the current guidelines are open to interpretation and that the variation in the results obtained regarding the structural safety is too great to be acceptable. Interpretations by the engineer are also included when deterministic methods are used, but probabilistic methods are more sensitive to the assumptions made and the differences in the results will therefore be greater.

In a literature survey it is concluded that residual service life predictions should not be expected to be valid for more than 10 to 15 years, due to the large variability of the variables involved in the analysis. Based on these conclusions predictive models that are suitable for the inclusion of new data, and methods for the incorporation of new data are proposed. Information from the field of medical statistics and robotics suggests that linear regression models are well suited for this type of updated monitoring. Two test cases were studied, a concrete dam and a railway bridge. From the dam case, it was concluded that the safety philosophy in the deterministic dam specific assessment guidelines further development. Probabilistic descriptions of important variables, such as ice loads and friction coefficients, are needed if reliability theory is to be used for assessment purposes.

During the study of the railway bridge it became clear that model uncertainties for different failure mechanisms used in concrete design are lacking. If Bayesian updating is to be used as a tool for incorporation of test data regarding concrete strength info the reliability analysis, a priori information must be established. A need for a probabilistic description of the hardening process of concrete was identified for the purpose of establishing a priori information. This description can also be used as qualitative assessment of the concrete. If there is a large discrepancy between the predicted value and the measured value, the concrete should be investigated regarding deterioration due to, for example internal frost or alkali silica reactions.

Reliability theory is well suited for the assessment process since features of the reliability theory such as sensitivity analysis give good decision support for matters concerning both safety and service life predictions.

Keywords; service life, concrete, reliability theory, assessment, monitoring

SAMMANFATTNING

Möjligheten att använda tillförlitlighetsteori som ett verktyg för utvärdering av säkerhet och återstående livslängd av skadade konstruktioner har undersökts. Det framkommer att tillgängliga riktlinjer och stödjande dokument är öppna för tolkningar och detta leder till resultat med oacceptabla skillnader. Tolkningar förkommer även vid deterministiska beräkningar men tillförlitlighetsteorin är känsligare för gjorda antaganden och skillnaderna i resultaten blir därför större.

En litteraturstudie visar att livslängdsprediktioner inte är pålitliga mer än 10 till 15 år fram i tiden beroende på de stora osäkerheter som är kopplade till analysen. Baserat på dessa förutsättningar så föreslås prediktiva modeller som är öppna för införandet av ny information samt metoder för att göra detta. Inom medicinsk statistik och reglerteknik används modeller baserad på linjär regression för detta ändamål och för tillfällen då övervakning av en funktion behövs.

Två testfall har använts, en betongdamm och en järnvägsbro. Från fallet med betongdammen kan man fastslå att de deterministiska riktlinjer som används bör utvecklas vidare. Statistiska beskrivningar av viktiga parametrar såsom, islaster och friktionskoefficienter behövs om tillförlitlighetsteori skall användas för utvärdering dammsäkerhet.

Järnvägsbron visar att modellosäkerheterna för brottmoder som används inom betongkonstruktionen saknas. Används Baysiska metoder för att inkludera testdata i analyserna så bör det fastslås vad som kan användas som a-priori information. I det här sammanhanget framkom det att en stokastisk modell för betongens hållfasthetstillväxt behövs för att etablera a-priori informationen. En sådan här modell kan också användas för kvalitativa bedömningar av betongen, om där är stora skillnader mellan förväntade värde och uppmätta värde bör betongen undersökas med avseende på nedbrytningsmekanismer av typen inre frostskador eller alkali kisel syra reaktioner.

Tillförlitlighetsteori är väl lämpat för utvärdering av existerande konstruktioner då man bland annat får tillgång till känslighetsanalyser som ger bra beslutsunderlag för både säkerhetsutvärderingar och livslängdsuppskattningar.

Sökord; livslängd, betong, tillförlitlighetsteori, utvärdering, övervakning

TABLE OF CONTENTS

PREFACE ..... **I**

ABSTRACT ..... **III**

SAMMANFATTNING ..... **V**

1 INTRODUCTION **1**
1.1 Background 1
1.2 Objective 1
1.3 Methods 1
1.4 Significance of this research 2
1.5 Limitations 3
1.6 Outline of the thesis 3

2 ASSESSMENT PROCEDURE **5**
2.1 Background 5
2.1.1 Design vs. assessment 5
2.1.2 Service life predictions 6
2.1.3 Reliability analysis 7
2.2 Key issues of assessment 7
2.3 Proposed assessment approaches 9
2.4 Summary and comments 9

3 SERVICE LIFE PREDICTIONS **11**
3.1 General considerations 11
3.2 Deterioration mechanisms 11
3.2.1 Corrosion 11
3.2.2 Leaching 15
3.2.3 Service life design 18
3.3 Inspection and monitoring 19
3.4 Examples of probabilistic assessment and design 20
3.4.1 Swedish investigations 22
3.4.2 Dams 23
3.5 Summary and comments 25

4 BASIS OF DESIGN **27**
4.1 General considerations 27
4.2 Legal background 27
4.3 Limit states 27

4.3.1 Ultimate limit states 28
4.3.2 Serviceability limit state 28
4.4 Target safety index 28
4.5 Analysis method 33
4.6 Uncertainties in stochastic modelling 34
4.7 Material models 34
4.8 Geometric properties 37
4.9 Model uncertainties 38
4.10 Loads 40
4.10.1 Dead load 41
4.10.2 Train loads 41
4.10.3 Water pressure 41
4.10.4 Ice loads 42
4.11 Summary 42

5 RELIABILITY THEORY 43
5.1 General considerations 43
5.2 Methods of analysis 43
5.2.1 Numerical integration 45
5.2.2 Monte Carlo simulation 45
5.2.3 Second-moment concepts 45
5.2.4 First-order second-moment reliability method 47
5.2.5 Second-order reliability method 48
5.2.6 Sensitivities 49
5.2.7 Transformations 49
5.3 Time-variant reliability theory 50
5.3.1 Time-integrated approach 50
5.3.2 Discrete approach 51
5.4 Conditional probability 52
5.4.1 Bayesian updating 53

6 THE DAM 57
6.1 Introduction 57
6.2 General considerations 57
6.2.1 Structural system 58
6.2.2 Codes 59
6.2.3 Material 60
6.2.4 Damage 60
6.3 Owner's requirements 61
6.3.1 Deterministic requirements 61
6.3.2 Reliability requirements 63

6.4 Critical failure modes 63
6.4.1 Uplift pressure 64
6.4.2 Parameter study for normal load case and as-built geometry 66
6.5 Time-invariant reliability analysis 67
6.5.1 Limit state equations 67
6.5.2 Model uncertainty 69
6.5.3 Water level 71
6.5.4 Ice load 72
6.5.5 Friction coefficient 74
6.5.6 Summary of random variables 76
6.5.7 Results for the normal load case 77
6.5.8 Results for the exceptional load case 79
6.5.9 Summary of time-invariant reliability analysis 79
6.6 Monitoring 80
6.7 Incorporation of object-specific information 81
6.8 Time-variant reliability analysis 83
6.8.1 The leaching model 83
6.8.2 The recursive algorithm 84
6.9 Summary 85

7 THE RAILWAY BRIDGE 87
7.1 General considerations 87
7.1.1 Codes 88
7.1.2 Materials 89
7.1.3 Damage 91
7.2 Owner's requirements 93
7.2.1 Deterministic requirements 93
7.2.2 Reliability requirements 95
7.3 Deterministic analysis in the undamaged state 95
7.3.1 Main girders 96
7.3.2 The trough 98
7.4 Time-variant deterministic analysis of the bridge 101
7.4.1 Extrapolation of area loss 102
7.4.2 The shear capacity of the girders 103
7.4.3 Suspension capacity 104
7.5 Random modelling of concrete 105
7.5.1 Measured concrete properties 105
7.5.2 Statistical evaluation of concrete properties 107
7.5.3 Sample size investigation 108
7.5.4 Strength development of concrete 109
7.5.5 Uncertainties in the aging model 111
7.5.6 Transformation of compressive to tensile strength 111

7.5.7 Splitting tensile strength to tensile strength 112
7.5.8 Bayesian updating 113
7.5.9 Summary of the evaluation of concrete parameters 119
7.6 Random modelling 121
7.7 Random modelling of the suspension capacity 121
7.7.1 The limit state equation 122
7.7.2 Loads 122
7.7.3 Dynamic amplification factor 123
7.7.4 Reinforcement steel 123
7.7.5 Model uncertainty 124
7.7.6 Summary of the random variables 125
7.7.7 Results 125
7.8 Random modelling of the shear capacity of the trough .. 126
7.8.1 The limit state equation 127
7.8.2 Model uncertainties 127
7.8.3 Summary of random variables 129
7.8.4 Results 130
7.9 Random modelling of trough bending capacity 131
7.9.1 The limit state equation 131
7.9.2 Model uncertainties 133
7.9.3 Summary of random variables 133
7.9.4 Results 134
7.10 Time-variant reliability analysis 135
7.10.1 Method A 136
7.10.2 Method B 136
7.10.3 Extrapolated safety indices 138
7.11 Summary 139
7.12 Conclusions 140

8 SUMMARY AND CONCLUSIONS 143
8.1 General considerations 143
8.2 Assessment procedure 143
8.3 Basis of design 144
8.4 Test cases 145
8.4.1 The dam 145
8.4.2 The railway bridge 145
8.5 Further work 146

REFERENCES 149

APPENDIX A : THE DAM 159
Evaluation of σ_{tot} 159

APPENDIX B : THE RAILWAY BRIDGE 161
Geometry and geometrical properties of the bridge 161
Evaluation of concrete strength 162
Banverket (2000) 162
pr EN 13791:1999 163
Statistical evaluation 165
Damage 166
Dynamic amplification factor 167
Concrete cover on substructure 167
Test results regarding carbonation depth 169
Test results regarding chloride profiles 169
Measurement of current reinforcement area 172
Section forces 178

APPENDIX C : DISTRIBUTIONS FOR BAYESIAN UPDATING 183

1 INTRODUCTION

1.1 Background

The assessment of existing structures will become a more frequent task for engineers in the future due to the increasing age of existing infrastructure. The reasons for assessment can are various: different use may be proposed for the structure, new regulations with higher load requirements can be applied to the structure or there may be indications of ongoing deterioration in the structure. Deterioration is a common reason for assessment, making the prediction of the remaining service life an interesting task for safety and economical reasons. There is usually strong economical incentive for the postponement of repair or replacement of a structure, which may be in conflict with the safety of the structure.

Assessing the deteriorating concrete structures is often a task not suitable for one person alone due to its complexity, and should be performed by a group of experts from different fields of engineering such as structural engineering, materials science, chemistry and perhaps finite element analysis. Existing methods for service life assessment often describe the rate of different deterioration mechanisms deterministically, giving deterministic estimates of the residual service life. This is not a realistic approach since the uncertainties are very large for many of the governing parameters in the deterioration models. Probabilistic models provide a better decision support since important parameters can be identified via sensitivity analysis, and the residual service life can be presented as the probability of survival for the desired service life, instead of the Yes or No given by deterministic analysis. The introduction of probabilistic models also makes it possible to introduce information from monitoring into the decision process in a stringent manner. Apart from the management advantage of probabilistic models, the use of reliability theory for probabilistic structural design can also allow higher utilisation of existing structures. Higher utilisation is achieved since the design of the structure is no longer generic, but object specific. Reliability methods have, however, not yet gained general acceptance among engineers since they are considered to be “black box” solutions, and the method is also claimed to give whatever answer you want.

1.2 Objective

The aim of this study was to show a transparent assessment procedure for the residual service life assessment of concrete structures using reliability theory and statistical tools.

1.3 Methods

The use of reliability methods for assessment purposes is an unusual approach in Sweden. In this study an effort was made to collect information from international sources and to apply them to Swedish conditions. In order to do this, a review of the basis of design valid for design and assessment of Swedish structures was performed. A literature review was carried out to establish model uncertainties and load models used in the original calibration of the Swedish code system and to define the international knowledge base in the field.

Once the basis of design was established, two test cases were used to investigate the applicability and usefulness of reliability theory as a tool for assessment. Comparisons were made between deterministic and reliability results.

Finally, a simple model for the incorporation of information from testing and monitoring in the analysis was suggested. The model for the incorporation of new information is used for prediction of the residual service life of the test cases with respect to structural safety. In order to find simple algorithms suited both for manual and automated calculation, methods from statistical medicine and robotics were investigated.

In statistical medicine there are methods for diagnosis based on few samples. This is an important feature since the amount of information available on existing structures is limited. An effort was made to use these methods to determine deterioration rates and then to predict the future safety of the structure based on this information.

In robotics, recursive algorithms are frequently used to predict the future state based on what has happened up until now. This is an interesting approach for service life assessment when monitoring is to be employed and experiences from this field of research are incorporated into the reliability analysis related to monitoring.

1.4 Significance of this research

On an international level, the infrastructures needed in a modern society, such as bridges, hydropower dams, public buildings etc. represent an enormous replacement value and there are large economical benefits to be gained if the service life of existing structures can be extended without jeopardising safety. The replacement value of the concrete structures owned by the Swedish hydropower industry is estimated to be 15 milliards Euro. This considerable value creates a significant economical incentive for the development of better assessment and service life prediction methods.

More than 200,000 bridges in the USA (Dunker and Rabbat 1993) are deficient and estimates made in 1993 indicate that the cost of remedying all these bridges starts at about $90 milliards. In a more recent study by McClure (2002) it was shown that a major proportion of the bridges in USA are built of concrete and they are today between 25 and 50 years old (Table 1.1, Table 1.2). Deterioration rate studies show that these bridge types deteriorate slowly during their first 50 years, followed by a rapid decline during the following decades of their service life.

Table 1.1 Age of bridges in USA (McClure, 2002).

Age of bridge [years]	%
Older than 100	1.9
Between 75 and 100	5.1
Between 50 and 75	20.3
Between 25 and 50	41.0
Between 10 and 25	20.3
Younger than 10	11.1
Unknown	0.2

In addition to this, there are 12,000 bridges that are more than 100 years old. Approximately one quarter of the bridge inventory is obsolete and the cost of improving them is estimated to be more than $210 milliards.

In the USA, as in many other countries, a large proportion of existing bridges is made of concrete see Table 1.2. This fact makes the task of modelling the residual service life of concrete bridges very important from an economical point of view.

Table 1.2 Relation between different materials used in the construction of bridges, McClure (2002).

Material	%
Concrete	58.8
Steel	34.3
Wood/timber	6.0
Masonry	0.3
Aluminum /iron	0.4
Unknown	0.2

1.5 Limitations

This study is devoted to the modelling of the time-dependent safety of concrete structures; no detailed investigations regarding the resistance and load modelling part of the problem have been undertaken. Resistance models and load values together with information on their stochastic parameters have been collected from the literature. The starting point of the study is that the owner of a structure suspects that his structure no longer fulfils the safety requirements. The following questions must then be answered.

- Is the structure safe to use in its present state?
- If the structure is currently safe, for how long will it remain safe in the future?

The assessment process is limited to dealing only with the assessment of the present and future safety of deteriorating concrete structures. No efforts have been made to rank different repair methods that can be employed after the assessment has been completed.

The focus is on concrete structures since this is one of the main materials used for civil engineering constructions, but the suggested methodology is applicable to other materials since the core of the problem is the same. It is the two questions above that must be answered.

1.6 Outline of the thesis

This thesis is divided into the following chapters. Chapter two is devoted to a review of available assessment procedures. Chapter three focuses on service life prediction models, and background information on the deterioration mechanisms that are considered in the case studies. This chapter concludes with examples of probabilistic service life assessments from the literature.

In Chapter four the background information regarding the current Swedish building code system is reviewed, together with an international outlook. In Chapter five reliability theories are reviewed.

The suggested assessment procedure is applied in Chapter six and seven. A concrete dam is assessed in Chapter six and a railway bridge is assessed in Chapter seven. Vattenfall Utveckling AB has been helpful in providing information regarding the concrete dam. Banverket (the Swedish National Railroad Administration) in Malmö provided the bridge test case and has also provided assistance with material testing.

In Chapter eight the general conclusions are presented and in Chapter nine suggestions for further research are given. Appendix A contains calculations and test information regarding the dam and Appendix B gives the same type of information regarding the railway bridge. In Appendix C the applied a-posteriori and predictive distributions for Bayesian analysis are documented.

2 ASSESSMENT PROCEDURE

2.1 Background

A differentiation between structural design, and assessment of existing structures involving predictions of residual service life can be done since the available information differs in the different situations. In a design situation the deterministic code format used today is efficient and economical, but for the assessment situation there are reasons to use reliability theory. The same can be said for the prediction of the residual service life, deterministic models are not sufficient for the purpose of modelling something as variable as deterioration.

In the following section a short description is given of the procedure for a standard design, differences between design and assessment are pointed out and requirements on predictive models are down and the need for monitoring is discussed.

2.1.1 Design vs. assessment

Following the standard approach for structure design, a static system is defined and cross sections are assumed. Loads and load intensities influencing the structure are obtained from codes and load effects are calculated. The load effects are compared with the capacities of the structure and its cross sections. Design equations from codes are often used, especially for calculations of resistance (e.g. load bearing capacity). If the capacity is insufficient with the assumed cross section, a change in the geometry and/or of material quality is required, and a new static system is defined. New section forces are calculated, with associated re-design of the sections. This procedure is repeated until all design requirements are fulfilled.

When assessing an existing structure, the situation is different. Loads are in many cases still adopted from codes but cross sections; geometry and material properties of the structure are available. The objective of the assessment is to verify that the load carrying capacity of the cross sections is greater than the load effects originating from the loading. Load carrying capacities are often calculated using design equations; this use of design codes for assessment purposes is debatable since design codes are developed to be generic and to fit a very large number of different situations. The fact that codes are generic suggests that the degree of utilisation with respect to load carrying capacity may be low for special cases; reliability theory makes it possible to redress this problem.

Another significant difference between design and assessment is that in an assessment situation, a structure exists that is available for testing. The amount of available information is greater. This means that factors such, as material strength no longer need to be generic, but can be evaluated for the specific object. Since the structure exists in reality and not only on the drawing board, it is possible to gain further information about it if necessary, thereby reducing the uncertainties in different variables. In reliability theory, a reduced uncertainty leads to increased safety.

2.1.2 Service life predictions

As mentioned earlier, the reasons for assessment can vary, but a common reason for assessment is deterioration of structures. Several deterioration mechanisms can occur in concrete structures. Corrosion is the most frequent deterioration mechanism. Frost action is common in colder regions of the world. Amongst the less frequent deterioration mechanisms are various types of silica reactions taking place in the concrete, creating swelling and cracking of the entire concrete volume. Another deterioration mechanism is leaching. Leaching is a process where water dissolves the cement paste of the concrete and the concrete loses its internal structure.

When the safety of a structure is in question due to deterioration, the prediction of the future state becomes uncertain. This is due to large uncertainties in the local environment and the local conditions of the actual concrete and its status. If deterioration is present it is of interest to estimate the amount of degradation that is acceptable before the safety of the structure is jeopardised. Many existing deterioration models are dependent on several material and environmental parameters. These parameters need to be established, either by testing or by using values from the literature. In the same manner as for design codes, values from the litterateur are generic, and represent some kind of average value. If testing is performed, values are obtained that better reflect the current situation of the structure. Local climate and environmental factors are taken into account, improving the reliability of the assessment.

Moving from assessment of current load carrying capacity to service life predictions, the prime interest for a structural engineer is, according to Somerville (1992), not the development of degradation models and theoretical approaches, but their use. Somerville further states that a useful design method is made up of a number of essential elements.

- A behavioural model
- Criteria defining satisfactory performance
- Loads and actions under which these criteria should be satisfied
- Relevant characteristic material properties, which must be determinable
- Factors or margins to take account of vagaries and variability in the system

Apart from the behavioural model, reliability analysis, in combination with a stochastic approach, accounts for all of the points above. A criterion defining satisfactory performance is found via a target safety index, and loads can be evaluated by measuring or from a code; this is true both for static loads and environmental loads. Material test data can be converted to characteristic material properties via statistical analysis and the variability in the system is taken into account by use of reliability theory.

Stewart, Rosowsky and Val (2001) underlines that prediction of the behaviour of a deteriorating bridge is only accurate for 5 to 10 years, and for this reason risk ranking should not be attempted for longer periods of time.

2.1.3 Reliability analysis

By taking common structural design a step backwards, closer to its origin, higher utilisation is achievable for the structure. This backward step is achieved by using reliability theory, which is the basic tool for code calibration. Reliability analysis is a powerful tool that can improve and nuance the understanding of a structure and increases the utilisation of both load carrying capacities and service life for existing structures.

If reliability methods are to be used for both assessment of load carrying capacity and for residual service life estimation, the interpretation and utilisation of test results become important. Due to economical reasons, one wants to gain as much information as possible, at the lowest possible cost. Statistical methods of sampling and the design of experiments used in other industrial branches, such as chemistry and manufacturing industries, give a high degree of utilisation of the money spent.

2.2 Key issues of assessment

According to Schneider (1994) it is of great importance that the procedure used during the assessment of existing structures is formulated to make sure that no legal difficulties arise. The key issue when assessing an existing structure is safety, and in Figure 2.1 the options available for the assessing engineer are shown. A large responsibility is placed on the assessing engineer. Based on limited means and small fees, it is up to the engineer to decide whether the structure is safe to use or if additional investigations should be carried out.

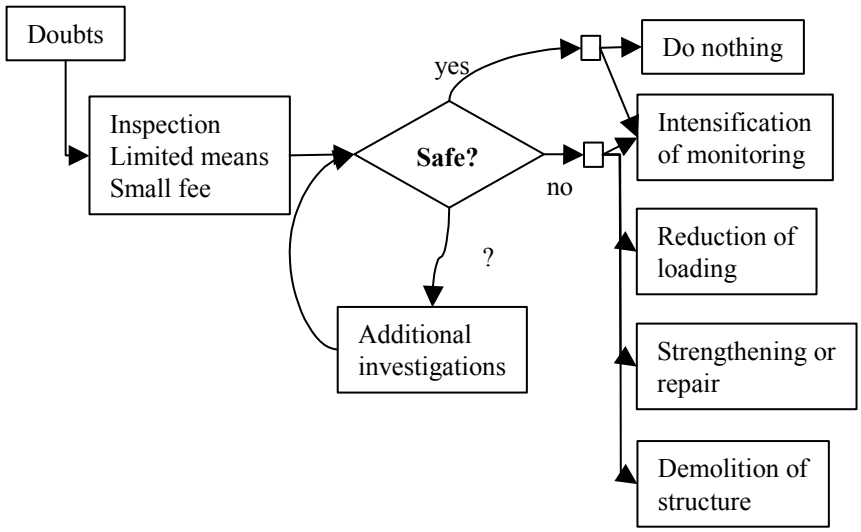

Figure 2.1 The key question, from Schneider (1994).

For the purpose of creating a dialogue between the owner of the structure being assessed and the engineer performing the assessment, a three-phase investigation process is suggested by Schneider (1994). It consists of a Preliminary Evaluation, a Detailed Investigation and a

phase called Finalising the Decision among a "Team of Experts". A similar approach is suggested in CONTECVET (2001), where both preliminary and a detailed investigation are used.

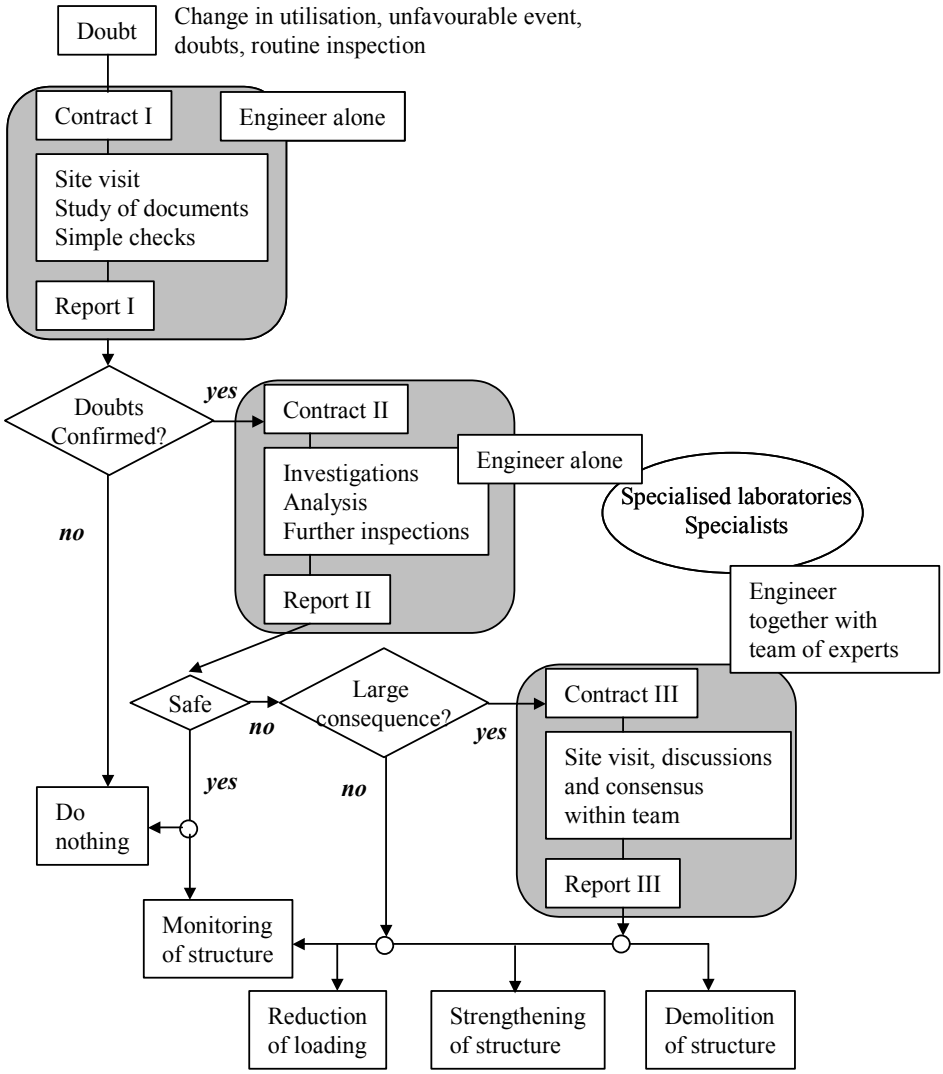

Figure 2.2 Phases in the process of assessment, from Schneider (1994).

Schneider (1994) suggests that the consensus of a group of experts should be used as a substitute for codes; in principle the acceptance of increased risk should be left to this team of experts.

In Schneider (2000) a discussion is presented regarding appropriate safety levels, taking the cost of the reduction of risks into account. Schneider states that the acceptable life-saving cost is a matter of judgement and it should be discussed within society. Thoughts in this direction should be considered when deciding upon target safety indices for existing structures, and they are under consideration as shown in Section 4.4.

2.3 Proposed assessment approaches

In order to perform an assessment in the most cost-effective manner the contractual scheme in Figure 2.2 could be kept in mind, and a working scheme proposed by Enevoldsen and Jensen (2000) can be used. They propose a probabilistic approach for the assessment of an existing structure. In their approach it is assumed the bridge in question does not have to fulfil the specific requirements in the general code, as long as it fulfil the safety level defined in the governing background documents for the code.

They further state that a probabilistic approach increases the possibility of including new information on the status of the structure in the analysis. Another benefit is that the safety level becomes more differentiated than simply safe or not safe, the result gives an indication of how unsafe the bridge is. A third advantage is the possibility of calculating how the safety varies with time. Their approach identifies the critical sections using deterministic models, and the critical sections are thereafter analysed using the more costly probabilistic analysis. Enevoldsen and Jensen (2000, 2001) suggest a 10-phase procedure for establishing a safety-based Bridge Management Plan see Table 2.1. This procedure can be adjusted to suit all structures.

Table 2.1 Safety-based bridge management plan (Enevoldsen and Jensen, 2000,2001).

Phase	Action
0	Fact-finding (previous inspections, analyses etc.)
1	Formulation of problem
2	Safety requirements for the bridge
3	Development of deterministic models for failure
4	Development of a probability-based safety model for critical failure modes
5	Modelling of random variables
6	Calibration of the safety of the un-deteriorated bridge
7	Calculation of the safety when taking deterioration into account
8	Analysis of various repair and rehabilitation actions
9	Requirements to the visual appearance of the bridge
10	Making the cost-effective management plan

2.4 Summary and comments

The objective of assessing an existing structure subjected to deterioration, without the intention of repairing it, is to answer the following two questions

1. Is the structure safe to use now?
2. For how long will it remain safe to use?

To answer the first question the approach suggested by Enevoldsen and Jensen (2000) was adopted, i.e. the safety requirements are stated based on the legal documents relevant to the structure. When the safety requirements have been established, deterministic models are used to find critical failure modes and sections. In this phase it is important to have access to relevant deterioration models describing how the load carrying capacity is affected by ongoing deterioration.

It is now time to model the stochastic variables that are involved in the critical failure equation. After the modelling of the stochastic variables, a reliability calculation can be performed and the predictive models used to verify the future reliability of the structure taking deterioration into account.

It is important to choose deterioration models based on parameters that can be monitored. Since the prediction of the future behaviour is very uncertain regular monitoring is proposed. A good approach is to limit the predictions of the future state to be valid for five to ten years, and that period of time go back and observe what has actually happened and compare it with the predicted result.

Effort should be made to create recursive algorithms for this purpose from the start. A system should be ready and waiting for information from the latest inspection. After the incorporation of this information into the system the future safety of the structure can be predicted with a higher degree of confidence.

3 SERVICE LIFE PREDICTIONS

3.1 General considerations

This thesis is the result of an interdisciplinary study, involving reliability theory, material science with the focus on deteriorating concrete, as well as some aspects regarding monitoring. In Chapter 4 Basis of Design, the basis for probabilistic design and assessment for Swedish conditions are reviewed and reliability theory is dealt with in Chapter 5.

In this chapter a short background is given concerning the deterioration models for corrosion and leaching, considered in this thesis. The requirements of a good service life model, and a short review of different approaches suggested for service life design are discussed. Basic principles of inspection and monitoring of structures are also described. Finally, some examples of probabilistic-based assessment are reviewed.

3.2 Deterioration mechanisms

A number of deterioration mechanisms affect concrete: freeze-thaw, steel corrosion, alkali silica reactions, corrosion etc. The literature review here is limited to corrosion and leaching since these two mechanisms were considered in this study.

3.2.1 Corrosion

Much work has been done on reinforcement corrosion, both on a physical level, to increase the understanding of the mechanisms, and on a probabilistic level. The state of the art regarding deterioration of concrete is extensively discussed by Duracrete (1998), where the focus is on finding suitable models for probabilistic analysis. Many lengthy and complex expressions, involving several different parameters, are presented. The number of parameters and the number of investigations needed to determine the statistical properties of the parameters is one of the main reasons for using as simple expressions as possible.

In Tuutti (1982) a broad survey of corrosion process is presented, and the idea of dividing the process into an initiation phase and a propagation phase was introduced see Figure 3.1. This concept made it possible to model the process in a more accurate manner. The initiation phase can be separated into two different models, based on the reason for corrosion. A common reason for the onset of corrosion of reinforcement is that the high pH value in the concrete that passivates the steel is reduced below a critical value, either by carbonation or by chloride ingress. The pH value in concrete is approximately 13 and corrosion is initiated when it falls below 8-9.

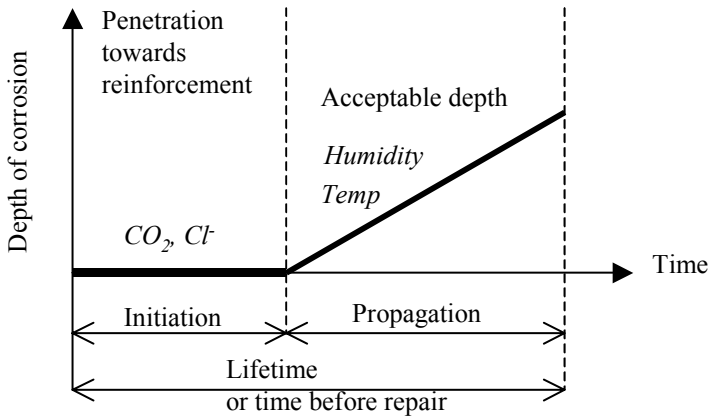

Figure 3.1 Schematic sketch of steel corrosion sequence in concrete from Tuutti (1982).

The corrosion process is of electrochemical nature, i.e. oxidation of the metal is counterbalanced by the reduction of another substance (Figure 3.2). This means that anodes and cathodes with different electrochemical potential develop. At the anode the metal is oxidised and transformed into a different chemical compound. This process results in rust leading to a reduction in the reinforcement area, affecting the safety of the structure. Another consequence of the rust is that it reduces the bond between the reinforcement and the concrete, and without a bond there is no use of the reinforcement. Bond reduction takes place when the swelling of the corroding products cracks the cover. Before cracking of the cover there is an increase in bond strength.

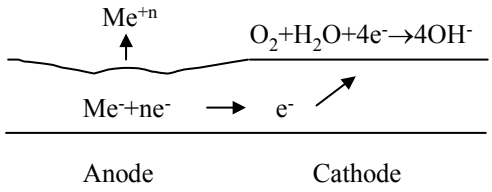

Figure 3.2 Simplified mechanism of the electrochemical process of corrosion (CONTECVET 2001).

As mentioned earlier there are two common types of corrosion: that initiated by carbonation leads to homogenous corrosion of the reinforcement bar (Figure 3.3) and that initiated by chloride ingress leads to pitting (Figure 3.4). Ingress of ions other than chlorides can also lead to corrosion, but chlorides are the most common. Pits are created in the reinforcement leading to a local and more rapid loss of area than in corrosion due to carbonation.

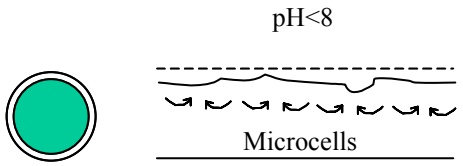

Figure 3.3 Area loss due to carbonation (CONTECVET, 2001).

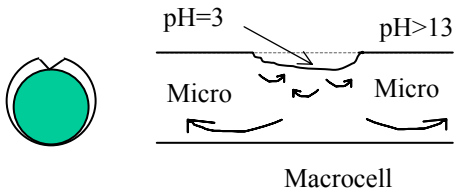

Figure 3.4 Area loss due to chlorides (CONTECVET, 2001).

According to Tuutti (1982), the initiation period depends on the following factors, which control the rate of diffusion of carbon dioxide and chlorides.

- The concentration difference between the ambient environment and the initial concentration in the material in which the substance diffuses.
- The thickness of the concrete cover.
- The permeability of the concrete.
- The threshold values at which the corrosion process is initiated. Sandberg (1998) studied the threshold values for initiation of corrosion in marine concrete.

According to Tuutti (1982) the following factors have the greatest influence on the rate of corrosion after it has been initiated:

- The moisture content of the concrete expressed in terms of the relative humidity in the pore system of the concrete.
- The temperature in the vicinity of the corroding steel.
- The chemical composition of the pore solution surrounding the steel. The pore solution in hardened concrete is water containing dissolved chemicals, located in the air pore system.
- The porosity of the concrete.
- The thickness of the concrete cover.
- The environmental variations along the reinforcement. These variations can originate from carbonation or chloride ingress. Cracks can, for instance, create variations in chloride concentrations.

The first part of the corrosion process is of no significance for the safety of the structure since the concrete, the bond and the reinforcement are intact. Estimation of the initiation time is, however important, when estimating the time-averaged corrosion current (I) via the

residual reinforcement area. If the age of the structure is known and the initiation time can be estimated, it is possible to calculate the corrosion rate using Faraday's law (Eq. 3.1), see e.g. Fagerlund (1996). Note the linear relation between time and weight loss; this is a feature that will become useful later on.

$$\frac{q}{M} = \frac{I \cdot t_{corrosion}}{|z|F} \qquad \textbf{Eq. 3.1}$$

q is the weight loss per unit length, M corresponds to the mole weight of iron, 55.8 g/mol, z is the valence of iron, which is +2 for corroded iron, F is Faraday's constant, which is 96,500 As, and $t_{corrosion}$ is the duration of the corrosion. Assuming a density of 7.8 kg/cm^3 for iron, the weight loss q, can be transformed into an area loss, $t_{corrosion}$ is calculated using Eq. 3.2:

$$T = t_{initation} + t_{corrosion} \qquad \textbf{Eq. 3.2}$$

where T is the age of the structure and $t_{initation}$ is the time taken for initiation.

The importance of a good estimate of the initiation time is shown in Figure 3.5. Point A corresponds to the observed reinforcement at the time. If the estimated initiation time varies between points B and C, the predicted area loss will fall between D and E i.e. a considerable difference in the predicted residual service life can be expected.

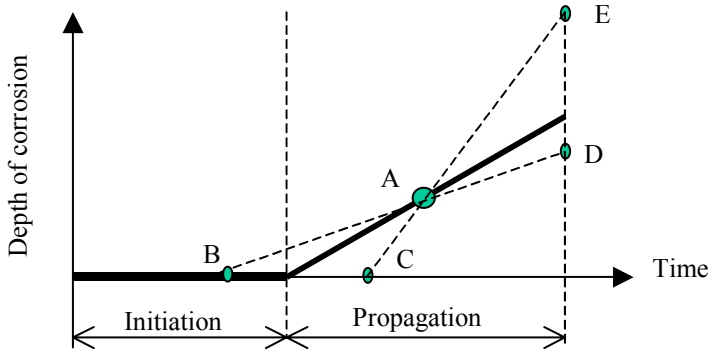

Figure 3.5 Influence of correct estimation of initiation time.

It is also possible to measure the corrosion rate with instruments. These measurements should, according to CONTECVET (2001), be performed over a 12-months period, with a frequency such that the difference between the seasons is observed, if one measurement is chosen instead of a series of measurements over a longer period, this single value must be calibrated against the humidity in the concrete. Cores should be taken from the structure and conditioned to a predefined relative humidity. Then the resistivity of the concrete is measured and is used to calibrate the corrosion rate. The dependence of resistivity on moisture content makes it necessary to measure the corrosion rate at several times during the year, since climate variations lead to variations in relative humidity in the concrete.

Tang (2002) summarised the current knowledge on corrosion intensity measurements and compared different commercially available instruments. Measuring is performed commercially with equipment that measures the polarisation resistance and equipment using the galvanostatic pulse technique. Both methods measure a pulsed current but the galvanostatic method employs only a very short time. The analysis of this pulse, gives a 10-100 times higher corrosion rate than equipment using longer pulses for the measurement. It is difficult to determine the correct answer since the extrapolated corrosion rate should also be related to the corrosion history of the structure, and this is of course difficult to establish.

An important part of service life prediction lies in defining what is meant by service life. Views on this vary between the structure owners. Examples of different service life definitions are given by Thoft-Christensen (2000, 2002) amongst others. One definition of the service life is the time from construction until the initiation of corrosion.

Another common definition is that the service life has come to an end when the corrosion opens up cracks on the concrete surface. Cracking is related to the swelling of the steel after corrosion. Swelling takes place since the chemical compound formed, i.e. rust, has a larger volume than steel. This gives:

$$T_{service} = t_{initation} + \Delta t_{crack} \qquad \text{Eq. 3.3}$$

where $T_{service}$ is the service life, $t_{initation}$ is the time until initiation and Δt_{crack} is the time from initiation of corrosion to the first visible crack on the concrete surface.

Thoft-Christensen further states that when performing service life calculations for concrete subjected to chloride ingress, the calculation should be divided into six steps, and a separate model be used for each step involving several different random variables.

1. Chloride penetration of the concrete.
2. Initiation of corrosion.
3. Evaluation of corrosion of the reinforcement.
4. Initial cracking of the concrete.
5. Evaluation of cracks in the concrete.
6. Spalling.

As an alternative, one could use empirical models as suggested by, amongst others, Chan and Melchers (1993). This kind of empirical model is useful as a tool for the assessment of residual service life, of for instance, corroding concrete structures. The amount of corrosion (c) is described as a non-linear function of time (Eq. 3.4) with k and n as empirical constants taking into account the environmental conditions:

$$c = kt^n \qquad \text{Eq. 3.4}$$

where t is time

3.2.2 Leaching

In Ekström (2001) leaching is described as a problem for concrete dams and other concrete structures in the hydropower industry in many countries. Leaching is a process where water

dissolves ions from the cement creating increased permeability, increased porosity and reduced strength of the concrete. Due to the change in permeability and porosity there is a change in the internal pore pressure, which to some extent, creates internal stresses in the concrete, as well as a change in the uplift pressure distribution. There are also synergy effects between leaching and other deterioration mechanisms, mainly frost.

Ekström (2001) modelled leaching of concrete in hydropower dams with a flow pipe model. This means that the concrete is assumed to dissolve from the walls of pipes due to flowing water. In order to model the behaviour, the mass balance of the flow pipe was studied and based on the amount of leached concrete; the change in porosity can be calculated. Since the relation between porosity and compressive strength is known, it is possible to calculate the variation in concrete strength with time.

Fagerlund (1996, 2000) briefly described the theory behind leaching as dissolving of lime from the pore walls in the concrete. In order for the dissolution to continue there must be a flow of water through the concrete and the water pressure gradient acts as a driving force for the process in a number of cases. The different types of leaching that can occur are:

1. Surface leaching with no erosion and no water pressure gradient, cement is only dissolved at the surface of the concrete
2. Surface leaching with erosion and no water pressure gradient
3. Homogeneous internal leaching under a water pressure gradient
4. Semi-homogeneous internal leaching under a water pressure gradient
5. Selective leaching in defects and cracks under a water pressure gradient

The effects of leaching can be calculated using a relation between water flow and dissolution. For cases 3 to 5 there are different scenarios for the future state of the concrete due to leaching. Leaching can proceed without creating any change in permeability, or there can be a gradual increase in permeability. If there is an increase in permeability this can be directly proportional to the leaching or it can increase progressively with leaching.

When the permeability of the concrete increases progressively with increased leaching, Fagerlund (2000) suggests the following expression for extrapolation of the future states of the concrete. The mass water flux (q_w) [kg/(m^{2}s)] is described by Eq. 3.5:

$$q_w = B\frac{\Delta P}{\Delta x} \qquad \textbf{Eq. 3.5}$$

where $\Delta P/\Delta x$ is the pressure gradient and B is the permeability

The total amount of lime (Q) [kg/m^2] that is leached from the concrete volume of a streamline tube with a given pressure gradient and unit area is as shown in Eq. 3.6:

$$Q = q_w st = B\frac{\Delta P}{\Delta x} st \qquad \textbf{Eq. 3.6}$$

where s [kg/kg] is the average concentration of lime in the out-flowing water and t is time.

The equation suggested below for the extrapolation of leaching does not describe the physics behind leaching, and must be calibrated with measurements made at different times in order

to be useful. In a simplified analysis the ratio between the average permeability after leaching (B) and the initial average permeability (B_i) is used:

$$\frac{B}{B_i} = \left[1 + \frac{\Delta X_Q}{1 - X_i}\right]^k \qquad \textbf{Eq. 3.7}$$

where X_i [m^3/m^3] is the initial volume fraction of the solid phase in the cement paste, ΔX_Q [m^3/m^3] is the decrease in cement paste (X) caused by leaching and k is a constant greater than one.

The dissolved paste volume is proportional to the dissolved weight

$$\Delta X_Q = v_s Q_v \qquad \textbf{Eq. 3.8}$$

where v_s [m^3/kg] is the specific volume of the dissolved material, and Q_v [kg/m^3] is the total amount of dissolved lime per cubic metre of concrete.

Insertion of Eq. 3.7 and Eq. 3.8 into Eq. 3.6 and multiplication with by length of the streamline tube (L), followed by integration over time gives the total amount of leached lime (see Eq. 3.9):

$$Q_v L = \int_0^t B_i \left[\frac{1 + v_s Q_v(t)}{1 - X_i}\right]^k \frac{\Delta P}{\Delta x} s dt \qquad \textbf{Eq. 3.9}$$

where $Q_v(t)$ is a non-linear function of the amount of dissolved lime.

If an inspection is now performed it is possible to calculate the amount of dissolved lime ($Q_{v,0}$), from the time to construction until the time of inspection (t_0).

$$Q_{v,0}\left[(1 - X_i) + v_s Q_{v,0}\right]^k L = \int_0^{t_0} B_i \left[(1 - X_i) + v_s Q_v(t)\right]^k \frac{\Delta P}{\Delta x} s dt \qquad \textbf{Eq. 3.10}$$

$Q_v(t)$ is derived from Eq. 3.10 and insertion into Eq. 3.9 gives Eq. 3.12, which can be used for extrapolation of the future leaching under the assumption that the pressure gradient is not influenced by the leaching:

$$Q_v L = \int_0^t q_{w,0} \left[\frac{(1 - X_i) + v_s Q_v(t)}{(1 - X_i) + v_s Q_{v,0}}\right]^k s dt \qquad \textbf{Eq. 3.11}$$

where $q_{w,0}$ is calculated as:

$$q_{w,0} = B_i \left[1 + \frac{v_s Q_{v,0}}{1 - X_i}\right]^k \frac{\Delta P}{\Delta x} \qquad \textbf{Eq. 3.12}$$

Modelling leaching is a complex task, involving many parameters that must be evaluated. Instead of using the expressions above, a simpler expression will be proposed and used below.

3.2.3 Service life design

Engineers have previously performed durability design simply by fulfilling "deemed to satisfy" rules according to the Duracrete Design Framework (1997). In a series of reports a new concept for durability design is suggested using the probabilistic framework developed for code calibration, (see Figure 3.6). This is expected to give the designer a good opportunity to tailor solutions for specific cases.

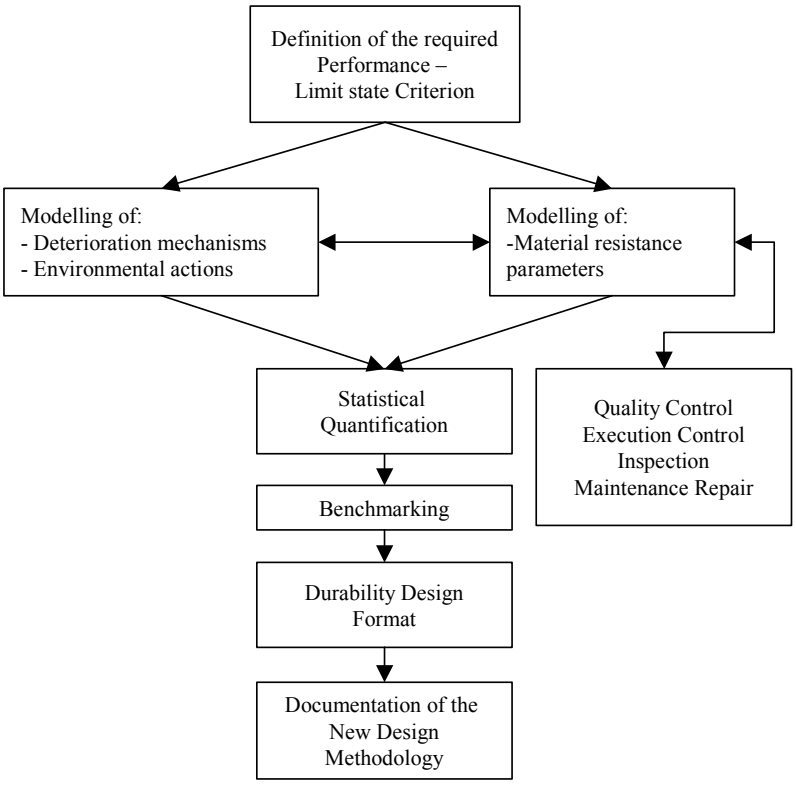

Figure 3.6 Durability design according to the Duracrete project (from Duracrete, 1997).

In the same manner as for structural design, a limit state must be specified in terms of the occurrence of an unwanted event. In the Duracrete framework it is proposed that the modelling be based on equations describing the resistance of the material to environmental action. No connection is made between the material resistance and the load carrying capacity.

Three different limit state functions for durability problems have been formulated by the Duracrete framework, in compliance with the three different time-variant approaches presented in Section 5.3.

3.3 Inspection and monitoring

The assessment of residual service life is associated with considerable uncertainties, due to a lack of knowledge and variation in the local environment. If the assessment is coupled to a monitoring system, predictions can be made more accurate by updating the parameters at regular intervals. Even if monitoring takes place, it is advisable not to make predictions for time periods longer than approximately 10 years (Stewart, Rosowsky and Val 2002). This means that monitoring of a structure should be closely related to a management plan for the damaged structure.

Lindbladh (personal communication) describes the Swedish bridge management system coupled to a bridge inspection handbook (Vägverket 1993a, 1993b, 1996a, 1996b). Within the bridge inspection system it is also stated that an ocular inspection should be performed every third year. The system classifies bridges into the following categories:

0 Undamaged at the time of inspection occasion, defective function not expected within 10 years
1 Defective function expected within 3-10 years
2 Defective function expected within 3 years
3 Defective function at the time of inspection

Bickley and Liscio (1997) pointed out that the rate of ongoing deterioration between different parking structures is highly variable and depends on many local factors, such as chloride content, corrosion levels, repair methods etc. In order to evaluate the need and timing for repairs and to assess the performance of different repair methods, annual monitoring was used to map the ongoing deterioration. One of the main conclusions of this monitoring was that enough information was gained to make accurate predictions of when further repairs would be needed. Maage et al. (1996) further emphasized the need for service life estimates based on inspection and testing with respect to corroding structures.

Broomfield, Davies and Hladky (2002) stated that long-term monitoring of corrosion in new or existing concrete structures is possible today and emphasized the possibility of using monitoring as a tool for maintenance planning and service life prediction.

Faber (2002) gave a description of a framework for risk-based inspection. The basic idea is to make sure that complicated structural systems are designed so as to ensure economical operation throughout their service life and, during this time, live up to acceptance criteria with respect to the safety of personnel and risk to the environment. Planning of inspection involves identification of what to inspect, how to inspect it and how often to inspect it. It was concluded that deterioration processes are highly uncertain and are best described in probabilistic terms. The high uncertainty leads to the conclusion that there will always be a certain probability that the structures will fail during operation. This makes it important to take the consequence of failure into consideration; consequences such as fatalities, or injuries, costs and their importance for operation of the structure.

It is further stated by Faber (2002) that quantification of risks should not only be made on a component level, but by summing the risks to obtain a value for the installation as a whole. Different inspection strategies involving different degrees of effort, cost and quality have

different effects on the risk. By comparing the calculated risks using different inspections strategies, the strategy with the smallest associated risk can be identified and implemented.

Soerensen and Faber (2002) used a 50 m long welded stiffener in a bridge structure with a 50-year service life as an example of risk-based inspection. The stiffener is exposed to fatigue stresses and the risk-based planning framework of inspections suggested by Faber (2002) is used as decision support when choosing between visual inspections and measurements. During the investigation, the inspection plan was optimised for two different assumptions. Equidistant inspection times were one assumption, and constant annual failure probability at the time of inspection was the other assumption. It was seen that the uncertainty related to the stress range had a significant impact on the most cost-effective inspection and repair plan for both assumptions.

Goyet et a.l (2002) reported another example of risk-based inspection. A welded detail on a floating production, storage and offloading installation for the offshore industry was investigated. The ship hull contains thousands of single details of the same type. The first step in the planning was to establish an acceptance criterion for the safety of the offshore structure. The next step was to collect as much data as possible about the system; this was done in order to perform risk screening. The purpose of risk screening was to establish an overview of the system and to identify systems and components with regard to their contribution to the overall risk of the system. The last step was to define inspection schedules and decide how to update the inspections plans. They concluded that the theoretical framework work after 25 years of development, and can be used in the industry, but that there still is a lack of good models for physical phenomena such as corrosion.

3.4 Examples of probabilistic assessment and design

Reliability-based assessment of structures is today used for all types of structures. In this literature review a few examples of reliability-based assessment are presented together with some examples where reliability theory is used for service life predictions. A large number of service life calculations for existing bridges subjected to assessment can be found in the literature, many of these are of an academic nature. They are often related to optimisation of the most cost effective repair and maintenance system.

Enright and Frangopol (1998a) investigated a three-span bridge. The load carrying system of each span consists of five simply supported concrete beams. The investigation showed that the bending capacities of the beams are critical. Reliability calculations were performed, using input from as built construction drawings for dimensions and reinforcement ratios. All values from the drawings are assumed to be mean values and coefficients of variation were estimated from information found in the literature. The bridge was subjected to de-icing salts and Monte Carlo simulation was used to investigate the influence of chloride-initiated reinforcement corrosion. No comparisons were made of the load carrying capacity and the load, but the mean value and coefficient of variation for the ratio of the current resistance and the undamaged resistance were estimated.

The same bridge was investigated again by Enright and Frangopol (1998b) and the deteriorating load carrying capacity was compared with the load. System reliability theory was adopted instead of analysing the reliability of a representative beam and instead of

referring the probability of failure to a reference period it was calculated over time. Random variables for the resistance were chosen as before (Enright and Frangopol, 1998a) and load descriptions were adopted from AASHTO. These traffic loads are described in detail by Nowak (1995).

Stewart and Rosowsky (1998) developed a model to investigate ultimate and serviceability limit states for continuous concrete slabs with respect to bending capacity and chipping of the cover due to corrosion. Interaction between transversal cracks, diffusion of chlorides as well as initiation of corrosion was taken into consideration. Similar calculations regarding concrete bridges have been presented by Vu and Stewart (2000) and by Val, Stewart and Melchers (1998).

Probabilistic analyses were used by Estes and Frangopol (1999) to optimise bridge repair strategies. A bridge with nine steal beams, side by side, was first analysed to identify critical failure modes. Safety indices were calculated for 16 different cases, and these were then combined to form a time-variant reliability system, see Section 5.3. All loads were assumed to be time-invariant but the corrosion of the reinforcement in the concrete slab was included in the time-variant analyses. Based on this system, different repair criteria with related costs were investigated, and a cost-effective repair strategy was developed for the bridge. Results from the same investigation are, to some extent, given in Frangopol and Estes (1997).

With generic software for Monte Carlo simulation, together with software for optimisation Frangopol et al. (1997) performed life cost analysis of a bridge. The influence of corrosion was included in the analysis. An extensive parameter study for both the initiation phase and the propagation phase of the corrosion process was made with reference to bending moment and shear capacity. It was concluded that after taking into account material costs and expected lifetime costs, a more rational design than the conventional one is obtained using the probabilistic approach.

By taking into account the fact that a structure has been working properly, from the point in time when it was erected until today, uncertainties regarding the reliability of the structure can be reduced, according to Stewart and Rosowsky (1998). This means that progressive truncation can be done for the lower tail of the resistance with time. A result of this it can be shown that the probability of failure decreases with time (see Figure 3.7). A similar approach is used by Stewart and Rosowsky (1998), this investigation are based on Stewart (1997) where Monte Carlo simulations were used to describe the structural reliability of service proven-structures.

In a paper by Stewart, Rosowsky and Val (2002) the use of reliability-based bridge assessment in combination with risk ranking was investigated. Instead of focusing on the precise value of safety for a bridge, expressed as a safety index, the calculated safety index was used for comparison of different bridges and as a decision-making tool for prioritizing the need for repair.

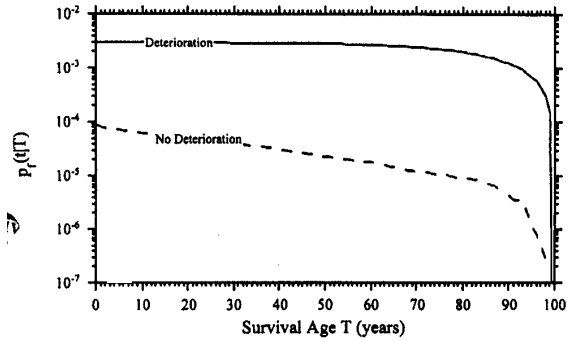

Figure 3.7 Time-variant reliability for an existing and functioning structure, from Stewart and Rosowsky (1998).

Efforts have also been made to transform the time-variant problem of deteriorating structures into a time-invariant problem. Mori and Nonaka (2001) stated that the target reliability index could be accurately achieved using approximate resistance reduction factors for different types of deterioration models. The models tested were linear, parabolic and square root dependent of time. This approach is the same as that used in the Swedish structural design codes, but here the loads were made time-invariant and partial safety factors were calibrated to give the required safety.

3.4.1 Swedish investigations

The Swedish National Road Administration, together with Rambøll, a Danish consultant, has performed reliability-based assessments of three Swedish bridges. Instead of performing repairs, immediately after an unsatisfactory deterministic classification, it was suggested that probabilistic evaluation be performed. A classification method that can be used to decide if it is useful to perform a probabilistic analysis is described by Enevoldsen and Pup (2000).

It is also stated in the reports by Rambøll that the legal basis of the analysis is given in BKR (1998), where it is stated that reliability-based methods for design in Sweden shall be based on methods described in ISO 2394-1998. Enevoldsen and Pup (2000) suggested that NKB 55 (1987) together with NKB 36 (1978) could be used to establish the target reliabilities (see Table 4.2). As can be seen in the table the target reliability depends on safety class and failure type.

The target safety index or failure probability, as defined in Table 4.2, is based on specific calculation requirements. The requirements define distributions for the random variables, the method to be used for the calculation of the safety index and a reference period for the loads. According to NKB 55 (1987) and NKB 36 (1978) the calculation of the safety index should be done using the first-order reliability method (FORM), see Section 5.2.4.

Some results of the probability-based assessment of a few Swedish cases, together with a few Danish cases are given in Enevoldsen (2000) and a formalized working procedure has been

presented by Enevoldsen and Jensen (2000, 2001) and a detailed presentation of the traffic load modeling is given by Rambøll (1999a).

Bridge T 531 (Rambøll, 1999b), is a continuous portal frame in two spans with an intermediate support consisting of three circular columns. A deterministic analysis has shown that the punching shear capacity of the middle column is decisive for the load carrying capacity of the bridge. A punching shear capacity model from the Handbook for Concrete Constructions (AB Svensk Byggtjänst, 1990) was used to describe the failure limit state in the subsequent probabilistic modeling of the critical failure mode. The target index was chosen with reference to Table 4.2 with β equal to 4.75 for safety class 3. Calculations showed that the punching shear capacity could be increased from 188 kN to 248 kN. Distribution functions, coefficients of variation and model uncertainties were chosen according to NKB 36. The increase in capacity arises from the combination of finite element analysis of the punching shear force and the probabilistic calculations.

Bridge C 295 (Rambøll, 1999c) is a continuous post-tensioned three-wall box girder; the box girder is supported on circular columns at all supports. According to a deterministic analysis the torsion capacity of the box girder was insufficient. From Table 4.2 a target safety index of 4.26 was chosen and distribution functions, coefficients of variation and model uncertainties were chosen according to NKB 36 (1978). The load carrying capacity was increased from 115 kN to 240 kN, mainly due to a change in model for the torsion capacity and not due to the probabilistic part of the new analysis.

Bridge E 129 (Rambøll, 1999d) is a post-tensioned beam bridge with a single span of 49.4 m. According to a deterministic classification made after the Swedish bridge assessment code (Vägverket, 1998) it was found that the tension capacity of the concrete in the serviceability limit state is critical. A target safety index range of $1.3 \leq \beta \leq 2.3$ was chosen with reference to ISO 2394 (1986). After a probabilistic analysis with distribution functions, coefficients of variation and model uncertainties chosen according to NKB 36 (1978), the critical load could be increased from 170 kN to 215 kN.

Carlsson (2002) has investigated the coefficients of variation for traffic loads on Swedish bridges with spans shorter than 40 m. The investigation was based on the same weight-in-motion measurements of the axle loads used by Getachew (2000) for the evaluation of traffic queues on long bridges. Carlsson (2002) investigated the possibility of differentiating between bridges located on roads with small traffic volumes and bridges located on roads with high traffic volumes. The traffic load effect can be expected to depend on the traffic intensity on the investigated bridge. A comparison was also made between the safety indices achieved when using NKB 55 (1987), NKB 36 (1978) and JCSS (2002) for some examples. This comparison showed that the highest safety indices were achieved when NKB 55 and JCSS were used; NKB 36 gave generally lower safety indices.

3.4.2 Dams

Bowles and Anderson (2001) wanted to kill the myths regarding probabilistic safety analysis of dams. One myth is that the methodology is expensive and extensive, and it is only used to justify whether a dam should be attended to or not. Another myth according to the authors

is that the method is only used for economical planning, where a price tag is put on human life. As well as these objections, it is also said that traditional engineering tools have been abandoned and that reliability analyses are of limited use since too little information is usually available to make the analyses reliable.

The response of Bowles and Anderssson to these objections was that the statistical approach provides a stringent framework that makes it possible for engineers and other experts to perform valid estimates. It is also a tool for communication between experts and decision makers. This is considered an important advantage since the number of people with a technical background in managerial positions is decreasing.

Many existing dams cannot resist loads and fulfil the safety demands of new codes according to Ellingwood and Tekie (2001). A rational safety analysis can be achieved by performing a probabilistic analysis of the dam. This can be used to show, in terms of probabilities, to what extent a dam can resist specific events. Different failure modes, such as the position of the resultant, sliding of the dam, overtopping etc, can be calculated as failure probabilities.

In ICOLD (2000) several papers deal with probabilistic risk analysis and the safety of dams. With few exceptions, the risks are based on estimates instead of analyses based on reliability theory.

Xiutang et al. (2000) have investigated the failure probability of a large gravity dam on a rock foundation. It was recognised that several different failure modes could occur and the reliability of the dam was calculated for a series system of the failure modes. i.e. the failure modes taken into consideration are sliding, stresses at upstream edge and downstream edge as well as overturning. For the evaluation of the dam of the Three Gorges, Xiutang et al. used the following random variables, see Table 3.1 and Table 3.2.

Table 3.1 Main statistical characteristic of random variables for the Three Gorges, from Xiutang et al. (2000).

Variable	Mean	Variance	Distribution
Upstream water head	$0.912 \cdot H$	$0.26 \cdot H^{0.27}$	Normal
Uplift coefficient	0.25	0.038	Extreme
Friction coefficient	1.107	0.1203	Normal
Cohesion	1.22 MPa	0.215	Lognormal
Compressive strength of concrete	33.56 MPa	0.145	Normal
Tensile strength of concrete	2.78 MPa	0.141	Normal
Young's modulus of concrete	32.61 GPa	0.115	Lognormal

The values given for the variance and standard deviation of the friction coefficient are of interest for comparison with Swedish conditions.

Table 3.2 Statistical characteristics of random variables for the Three Gorges, from Xiutang et al. (2000).

Variable	Mean	SD	COV	Distribution
Uplift coefficient	0.186	0.056	0.3	Normal
Friction coefficient	1.2	0.226	0.22	Normal
Cohesion	0.9 MPa	0.324	0.36	Normal / Lognormal
Compressive strength of concrete	18.40 MPa	4.408	0.22	Normal

3.5 Summary and comments

Corrosion is a common deterioration mechanism in reinforced concrete structures. The corrosion process can be divided into two phases, an initiation phase and a propagation phase. Several mathematical models exist for both phases but the influence of corrosion on the load carrying capacity of a structure has been less well investigated. A linear relation between time and area loss can be assumed for the propagation phase. This is a useful feature for the incorporation of new information from monitoring or inspection and for the purpose of extrapolation of the residual reinforcement area.

Leaching is a process where lime is dissolved from the concrete by flowing water, leading to increased porosity and reduced strength of the concrete. Leaching may develop with time in various ways. A safe assumption is to model the leaching process as being proportional to the change in permeability. None of the reviewed expressions used to describe the leaching process is suited for integration into a monitoring programme, and a simpler expression will be suggested for leaching.

It is reported that service life predictions should not be expected to be accurate for longer periods than 5-10 years. This coincides well with the bridge inspection system used in Sweden by both the National Road Administration and the National Railroad Administration, where ocular inspections are performed every three years and more thorough inspections are performed every six years (Vägverket, 1993a). With this inspection routine as a base, it should be possible to implement results from inspections or monitoring of critical sections and parameters and incorporate them into recursive reliability analysis used for residual service life assessments. The goal of this system should be to prolong the service life for a few percent of the damaged bridges. If repair can be postponed until the next inspection interval money can be saved.

Probabilistic methods can easily be misused and result in “black-box” solutions giving whatever answers you want. Special effort must be made to document the analysis in detail, and the assumptions behind it. An increase in transparency is in accordance with suggestions made by Schneider (1994), that the whole assessment process should be divided into different contracts to increase the communication between the assessing engineer and the owner of the structure. Increased communication will also increase the understanding of the process from both sides.

Experience shows that it is often a change of design equations and analysis method that leads to the greatest gain in load carrying capacity when performing reliability-based

assessments. From earlier experience it could also be concluded that NKB 55 (1987) together with NKB 36 (1978) and ISO 2394-1998 contain the legal background for probabilistic design and assessment in Sweden.

4 BASIS OF DESIGN

4.1 General considerations

In this chapter the legal basis for reliability analysis of Swedish structures is reviewed and different aspects of probabilistic modelling are compared with the International Organisation for Standardisation (ISO), Joint Committee of Structural Safety (JCSS) and European Norm (EN) publications.

The relevant aspects are limit state definitions, target safety indices and analysis methods. Uncertainties in stochastic modelling, material models, geometric properties and load models are reviewed. Regarding probabilistic modelling, the aspects dealt with are limited to those of interest for the two test cases in this thesis. Emphasis is put on concrete structures and the loads of interest, i.e. dead weight, ballast, water pressure and train loads.

4.2 Legal background

Probabilistic design is seldom used in Sweden but, according to BKR (2000), in which the Swedish Design Regulations are stated, probabilistic design may be used. Reference is made to ISO 2394-1998 and NKB 55 (1987). Generic information and definitions from ISO 2394-1998 are also valid for Swedish conditions.

BKR (2000) states that NKB 55 (1987) can be used as a background document for code calibration and design. NKB 55 is closely related to NKB 36 (1978), which contains most of the information in NKB 55 together with some information that has been taken out in NKB 55. NKB 36 is in some cases needed to make NKB 55 operational.

4.3 Limit states

NKB 55 states that the design methods used should be based on scientific theories and statistical interpretation of experimental data, and that the safety class should be dependent on the extent of injury and social consequences following a failure. The classification of structural elements into safety classes is done with regard to the extent of injury to persons associated with failure of the element as follows.

- Safety class 1 (low), little risk of serious injury to persons
- Safety class 2 (normal), some risk of serious injury to persons
- Safety class 3 (high), great risk of serious injury to persons

It is also indicated in the first section of NKB 55 that the failure type and the degree of control during design and execution should affect the safety index. Ductile failures with extra load carrying capacity in the form of strain hardening are considered safer than ductile failures (normal) without any extra load bearing capacity. Brittle failures or instability failures are considered most hazardous.

Based on the safety class it is recommended that a differentiated scale of control measures be taken, regarding design calculation, material properties, execution of the structure, use of the structure and the condition of the structure. Stricter control measures are required for higher safety classes.

4.3.1 Ultimate limit states

BKR (2000) states that load bearing structures in ultimate limit states should be designed so that safety is provided with respect to material failure and instability, during the construction of the structure, its service life and in the event of fire. Demands are also put on safety with respect to tilting, uplift and sliding together, through demands on design and detailing of buildings such that they can withstand accidental actions in a way that limits primary damage. The damage should not give rise to progressive collapse and destruction of other parts of the structure than the damaged part or parts adjacent to the damaged one. These demands on the limit state are also stated in NKB 55 (1987).

ISO 2394-1998 and ISO/CD 13822 have the same approach to the limit states as NKB 55. JCSS (2002) follows the definitions given in ISO 2394-1998. In EN 1990 it is also stated that time-dependent effects such as for instance fatigue should be related to the ultimate limit state.

4.3.2 Serviceability limit state

This limit state is related to normal use and durability. Examples of relevant criteria are deformation, cracking, local damage or damaged due to vibrations (see NKB 55, 1987). In ISO 2394-1998 and ISO/CD 13822 fatigue is related to the serviceability limit state, contrary to what is stated in EN 1990. It is also stated that local damage, which may reduce the service life of the structure, should be related to the serviceability limit state. JCSS (2002) follows the definitions given in ISO 2394-1998.

4.4 Target safety index

BKR (2000) states that the target safety index for a structural element should be calculated according to ISO 2394-1998 and should have the target values given in Table 4.1 for different safety classes. The reference period is one year.

Table 4.1 Safety class and safety index according to BKR (2000).

	Safety index
Safety class 1	≥ 3.7
Safety class 2	≥ 4.3
Safety class 3	≥ 4.8

It is also stated in BKR (2000) that in design with respect to accidental actions the safety index shall be not less than 3.1 and if there is a risk of progressive collapse the value should

be no less than 2.3. The safety indices in Table 4.1 are for a reference period of one year. It is also stated that values of the partial factors in the ultimate limit states have been calculated with respect to the above values of β and are based on calibration in accordance with NKB 55 (1987). If a probabilistic method is used, design should be based on the rules relating to the method of partial factors.

The explicit values of the target safety indices given in NKB 55 are the same as those given in Table 4.1. These values are valid for the ultimate limit state for permanent and variable loads with a ductile failure. The relation between the target safety index and the failure mode is not mentioned in BKR (2000).

According to NKB 55 the calibration of partial factors is to be carried out based on the following assumptions.

- Random variables in the limit state are defined.
- The random variables are uncorrelated, and have known distribution functions.
- The random variables are assumed to be normally distributed or lognormally distributed.
- The limit state function describes one condition for a single structural element or a section of a structural element.

Even if the basic assumptions presented above are not valid it is still possible analyse the problem. If the variables are correlated, the method can be generalised to fit correlated variables. If a variable cannot be assumed to be normally or lognormally distributed, but has another cumulative distribution function or density function, this distribution can be approximated by a normal distribution at the design point.

In NKB 36 (1978) the predecessor of NKB 55 (1987), differentiated target safety indices are suggested based on the failure types described in Section 4.3, see Table 4.2.

Table 4.2 Safety class and safety index according to NKB 36 (1978).

	Failure type		
	Ductile	Normal	Brittle
Safety class 1	3.1	3.7	4.2
Safety class 2	3.7	4.2	4.7
Safety class 3	4.2	4.7	5.2

In NKB 36 the following assumptions are made.

- For each variable action, the reference period is divided into r intervals of equal length representing the time during which the individual action is acting upon the structure with constant intensity.
- The occurrence or non-occurrence of the action in each time interval corresponds to repeated trials with a probability p of occurrence.
- Given that the action occurs, the distribution of intensity is $F_i(x)$.
- Intensities corresponding to different time intervals are stochastically independent.

- Occurrence and intensities of different actions are independent.

According to NKB 36 the distribution function, $F_{max}(x)$, of maximum intensity within the reference period can be expressed as:

$$F_{\max}(x) = (1 - p(1 - F_i(x)))^r \qquad \text{Eq. 4.1}$$

where $F_i(x)$ is a distribution function, and p and r are empirical parameters.

If sufficient statistical data are lacking, the distribution function $F_i(x)$ may be assumed to be normal and the values of the parameters p and r may be based on experience. For the purpose of describing load regulations in a probabilistic manner, the distribution type of each action must be defined due to the sensitivity of the failure probability to the choice of distribution function. This so-called "tail sensitivity problem" is addressed by, amongst others Melchers (1999) and is considered to be essential during code calibration. Due to the tail sensitivity of the failure probability the safety index can be "adjusted" up or down by choosing an appropriate distribution type.

In ISO 2394-1998 the target safety index is differentiated with respect to the relative cost of safety measures. It is suggested that economic optimisation be done in a formal manner, using an equation of the following type:

$$C_{tot} = C_b + C_m + \sum P_{f,lifetime} C_f \qquad \text{Eq. 4.2}$$

where C_{tot} is the total cost during the lifetime of the structures, C_b is the building cost, C_m is the cost of maintenance and demolition, $P_{f,lifetime}$ is the lifetime probability of failure and C_f is the cost of failure.

Eq. 4.2 is highly simplified and not suitable for practical use, but the idea of coupling the target safety index to economical factors is interesting for the purpose of assessment where the cost of a small increase in safety can be very high, compared with the same safety increase for a new structure.

The values given in Table 4.3 were calibrated based on the assumption of lognormal or Weibull models for resistance variables, normal models for permanent loads and Gumbel extreme value models for variable loads.

Table 4.3 Target safety index according to ISO 2394-1998, one-year reference period.

Relative costs of safety measure	Consequence of failure			
	Small	Some	Moderate	Great
High	0	1.5	2.3	3.1
Moderate	1.3	2.3	3.1	3.8
Low	2.3	3.1	3.8	4.3

No formal requirements for country-specific codes are coupled to the values in Table 4.3, but suggestions for appropriate values are given. The use of this table can be exemplified as follows.

- In the serviceability limit state the target safety may be 0 if the limit state is reversible and the cost of preventing failure is high.
- In the serviceability limit state the target safety be 1.5 if the limit state is irreversible and the cost of preventing failure is high.
- A target safety index of 2.3 may be used for fatigue if it is possible to inspect the detail.
- If inspection is not possible, a higher target safety index should be used; a value of 3.1 is suggested.
- In the ultimate limit state the value 3.1, 3.8 or 4.3 may be used, depending on the safety classes.

ISO/CD 13822 further emphasizes the possibility of reducing the target safety index based on socio-economical reasons. Another difference between ISO 2394-1998, which deals with design of new structures, and ISO/CD 13822, which deals with assessment of existing structures, is the change of reference period. The reference period in ISO 2394-1998 is one year while the remaining service life suggested as reference period in ISO/CD 13822 leading to a higher annual probability of failure. In ISO/CD 13822 this is considered acceptable for the serviceability limit state, but not for the ultimate limit state, where a shorter reference period is required, giving a smaller annual probability of failure. Eq. 4.4 can be used to transform safety indices for one-year reference periods to arbitrary reference periods.

All assumptions made in t the calculation of the safety index are the same for ISO/CD 13822 as those in ISO 2394-1998. Proposed target safety indices according to ISO/CD 13822 are given in Table 4.4.

Table 4.4 Target safety index according to ISO/CD 13822.

Limit states		β_{target}	Reference period
Serviceability	Reversible	0	Intended remaining working life
	Irreversible	1.5	Intended remaining working life
Fatigue	Inspectable	2.3	Intended remaining working life
	Not inspectable	3.1	Intended remaining working life
Ultimate	Very small consequences of failure	2.3	L_s – constant reference period for safety (10 years)
	Small consequences of failure	3.1	L_s – constant reference period for safety (10 years)
	Moderate consequences of failure	3.8	L_s – constant reference period for safety (10 years)
	Serious consequence of failure	4.3	L_s – constant reference period for safety (10 years)

Economic aspects are also used in JCSS (2001) and the JCSS Probabilistic Model Code (2002) as a starting point for the establishment of the target safety index during assessment of existing structures, together with the consequence of failure, see Table 4.5.

Table 4.5 Tentative target safety index according to JCSS (2001) and JCSS (2002) for a one-year reference period and ultimate limit state.

Relative cost of safety measure	Consequence of failure		
	Minor	Moderate	Large
High (A)	3.1	3.3	3.7
Normal (B)	3.7	4.2	4.4
Low (C)	4.2	4.4	4.7

In order to determine a suitable value for the target safety index the following equation is introduced:

$$\frac{C_b + C_f}{C_b} \qquad \text{Eq. 4.3}$$

where C_b is the building cost and C_f is the cost of failure.

A structure can be assigned to the consequence class, "Minor consequences of failure" if the value of Eq. 4.3 is less than approximately 2. Agricultural structures such as silos and masts can be assigned to this consequence class. If the value of Eq. 4.3 is between 2 and 5 and the risk to life, given failure is moderate or if the economic consequences are considerable the structure can be assigned to the consequence class "Moderate". If Eq. 4.3 renders a value between 5 and 10 and the risk to life can be considered high, the structure is assigned to the consequence class "Large consequence".

For the serviceability limit state, JCSS (2002) differentiates between the reversible and irreversible limit state. Tentative target reliability indices are shown in Table 4.6 for the case of irreversible limit state.

Table 4.6 Tentative target safety index according to JCSS (2002) with a one-year reference period and the irreversible limit state.

Relative cost of measure	Safety index
High	1.3
Normal	1.7
Low	2.3

In the same manner as in NKB 55 and ISO 2394-1998, EN 1990 safety index has 3 levels. These levels are called reliability classes (*RC*) instead of safety classes, see Table 4.7. If EN 1990 is used for design with partial factors from Annex A1 and design equations from the Eurocodes EN 1991 to EN 1999, a safety index greater than 3.8 is expected for a 50-year reference period. Reliability class 3 is not considered here since these structures require individual consideration.

Table 4.7 Recommended minimum values of safety index β in the ultimate limit state according to EN 1990.

Reliability class	Minimum value for β	
	1 year reference period	50 year reference period
RC 1	4.2	3.3
RC 2	4.7	3.8
RC 3	5.2	4.3

In the evaluation of these values lognormal or Weibull distributions were used for material and structural resistance parameters and model uncertainties. Normal distributions are usually used for dead load, and for non-fatigue verifications normal distributions have been used for variable actions, even if extreme value distributions would have been more appropriate, according to EN 1990.

The relation between the values of β for different reference periods can be calculated using Eq. 4.4. This relation is only valid if the main actions have statistically independent maximum for each year.

$$P(t < n) = 1 - (1 - p_1)^n \qquad \text{Eq. 4.4}$$

Here t is time, n is the reference period in years, p_1 is the probability of failure with a one-year reference period and $P(t<n)$ is the failure probability within the reference period n.

Nowak and Saraf (1996) presented results from a calibration for bridges designed according to the AASHTO code of 1992. In their calibration a target safety index of 3.5 was achieved for the ultimate limit state for structural elements with a reference period of 50 years. For the serviceability limit state a similar process gave a corresponding target safety index of 1.0.

4.5 Analysis method

In BKR (2000) reference is made to ISO 2394-1998 for the method used to calculate the safety of an element. Three types of methods are suggested for time-invariant analysis. These are: analytical methods, such as FORM (see Section 5.2.4) and SORM (Section 5.2.5), Monte Carlo simulation (Section 5.2.2) and numerical integration (Section 5.2.1).

It is suggested in ISO 2394-1998 that the time-variant problems be transformed into time-invariant problems. Two types of time-variant problems are likely to occur; overload failure or cumulative failure. In the case of overload failure a single action process can be replaced by a random variable with a mean value equal to its expected maximum value over a chosen reference period. In the case of cumulative failure, such as fatigue or corrosion, the entire history of the load up to the point of failure is of interest.

4.6 Uncertainties in stochastic modelling

When establishing a limit state equation, different random variables are introduced, for example, concerning geometric properties of the structure, material properties, loads and model uncertainties. Besides the uncertainties regarding the values of the parameters, statistical uncertainties also arise during the evaluation of the values of the parameters.

Thoft-Christensen (2001a) breaks down the uncertainties into physical and statistical uncertainties. The former are related to actual values of material properties, loads and dimensions. Since these uncertainties are measurable they give rise to statistical uncertainties.

A third group of uncertainties, according to Thoft-Christensen, is model uncertainties, which describe how well a mathematical model fits the result of tests. This uncertainty can be described by a random variable x_m defined as in Eq. 4.5.

$$x_m = \frac{\text{response}}{\text{predicted responce using model}} \qquad \text{Eq. 4.5}$$

4.7 Material models

NKB 55 (1987) and NKB 36 (1978) both state that the difference between the strength of test specimens and their strength in the real structures should be taken into consideration. This is of special interest for concrete since there are significant differences between the standard cubes (SS 13 72 30) used for evaluation and the concrete in the finished structure. This relation can be expressed as:

$$f_r = \rho f \qquad \text{Eq. 4.6}$$

where f_r is the strength in the structure, f is the strength of the test specimen and ρ is the correction factor.

If the strength f and the correction factor ρ can be assumed to be uncorrelated, it is possible to estimate their mean values and variance. Assuming that both variables are lognormally distributed, the following relations are valid:

$$\mu_{fr} = \mu_f \mu_\rho \qquad \text{Eq. 4.7}$$

$$V_{fr} = \sqrt{V_f^2 + V_\rho^2} \qquad \text{Eq. 4.8}$$

where μ denotes the mean values and V the variances of each parameter.

Basic concrete properties are dealt with in a detailed manner in JCSS (2002). The *in situ* compressive strength ($f_{c,ij}$) at a particular point i in a given structure j is given by Eq. 4.9.

$$f_{c,ij} = \alpha(t,\tau)\left(f_{c0,ij}\right)^{\lambda} Y_{1,j} \qquad \text{Eq. 4.9}$$

where $f_{c0,ij}$ is the compressive strength, λ is a factor taking into account the systematic difference between *in situ* compressive strength and the strength in standard tests, $\alpha(t,\tau)$ is a factor taking into account age of the concrete at loading t [days], and the duration of

loading τ [days], and $Y_{1,j}$ is a lognormal random variable representing variations due to the special curing and hardening conditions of the *in situ* concrete in structure *j*. Data and distribution parameters of $Y_{1,j}$ are given in Table 4.8. $f_{c0,ij}$ is used as a basic strength to which all strengths parameters are related.

Table 4.8 Data and distribution parameters $Y_{i,j}$ from JCSS (2002).

Variable	Distribution type	Mean	COV	Related to
$Y_{1,j}$	Lognormal	1.0	0.06	Compression
$Y_{2,j}$	Lognormal	1.0	0.30	Tension
$Y_{3,j}$	Lognormal	1.0	0.15	E-modulus
$Y_{4,j}$	Lognormal	1.0	0.15	Ultimate strain

According to JCSS (2002) the strength development of the concrete is taken into consideration by $\alpha(t,\tau)$, a deterministic function, which takes into account the concrete age at loading and the duration of loading. The function is given by:

$$\alpha(t,\tau) = \alpha_1(\tau)\alpha_2(t) \qquad \text{Eq. 4.10}$$

$$\alpha_1(\tau) = \alpha_3(\infty) + \left[1 - \alpha_3(\infty)e^{(-a_\tau \tau)}\right] \qquad \text{Eq. 4.11}$$

$$\alpha_2(t) = a + b\ln(t) \qquad \text{Eq. 4.12}$$

The coefficients in Eq. 4.11 can be set to $\alpha_3(\infty) \approx 0.8$ and $a_\tau = 0.04$ but in most applications $\alpha_1(t) = 0.8$ can be used instead of calculated values. *a* and *b* in Eq. 4.12 can be set to 0.6 and 0.12 respectively.

The basic compressive strength ($f_{c0,ij}$) can be evaluated using Eq. 4.13:

$$f_{c0,ij} = \exp\left(\left(U_{ij}\Sigma_j + M_j\right)\right) \qquad \text{Eq. 4.13}$$

where U_{ij} is a standard normal variable representing the variability within one structure, Σ_j is the standard deviation in structure *j*, and M_j is the logarithmic mean in structure *j*. These parameters are intended to be evaluated from *in situ* measurements. The variable *U* is related to the variability within a structure and if *i* and *k* represent different locations in structure *j* the correlation between the different locations can be expressed as shown in Eq. 4.14:

$$\rho\left(U_{ij}, U_{kj}\right) = \rho + (1-\rho)\exp\left\{\frac{\left(r_{ij} - r_{kj}\right)^2}{d_c^2}\right\} \qquad \text{Eq. 4.14}$$

where $d_c = 5$ and $\rho = 0.5$, and r_{ij} and r_{kj} are correlation coefficients.

If there are no direct measurements of the strength, recommendations are available for the values of the parameters in Eq. 4.9 and Eq. 4.13 in JCSS (2002). Values of Y_{ij} can be taken from Table 4.8, and if direct measurements are available these values can be taken as parameters of an equivalent a priori sample with size n'=10 in a Bayesian updating of Σ_j and M_j.

Bayesian updating implies that conditional probabilities are used (see Section 5.4). Bayesian updating can, for instance, be used when testing is done with only a few samples, and information is available from a larger number of samples. The available information is denoted a priori information. Bayes' theorem is then used to weigh the two sources of information together. During this process the mean value and the standard deviation of the parameter that is updated are assumed to be random variables themselves. In JCSS (2000) this method is suggested as a tool for the evaluation of concrete strength following the scheme described below.

The random variable $x_{ij}=\ln(f_{c0,ij})$ is normally distributed if the mean value and standard deviation are obtained from an ideal infinite sample. When this is not the case these parameters must be treated as random variables. For the assumptions valid for the concrete strength describe with Eq. 4.9, x_{ij} has a student distribution according to

$$F_x(x) = F_{tv''}\left[\frac{\ln(x/m'')}{s''}\left(1+\frac{1}{n''}\right)^{-0,5}\right] \qquad \text{Eq. 4.15}$$

where $F_{tv''}$ is the student distribution for υ'' degrees of freedom, and the values of m'', n'', s'' and υ'' depend on the amount of specific information that is available from the new sample.

$f_{c0,ij}$ can now be represented as:

$$f_{c0,ij} = \exp\left(m'' + t_{v''}s''\left(1+\frac{1}{n''}\right)^{0,5}\right) \qquad \text{Eq. 4.16}$$

The tensile strength ($f_{ct,ij}$) is related to the compressive strengths by:

$$f_{ct,ij} = 0,3 f_{c,ij}^{2/3} Y_{2,j} \qquad \text{Eq. 4.17}$$

where $Y_{2,j}$ is given in Table 4.8.

The modulus of elasticity ($E_{c,ij}$) can be expressed as:

$$E_{c,ij} = 10,5 f_{c,ij}^{1/3} Y_{3,j} \frac{1}{1+\beta_d \varphi(t,\tau)} \qquad \text{Eq. 4.18}$$

where β_d is the ratio of permanent load to the total load and $\varphi(t,\tau)$ is the creep coefficient. β_d is generally between 0,6 and 0,8 and $Y_{3,j}$ is given in Table 4.8.

The ultimate compressive strain ($\varepsilon_{cu,ij}$) is given by:

$$\varepsilon_{cu,ij} = 6\cdot 10^{-3} f_{c,ij}^{-1/6} Y_{4,j}\left(1+\beta_d \varphi(t,\tau)\right) \qquad \text{Eq. 4.19}$$

where $Y_{4,j}$ is given in Table 4.8.

ISO 2394-1998, ISO/CD 13822 and EN 1990 do not consider details on this level.

4.8 Geometric properties

NKB 55 (1987) states that geometric properties can be regarded as deterministic variables if they are related to calculations of load effects. Such properties may be the spans between beams and the dimensions used for calculation of moments of inertia as a basis for the analysis of statically indeterminate systems of the first order. If the moments of inertias are used for second-order stability analysis, geometric properties should be regarded as random variables. Dimensions used to describe resistance should be considered as random variables with lognormal distributions.

NKB 36 (1978) promotes the same approach expect that any geometrical data of importance should be regarded as random variables. If a value of the geometrical property larger than the mean value is disadvantageous, a normal distribution should be used, whereas if a value smaller than the mean value is disadvantageous a lognormal distribution should be applied.

ISO 2394-1998 and ISO/CD 13822 adopt the viewpoint that all parameters of importance should be regarded as random variables but no recommendations are given regarding distribution functions. In EN 1990 no specific recommendations are given regarding the modelling of geometric properties, but the basic ideas in this publication are closely related to ISO 2394-1998.

In JCSS (2002), recommendations are given for cross-section dimensions giving rise to dead loads. The recommendations are given as statistical characteristics of the deviation (Y) of the random variable (X) from a nominal value (X_{nom}), see Eq. 4.20.

$$Y = X - X_{nom} \qquad \textbf{Eq. 4.20}$$

This means that when applying the random variable (X) in a limit state equation it should be expressed as:

$$X = X_{nom} + Y \qquad \textbf{Eq. 4.21}$$

Suggestions are also given for coefficients of variation for reinforcement areas, and dimensions of concrete structures. For concrete structures detailed suggestions are made. External dimensions can be expected to have a mean deviation, μ_y, between 0 and 3 mm, as shown in Eq. 4.22 and a standard deviation as shown in Eq. 4.23. These recommendations are valid up to dimensions of 1000 mm.

$$0 \le \mu_y = 0.003 x_{nom} \le 3\,\text{mm} \qquad \textbf{Eq. 4.22}$$

$$\sigma_y = 4\,\text{mm} + 0.006 x_{nom} \le 10\,\text{mm} \qquad \textbf{Eq. 4.23}$$

Statistical data show that the average concrete cover on top steel is systematically larger than the nominal values with a large scatter. The following suggestions are made for the deviation, $5 \le \mu_Y \le 15$ mm and $5 \le \sigma_Y \le 15$ mm. For bottom steel, the scatter is even larger, and thought to be due to the variety of spacers used. Deviation of the position of the bottom steel is suggested to have the following variation, $-20 \le \mu_Y \le 20$ mm and $\sigma_Y \cong 5$ mm.

Effective depths of concrete beams are also associated with large variations. In this case the following suggestions are made, $\mu_Y \cong 10$ mm and $\sigma_Y \cong 10$ mm. According to JCSS (2002)

can the deviation of all geometric properties be modelled with normal distributions and recommended limits are given in Table 4.9.

Table 4.9 Recommended bounds regarding deviations of geometric properties from JCSS (2002).

Structural element	μ_y [mm]	σ_y [mm]
Column and wall	0 to 5	5 to 10
Slab, bottom steel	0 to 10	5 to 10
Beam, bottom steel	-10 to 0	5 to 10
Slab and beams, top steel	0 to 10	10 to 15

Details on this level are not dealt with in ISO 2394-1998, ISO/CD 13822 or in EN 1990.

4.9 Model uncertainties

In NKB 55 (1987) the separated limit state equation shown in Eq. 4.24 forms the basis for the definition of model uncertainties. It is further assumed that in many cases it is impossible to separate physical uncertainties from model uncertainties regarding the load, hence it is assumed that the model uncertainty is included in the mean value and standard deviation of the load.

$$R(a,\rho,f)-S(F_1\ldots F_n)\geq 0 \qquad \text{Eq. 4.24}$$

Here R is the resistance, a, f and ρ are different measurements and strengths, S is the load effect and $F_1 \ldots F_n$ are loads.

The resistance and load parts can be written as in Eq. 4.25 and Eq. 4.26, introducing uncertainties related to the design models S_0 and R_0, where C_{Si} describes load uncertainties, and C_R describes resistance uncertainties. As indicated in Eq. 4.25 the uncertainties are related to the loads included in the load descriptions below.

$$S(F_1\ldots F_n)=S_0(C_{S1}F_1\ldots C_{Sn}F_n) \qquad \text{Eq. 4.25}$$

$$R(a,\rho,f)=R_0(a,\rho,C_R f) \qquad \text{Eq. 4.26}$$

All the uncertainties introduced are assumed to be lognormally distributed with a mean value 1.0 and a coefficient of variation that represents the uncertainty. In cases when the resistance and load cannot be separated in the limit state function another solution must be found. If equilibrium is used as the limit state function, no model uncertainties should be applied. NKB 36 (1978) is more detailed in its description of model uncertainties. Account is taken of model uncertainties related to material properties via a judgement factor denoted I_m and a similar judgement factor for actions I_f. I_m is assumed to be lognormally distributed with a mean value of 1.0 and a coefficient of variation V_{I_m}, and is introduced through multiplication by the material parameter in question. I_f is assumed to be normally distributed with a mean equal to 0 and a standard deviation V_{I_f}. The judgement factor (I_f)

is added to the basic actions. As help for the code writer the following suggestions (see Table 4.10 to Table 4.12) are made for the coefficients of variation to use with Eq. 4.27:

$$V_{I_m} = \sqrt{V_{I_1}^2 + V_{I_2}^2 + V_{I_3}^2 + 2\left(\rho_1 V_{I_1} + \rho_2 V_{I_2} + \rho_3 V_{I_3}\right) V_m} \qquad \text{Eq. 4.27}$$

where V_{I_i} takes into account uncertainties related to the calculation model, deviation in strength between the material in the structure and the specimen as well as the degree of control, see Table 4.10 to Table 4.12.

Table 4.10 Coefficient of variation (V_{I_1}) and the correlation coefficient ρ_1, from NKB 36 (1978).

	Accuracy of the calculation model		
	Good	Normal	Bad
V_{I_1}	0.04	0.06	0.09
ρ_1	-0.3	0	0.3

Table 4.11 Coefficient of variation (V_{I_2}) and the correlation coefficient ρ_2, from NKB 36 (1978).

	Possible deviation in the strength of materials in the structure compared with that derived from control specimens		
	Small	Medium	Large
V_{I_2}	0.04	0.06	0.09
ρ_2	-0.3	0	0.3

Model uncertainties regarding actions are assigned to the standard deviation of the judgement factor I_f. For permanent actions this standard deviation is 5% of the expected mean value.

Table 4.12 Coefficient of variation (V_{I_3}) and the correlation coefficient ρ_3, from NKB 36 (1978).

	Degree of control on site		
	Strict	Normal	Slack
V_{I_3}	0.04	0.06	0.09
ρ_3	-0.3	0	0.3

In JCSS (2002) recommendations are given for model uncertainties when calculating the response of a structure. The model uncertainties are described either by Eq. 4.28 or Eq. 4.29.

$$Y' = \theta f(X_1 \ldots X_n) \qquad \text{Eq. 4.28}$$

$$Y' = \theta + f(X_1 \ldots X_n) \qquad \text{Eq. 4.29}$$

Y' is the load effect or resistance, θ is the model uncertainty, f is a function and $X_1 \ldots X_n$ are random variables. Proposed statistical properties for θ are given in Table 4.13. Eq. 4.28 is used when θ is lognormally and Eq. 4.29 when θ is normally distributed.

Table 4.13 Recommended probabilistic models for model uncertainties, from JCSS (2002).

Model type	Distribution	Mean	COV
Load effect calculation			
Moments in frames	Lognormal	1.0	0.10
Axial forces in frames	Lognormal	1.0	0.05
Shear forces in frames	Lognormal	1.0	0.10
Moments in plates	Lognormal	1.0	0.20
Stresses in 2D solids	Normal	0.0	0.05
Stresses in 3D solids	Normal	0.0	0.05
Resistance models, steel (static)			
Bending moment capacity	Lognormal	1.0	0.05
Shear capacity	Lognormal	1.0	0.05
Welded connection capacity	Lognormal	1.15	0.15
Bolted connection capacity	Lognormal	1.25	0.15
Resistance models, concrete (static)			
Bending moment capacity	Lognormal	1.2	0.15
Shear capacity	Lognormal	1.4	0.25
Connection capacity	Lognormal	1.0	0.10

Mean values greater than 1 indicate that the models related to the model uncertainties are calibrated to give results corresponding to values at lower percentiles than the mean response.

Details on this level are not available in ISO 2394-1998, ISO/CD 13822 or EN 1990.

4.10 Loads

Loads on structures are often classified with respect to time variation or spatial variation of the loads. In a time-related classification the loads may be permanent, variable or exceptional i.e. accidental loads. With regard to spatial variation the loads can be either fixed or free.

A structure also often suffers from to deterioration. Deterioration can also be regarded as a load. Modelling of durability for concrete structures is dealt with in great detail in Duracrete (1997), a EU-funded research programme with the objective of defining a framework for durability design of new concrete structures. Some of the findings of this research programme are also useful for assessment purposes in combination with JCSS (2002).

In this section, recommendations for probabilistic modelling are summarised for the loads considered in this thesis. For further information regarding modelling the reader is referred is to the literature. The information presented below has been taken from NKB, JCSS and Duracrete.

4.10.1 Dead load

In NKB 55 (1987) no specific values are recommended for the coefficient of variation with regard to the dead load. NKB 36 (1978) is more specific and concrete is said to have a mean density between 23 and 25 kN/m^3 with a COV of 4%, JCSS (2002) gives the same recommendation for the COV but uses 24 kN/m^3 as a mean value for ordinary concrete. No recommendations could be found for the probabilistic modelling of ballast in the literature, but it is permanent in nature, likely to have a larger variability than the dead load.

4.10.2 Train loads

In a European perspective two train load models are used according to Calgaro (1998). They are called Load Model 71 and Load Model SW. These models are also used in the Swedish Rail Bridge Design Code. Calgaro does not give any probabilistic design values for the load intensities. However, James (2001) and James and Karoumi (2001) have evaluated on-site measurements of train loads from different locations in Sweden in order to evaluate a possible increase in permissible axle loads on railway bridges. From their work it can be seen that the mean value of axle loads on the iron-ore rail track in the north of Sweden is 247 kN, with a standard deviation of 12.2 kN. These values were estimated from a 3-month test period with 250 kN as the permissible axle load.

Since the bridge investigated in the present study is located in the vicinity of Malmö and no iron ore trains traffic the line these data are not suitable for the current application. The traffic around Malmö is a combination of heavy traffic and lighter passenger trains with a permissible axle load of 225 kN. For the present study measurements from Hallsberg, a large railway junction in the central Sweden, are more representative, according to James (2002). Measurements at this location have been performed with a permissible axle load of 225 kN, giving a mean value of 199 kN with a standard deviation of 18.7 kN. All load data presented in this thesis are annual maximum axle loads.

4.10.3 Water pressure

In NKB 55 (1987) and NKB 36 (1978) it is suggested that water pressure should be divided into two parts: a permanent part and a variable part. The permanent part is the mean water pressure, and the difference between the current water pressure and the permanent water pressure should be regarded as a variable load.

4.10.4 Ice loads

In NKB 55 (1987) and NKB 36 (1978) ice loads are described by a characteristic intensity of 50-150 kN/m, but no information is given about the distribution or coefficient of variation for the loads.

4.11 Summary

Reliability analysis is permitted for the assessment of Swedish concrete structures, according to BKR (2000). Here reference is made to NKB 55 (1987) and ISO 2394-1998 for details. The information in ISO 2394-1998 is generic and not applicable for practical use. NKB 55 is more advanced but it does not contain enough guidance to be useful on its own. If NKB 55 is to be used for practical purposes, additional information that is needed can be found in NKB 36 (1978).

In NKB 55 information is given about target safety indices, and these are related to the assumptions made when they were originally calibrated from earlier practice. The target safety index is related to loads with a one-year reference period, i.e. it is the annual maximum value of the load that is of interest. Design is performed for sections or structural elements, not structural systems.

The basis of the analysis is a limit state function with uncorrelated random variables, and the safety index or probability of failure is calculated using analysis methods such as FORM (see Section 5.2.4). It is also assumed that random variables describing resistance parameters are lognormally distributed and random variables describing loads are normally distributed. If deviations are allowed from these assumptions, one is suddenly comparing different things and the tail sensitivity problem becomes apparent, see e.g. Melchers (1996).

As well as the distribution functions, model uncertainties are very important for the outcome of an analysis. The result is affected by the actual value of the uncertainty but also by the manner, which it is applied in the analysis.

In comparison with EN 1990, ISO 2394-1998 and ISO/CD 13822 are NKB 55 and NKB 36 detailed and better suited for practical use. Both the ISO publications recommend that socio-economic considerations be allowed to affect the target safety. This is an interesting feature for assessment purposes but needs to be investigated further. Lower nominal safety for older structures then newer structures is not officially accepted in Sweden, but it is a pragmatic approach that should be investigated.

JCSS (2002) differs from all the others, with its very detailed guidelines and statistically advanced methods in many aspects of probabilistic analysis. The large amount of available information is advantageous, but the advanced statistics make it difficult to use.

5 RELIABILITY THEORY

5.1 General considerations

Reliability with reference to structures is linked to the consistent evaluation of the safety of the structure, according to Madsen et al. (1986). Consistency is needed since the fluctuation of loads and the variability of material properties and uncertainties regarding the analytical models mean that there is a probability that the structure will not perform as intended. Although this probability in current practice is generally very small, there is a need to control the risk of non-performance in a rational way. A solution to this problem is to use statistical tools in structural design as well as in reassessment of existing structures.

Thoft-Christensen and Baker (1982) stated that structural reliability theory is the rational treatment of uncertainties in structural engineering. This leads to a fundamental problem since many of the design parameters are unknown at the design stage. According to JCSS (2001) a substantial part of the uncertainty arises from lack of information, as little is known for example about the actual wind or snow load. There is also a considerable uncertainty related to matter such as the concrete quality actually achieved during casting.

To take into account these uncertainties in modern everyday design, the partial factor system was developed. This format is used in many design codes, such as EN 1990 and the Swedish design guidelines BKR (2000). A partial factor system can be described as a level 1 method of safety checking according to, e.g., Thoft-Christensen and Baker (1982). Level 1 analysis indicates that the reliability is provided on a structural element basis, by the use of partial safety factors related to predefined nominal values of the structural and load variables. All calculations are performed on a deterministic level. According to JCSS (2001) this method is less suitable for the assessment of existing structures.

Probability-based design can be performed by level 2 or level 3 methods, see e.g. Thoft-Christensen and Baker (1982). Level 2 design methods involve iterative procedures to find an approximation of the failure probability of a structure or a system. This procedure requires idealisation of the failure domain and is often associated with a simplified representation of the joint probability distribution of the variables. Level 2 methods are used in many cases for the calibration of partial factors in design codes.

Level 3 approaches are described as calculations to determine the exact probability of failure for a structure or a structural component. This is achieved using a full probabilistic description of the joint occurrence of the various quantities that affect the response of the structure taking into account the true nature of the failure domain.

5.2 Methods of analysis

The outcome of level 2 and level 3 methods described above is a probability of failure or a safety index. There are several different methods of calculating the failure probability, and descriptions of the methods can be found in Thoft-Christensen and Baker (1982), Ditlevsen

and Madsen (1996), Madsen, Krenk and Lind (1986) and Melchers (1999). According to Melchers (1999) the methods can be grouped into direct integration, simulation and second-moment methods. The basis of reliability theory is that the relevant parameters used to describe the relationship between load and resistance in the limit state equations are random variables.

A random variable may be described by its distribution function and associated parameters. An imaginary situation when the load (S) and resistance (R) are described by single parameters is used as a starting point to define the probability of failure and the safety index. The failure probability (p_f) is then defined as follows.

$$p_f = P(R - S \leq 0) \qquad \textbf{Eq. 5.1}$$

If the basic variables R and S are defined as independent random variables with continuous distributions, the probability of failure can be written as:

$$p_f = \int_{-\infty}^{+\infty} \int_{-\infty}^{s \geq r} f_R(r) f_S(s) dr ds \qquad \textbf{Eq. 5.2}$$

where f_R is the probability density distribution function for R and f_S is the probability density function S. This integral is illustrated in Figure 5.1.

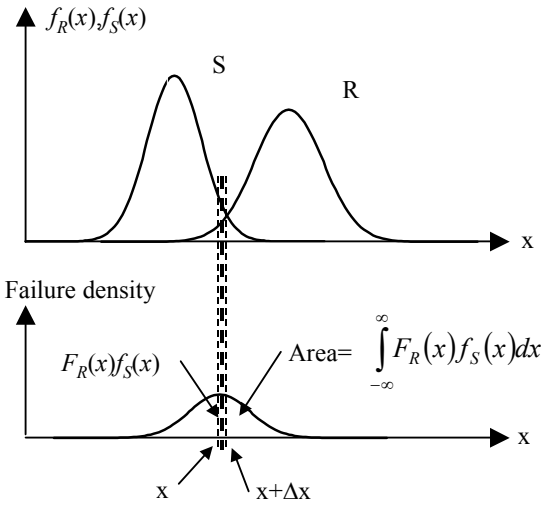

Figure 5.1 Basic *R-S* problem: $f_R(\,)$ $f_S(\,)$ representation, from Melchers (1999).

Eq. 5.2 can be reformulated to Eq. 5.3, corresponding to the situation shown in Figure 5.2.

$$p_f = \int_{-\infty}^{+\infty} F_R(x) f_S(x) dx \qquad \textbf{Eq. 5.3}$$

where F_R is the cumulative distribution function for R and f_S is the probability density function S.

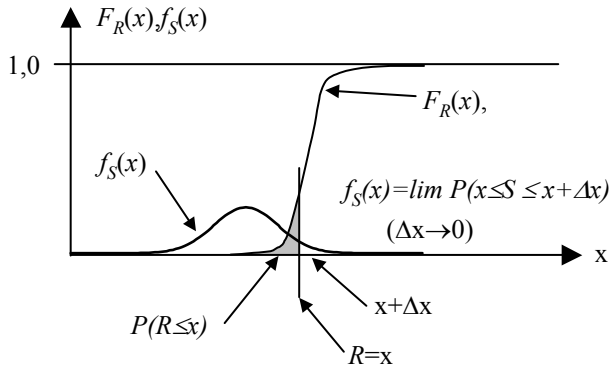

Figure 5.2 Basic *R-S* problem: $F_R(\ ) f_S(\ )$ representation, from Melchers (1999).

The integrals above can only be solved for certain cases and numerical integration or simulation must be used for the other cases.

5.2.1 Numerical integration

If no closed solution exists for the integrals in Eq. 5.2 and Eq. 5.3, it can be evaluated using numerical integration. Satisfactory results are achieved using the trapezoidal rule, but Simpson's rule or methods based on polynomials may be more appropriate (Melchers, 1999).

5.2.2 Monte Carlo simulation

Another way of solving the integrals is to use simulation techniques. The Monte Carlo technique involves random sampling, i.e. the value of a stochastic variable is randomly drawn from its distribution. Sampling is performed for all basic variables and the values are used to calculate *R* minus *S*. The number of times this value is less than 0, $n(R\text{-}S \le 0)$ is recorded and the probability of failure is the ratio of the number failures and the total number of trials (N_{trial}).

$$p_f = \frac{n(R - S \le 0)}{N_{trial}} \qquad \text{Eq. 5.4}$$

Monte Carlo simulation is only appropriate when the number of trials is smaller than the number of integration points that is needed for a numerical evaluation of the integral. Various methods are available for so called importance sampling to reduce the number of trials needed to achieve reliable estimates by simulation.

5.2.3 Second-moment concepts

The evaluation of Eq. 5.3 is easy if the limit state equation is a linear function of independent normally distributed variables. This type of solution is referred to as second-moment concept. Second-moment concepts are based on the fact that normally distributed

variables are described by their first two moments, i.e. mean value and variance. In this case, a limit state equation can be defined as:

$$M = R - S = 0 \qquad \text{Eq. 5.5}$$

where M is the limit state equation. Since R and S are normally distributed, and M is a linear function of R and S, M is also normally distributed. The mean value of M can now be calculated as:

$$\mu_M = \mu_R - \mu_S \qquad \text{Eq. 5.6}$$

where μ_M, μ_R and μ_S are the mean values of the limit state function, resistance and load, respectively.

It is also possible to calculate the standard deviation for the limit state equation (σ_M) as:

$$\sigma_M = \sqrt{\sigma_R^2 + \sigma_S^2} \qquad \text{Eq. 5.7}$$

where σ_R and σ_S are the standard deviations of the resistance and load, respectively. With this information the failure probability (p_f) becomes:

$$p_f = \Phi\left(\frac{0 - \mu_M}{\sigma_M}\right) \qquad \text{Eq. 5.8}$$

where Φ is the standard normal function.

The safety of a structure or the probability of failure can also be expressed using a reliability or safety index, β. The safety index is defined as the number of standard deviations by which μ_M exceeds zero, as shown in Figure 5.3.

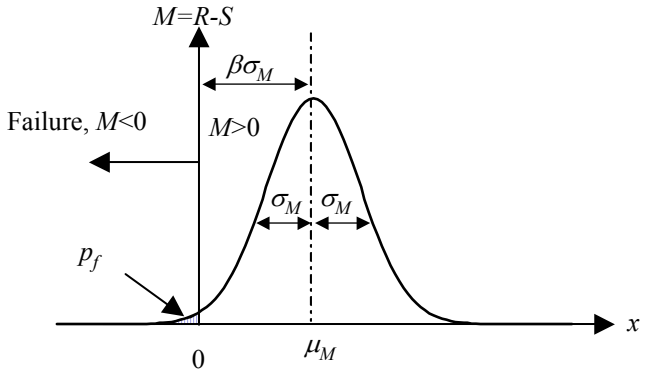

Figure 5.3 Distribution of safety margin *M=R-S*.

The safety index can be written as follows.

$$\beta = \frac{\mu_M}{\sigma_M} \qquad \text{Eq. 5.9}$$

Using Eq. 5.8 and Eq. 5.9 the probability of failure can now be defined as below.

$$p_f = \Phi(-\beta) \qquad \text{Eq. 5.10}$$

For a given probability of failure the safety index is given by the inverse of the standard normal distribution, as shown in Eq. 5.11.

$$\beta = -\Phi^{-1}(p_f) \qquad \text{Eq. 5.11}$$

When both R and S are normally distributed, the calculated probability of failure is exact, but when the parameters are described by other distribution functions the safety measure becomes nominal. Even if the exact probability of failure can be calculated the value should not be given a frequentistic interpretation since factors such as human error and human intervention are neglected. This means, for example, that a calculated probability of failure of 10^{-4} does not necessarily correspond to a failure rate of 1 out of 10,000 structures.

5.2.4 First-order second-moment reliability method

In the general case the failure or limit state condition R-$S \leq 0$ can be replaced by:

$$f(X) = f(x_1, x_2 \ldots x_n) \leq 0 \qquad \text{Eq. 5.12}$$

where the random vector X represents all the basic variables involved in the problem. The function $f(\ )$ is the limit state function defined in n-dimensional space. The limit state or failure surface $\partial\omega$, defined by $f(X)=0$, divides this space into two subspaces, the safe region and the unsafe region, see Figure 5.4. A consistent definition of safety index in this general context was proposed by Hashofer and Lind (1973).

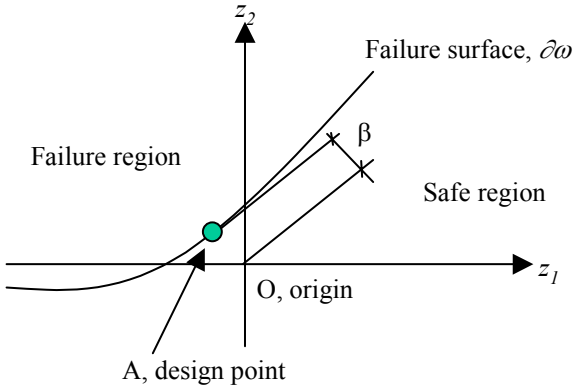

Figure 5.4 Schematic sketch of the Hashofer-Lind safety index, where z_1 and z_2 are arbitrary normalised parameters.

The first step when defining the Hashofer-Lind safety index is to normalise the set of basic variables. The new set of variables is denoted $Z = (z_1, \cdots z_n)$ and is defined by:

$$z_i = \frac{x_i - \mu_{X_i}}{\sigma_{X_i}} \qquad \text{Eq. 5.13}$$

where μ_{x_i} and σ_{x_i} are the mean and standard deviation of the random variable x_i.

Note that this definition gives μ_{z_i} =0 and σ_{z_i} =1. This mapping results in a failure surface in the *z*-coordinate system instead of the original failure surface in the *x*-coordinate system. The Hashofer-Lind safety index is defined as the shortest distance from the origin in the z-coordinate system to the failure surface, see Figure 5.4. For the special case when all random variables are normally distributed and independent, the relations given in Eq. 5.10 and Eq. 5.11 are still valid. In mathematical terms β is given by Eq. 5.14:

$$\beta = \min_{Z \in \partial\varpi} \left(\sum_{i=1}^{n} z_i^2 \right)^{1/2} \qquad \text{Eq. 5.14}$$

where $\partial\varpi$ is the failure surface in the *z*-coordinate system.

In the general case, a non-linear iterative method is used to calculate the safety index. A common basis for such methods is to expand the non-linear limit state function in a Taylor series at the design point, see Figure 5.4. It is then assumed that the failure function is differentiable. A unit vector $\overline{\alpha} = (\alpha_1, \ldots, \alpha_n)$ given by $\overline{OA} = \beta\overline{\alpha}$ where *A* is the design point, can be calculated from Eq. 5.15:

$$\alpha_i = \frac{-\frac{\partial f}{\partial z_i}(\beta\overline{\alpha})}{\left[\sum_{k=1}^{n} \left(\frac{\partial f}{\partial z_i}(\beta\overline{\alpha}) \right)^2 \right]^{1/2}} \qquad \text{Eq. 5.15}$$

where $(\beta\alpha_i, \ldots, \beta\alpha_n)$ are the coordinates of the design point.

The first-order reliability method (*FORM*) works essentially as the first-order second-moment method, described for the calculation of the Hashofer-Lind safety index. The difference is that the demand on normally distributed variables is not necessary. Instead, all the information about a variable is used and it can be described by an arbitrary distribution function. The arbitrary distribution function is then transformed into an equivalent normal distribution (see Section 5.2.6). This transformation is not elementary but once it has been done second-order calculation methods can be used.

5.2.5 Second-order reliability method

The second-order reliability method (*SORM*) is similar to the first-order reliability method but instead of approximating the failure surface by a linear, first order approximation, a second-order approximation is used. In both cases the approximation is performed using Taylor series expansion.

5.2.6 Sensitivities

During the calculation of the safety index (β) as shown in Eq. 5.14, a parameter denoted α is used, see Eq. 5.15. This parameter can be used to estimate the sensitivity of the safety index to the random variables involved in the limit state function. The sensitivity with respect to changes in the mean of the random variables is calculated as

$$\alpha_i = \frac{\partial \beta}{\partial z_i} \frac{1}{\|\alpha\|_z} \approx \alpha_i \qquad \text{Eq. 5.16}$$

where $\|\alpha\|_z$ is the length of the vector containing α values from Eq. 5.15. These sensitivities are often plotted as pie charts but in this thesis the results are mainly given in tables. It is also possible to investigate the sensitivity of β with respect to the variability of a variable, $\alpha_{\sigma,i}$.

$$\alpha_{\sigma,i} \approx -\beta \alpha_i^2 \qquad \text{Eq. 5.17}$$

5.2.7 Transformations

A basic random variable, X, with non-normal distribution must be transformed into an equivalent normally distributed random variable $Y \in N(\mu_Y, \sigma_Y)$ representing X in the vicinity of the design point. This is called the normal tail transformation; see e.g. Madsen, Krenk and Lind (1986) or Melchers (1999).

The parameters μ_Y and σ_Y are evaluated in a way that makes the values of the distribution functions and the probability density functions identical at a point x_i, i.e. the solution must fulfil the conditions below.

$$F_X(x_i) = F_Y(x_i) \qquad \text{Eq. 5.18}$$

$$f_X(x_i) = f_Y(x_i) \qquad \text{Eq. 5.19}$$

It can be shown that these conditions give

$$\mu_Y = x_i - \sigma_Y \Phi^{-1}(F_X(x_i)) \qquad \text{Eq. 5.20}$$

$$\sigma_Y = \frac{\Phi\left(\Phi^{-1}(F_X(x_i))\right)}{f_X(x_i)} \qquad \text{Eq. 5.21}$$

where $F(\ )$ is the cumulative distribution function, $f(\ )$ is the probability density function and Φ is the standard normal density function.

A standard normal variable $Z \in N(0,1)$ can now be introduced by the relation in Eq. 5.22 in the usual manner.

$$Z = \frac{Y - \mu_Y}{\sigma_Y} \qquad \text{Eq. 5.22}$$

The transformed random variables are used in solving the failure function according to the scheme presented as the solution to the Hashofer-Lind safety index. For each iteration step

in the solution of the Hashofer-Lind safety index, a new normal tail approximation is made if non-normal variables are used.

In the general case, when the basic variables may be correlated, the original random variables can be transformed into a new set of independent random variables. This can be achieved using the Rosenblatt transformation or the Nataf transformations, depending on the information available on the correlation between the variables, see e.g. Melchers (1999).

5.3 Time-variant reliability theory

For a time-variant problem, several approaches can be adopted. In this section the most common approaches are introduced and they are then discussed in the following sections. The probability of failure for an arbitrary period in time is given by Eq. 5.23.

$$p_f = P(R(t) \le S(t)) \qquad \textbf{Eq. 5.23}$$

This probability can, in principle, be evaluated in the same way as for a time-invariant problem, but would not have any practical meaning because a safety measure must be related to a finite time period.

The classical approach is to consider the time integration transferred to the load or load effect. This transformation is then assumed to represent the total time period and the load is modelled by an extreme value distribution. This concept is described in Section 5.3.1 and is the most common situation.

For practical purposes shorter time periods are considered instead of total time periods, such as the duration of a storm; extreme value theory is then applied within that time period. Simple statistical operations can often be applied to estimate the failure probability over the lifetime of the structure. This is explained in Section 5.3.2.

Another approach that can be used is calculate the safety margin:

$$Z(t) = R(t) - S(t) \qquad \textbf{Eq. 5.24}$$

where $Z(t)$ is the limit state margin.

The probability that $Z(t)$ is less than zero during the lifetime of the structure is calculated. The time at which $Z(t)$ becomes less than zero for the first time is called the "time to failure". This concept is not discussed in this thesis and the theory behind it is therefore omitted.

5.3.1 Time-integrated approach

In the time-integrated approach the probability of failure is expressed as:

$$p_f(t_L) = P[R \le S_{\max}(t_L)] \qquad \textbf{Eq. 5.25}$$

where $S_{max}(t_L)$ denotes the maximum load effect in the period $[0,t_L]$. The probability distribution for $S_{max}(\,)$ can be found either by fitting statistical data or by using data of shorter time periods that are extrapolated to describe extreme value distributions. This

approach assumes that the resistance is constant over time and failure occurs if $S_{max}( )$ is larger than R during the observed period.

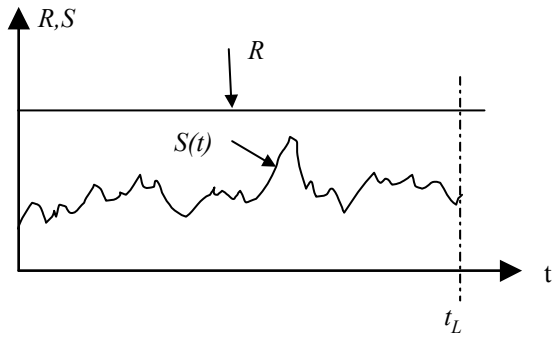

Figure 5.5 Realisation of load effect *S(t)* and resistance *R* with *R* as a time-independent random variable.

For a series of independent loads applied to the structure, the probability that the maximum load effect $S_{max}( )$ will be less than a given value x, is given by:

$$F_{S_{\max}}(x) = P(S_{\max} < x) = P(S_1 < x) \cdot \ldots \cdot P(S_n < x) = [F_S(x)]^n \qquad \text{Eq. 5.26}$$

where $F_{S_{\max}}$ is the cumulative distribution function for the maximum load effect and n represents the length of the reference period. For large values of n this expression approaches an extreme value distribution, which may then be used to describe $S_{max}( )$. The probability of failure for a given reference period (t_L) can now be calculated in the same way as for the time-invariant case, compare Eq. 5.3 and Eq. 5.27.

$$p_f = \int_0^{\infty} F_R(x) f_{S_{\max}}(x) dx \qquad \text{Eq. 5.27}$$

Note, however that the number of load applications n, is assumed to be statistically independent, which is not always fulfilled in reality.

5.3.2 Discrete approach

In the discrete approach the lifetime of the structure is divided into a number of discrete units n_L. This period is often one year, but it can also be a random variable linked to natural phenomena such as the duration of storms etc. These two cases are dealt with in different manners, but this presentation is limited to the case where the discrete unit time is determined deterministically.

A failure probability calculated using this method might then be the probability of failure per year. The one-year period is often used since wind and snow loads for instance have

annual maximum. If p_i is the failure probability for the i'th time unit and p_i is equal to p for all time periods t then:

$$P(T<t)=1-\prod_{i=1}^{t}(1-p_i)=1-(1-p)^t \qquad \text{Eq. 5.28}$$

where T is time and t is a time period.

If the product pt is sufficiently small Eq. 5.28 can be replaced by Eq. 5.29.

$$P(T<t)\approx 1-\exp(-tp)\approx tp \qquad \text{Eq. 5.29}$$

The probability of failure for a lifetime $[0,t_L]$ can then be expressed as below:

$$p_f(t_L)\approx 1-\exp(-t_L p)\approx t_L p \qquad \text{Eq. 5.30}$$

Another concept that is often used in combination with the discrete approach is the return period. A return period is the mean time between defined events. A generalised return period can be defined as:

$$\overline{T}_G=\frac{1}{p_{f_1}} \qquad \text{Eq. 5.31}$$

where $\overline{T_G}$ is the generalised return period and p_{f_1} is the failure probability for a unit time.

5.4 Conditional probability

The conditional probability of event B if event A has occurred can be written as

$$P(B|A)=\frac{P(B\cap A)}{P(A)} \qquad \text{Eq. 5.32}$$

or

$$P(B\cap A)=P(A)P(B|A) \qquad \text{Eq. 5.33}$$

Eq. 5.33 can be interpreted as follows. The probability of the occurrence of two events is equal to the probability of one event occurring multiplied by the conditional probability of the other event occurring, under the assumption that the first event has occurred.

Conditional probability is most easily explained with the aid of Figure 5.6. The fact that prior knowledge, in this case the event A, is known makes it possible to reduce the uncertainty regarding the events H_i

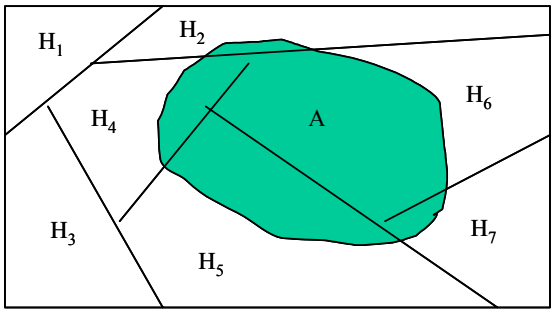

Figure 5.6 Outcome set divided into small outcomes, according to Blom (1984).

The probability of the event A can be written as follows.

$$P(A) = \sum_{i=1}^{n} P(H_i) P(A|H_i) \qquad \text{Eq. 5.34}$$

By using conditional probability it is now possible to write the event H_i, on condition that event A has happened as in Eq. 5.35.

$$P(H_i|A) = \frac{P(H_i \cap A)}{P(A)} = \frac{P(H_i)P(A|H_i)}{P(A)} = \frac{P(H_i)P(A|H_i)}{\sum_{j=1}^{n} P(H_j)P(A|H_j)} \qquad \text{Eq. 5.35}$$

Eq. 5.35 is usually referred to as Bayes' formula. Blom and Holmquist (1970) briefly describe the usefulness of Bayes' formula for point estimates of the mean and standard deviation of random variables.

5.4.1 Bayesian updating

The concept of conditional probability is often used to update parameters describing a random variable. The basic idea is to update prior probabilistic information about the parameters, with information from testing; this is often referred to as Bayesian updating. Examples of updating of material parameters based on prior information and new test data can be found in JCSS (2001).

The first step in Bayesian updating leads to a posteriori probabilistic model, which in its turn can be used to calculate a predictive probability distribution. The predictive probability distribution can then be used in reliability calculations. It is possible to obtain closed solutions in special cases. In JCSS (2001) and RCP Consult (1997) tables exists of continuous distribution functions used for Bayesian analysis, a few of these are reproduced in Appendix C and the background for these examples are further explained in the following section. If closed solutions do not exist numerical calculations can be performed based on conditional probability in the form of Bayes' theorem.

Suppose we want to model a random variable X, with unknown distribution $F_X(x)$. A common situation is that the type of distribution describing the random variable can be postulated but the parameters of the distribution $\boldsymbol{\theta}=(\theta_1, \theta_2,...,\theta_n)$ are unknown. In the Bayesian approach the parameters $\boldsymbol{\theta}$ are assumed to be random variables. The distribution of X can be denoted $F_X(x;\boldsymbol{\theta})$ in this case, to indicate that it depends on the unknown parameters $\boldsymbol{\theta}$.

In the following description it will be assumed that only one parameter θ is unknown, while the remaining parameters are known. Since θ is unknown it is a random variable with a distribution $F(\theta)$ and density $f(\theta)$. Let Y have the distribution $F(\theta)$, which is also called the prior distribution of the parameter θ. Now, the distribution $F_X(x;\theta)$ can be considered as the conditional distribution of X given that $Y=\theta$, i.e.

$$F_X(x;\theta) = F(x|\theta) = P(X \le x|Y=\theta) \qquad \textbf{Eq. 5.36}$$

Then, the distribution of X is given by

$$F_X(x) = \int_{-\infty}^{+\infty} P(X \le x|Y=\theta) f(\theta) d\theta = \int_{-\infty}^{+\infty} F(x|\theta) f(\theta) d\theta \qquad \textbf{Eq. 5.37}$$

In this way, uncertainties in parameters as well as the variability of data are considered simultaneously. Recall that $f(\theta)$ represent our priori information about the parameter θ. Now assume that we have observed n values of X, x_1, x_2,..., x_n. By including this knowledge in the analysis we can get at better estimate $f^{post}(\theta)$. By applying Bayes' formula (see Eq. 5.35), we obtain:

$$f^{post}(\theta) = f(\theta|x_1, x_{2,...}, x_n) = Cf(x_1, x_{2,...}, x_n|\theta) f(\theta) \qquad \textbf{Eq. 5.38}$$

where

$$C^{-1} = \int_{-\infty}^{+\infty} f(x_1, x_{2,...}, x_n|\theta) \cdot f(\theta) d\theta \qquad \textbf{Eq. 5.39}$$

Eq. 5.39 can be simplified if the observations x_i are assumed to be conditionally independent, which gives:

$$f(x_1, x_{2,...}, x_n|\theta) = f(x_1|\theta) f(x_2|\theta) \cdots f(x_n|\theta) = L(\theta) \qquad \textbf{Eq. 5.40}$$

where $L(\theta)$ is the likelihood function. By maximising $L(\theta)$, the maximum likelihood estimate of θ based on the new data x_i is obtained.

Introducing of Eq. 5.40 into Eq. 5.38 and Eq. 5.39 gives:

$$f^{post}(\theta) = CL(\theta) f(\theta) \qquad \textbf{Eq. 5.41}$$

with

$$C^{-1} = \int_{-\infty}^{+\infty} L(\theta) f(\theta) d\theta \qquad \text{Eq. 5.42}$$

Assuming that $F_x(x,\theta)$ is normal distributed, one can choose a form for the prior density $f(\theta)$ such that the posterior density will be of the same type as the prior density; this is called conjugate priors. In the case when the unknown parameter θ of a normal distribution is the mean value, μ_x, the prior density, f_{μ_x}, can be modelled by a normal distribution with a mean μ' and standard deviation σ', i.e.

$$f_{\mu_x}(\mu', \sigma') = \frac{1}{\sqrt{2\pi}\sigma'} \exp\left(-\frac{1}{2}\left(\frac{\mu_x - \mu'}{\sigma'} \right)^2 \right) \qquad \text{Eq. 5.43}$$

The posterior density can now be evaluated from Eq. 5.41 and Eq. 5.42. It can be shown that the posterior density is:

$$f_{\mu_x}^{post}(\mu_x) = \frac{1}{\sqrt{2\pi}\sigma''} \exp\left(-\frac{1}{2}\left(\frac{\mu_x - \mu''}{\sigma''} \right)^2 \right) \qquad \text{Eq. 5.44}$$

where μ'' is calculated as:

$$\mu'' = \frac{\frac{\mu'}{n} + \frac{\bar{x}}{n'}}{\frac{1}{n'} + \frac{1}{n}} \qquad \text{Eq. 5.45}$$

and σ'' is calculated as:

$$\sigma'' = \sqrt{\frac{\frac{\sigma_x^2}{n'}\frac{\sigma'^2}{n}}{\frac{\sigma'^2}{n'} + \frac{\sigma'^2}{n}}} \qquad \text{Eq. 5.46}$$

$$n' = \frac{\sigma_x^2}{\sigma'^2} \qquad \text{Eq. 5.47}$$

where $\bar{x}$ is the sample mean of the n observations and n' is the equivalent sample size for the prior distribution of μ_x.

The likelihood $L(\mu_x)$ of the observations is given by Eq. 5.48.

$$L(\mu_x) \propto \prod_1^n \frac{1}{\sqrt{2\pi}\sigma'} \exp\left(-\frac{1}{2}\left(\frac{x_i - \mu_x}{\sigma'} \right)^2 \right) \qquad \text{Eq. 5.48}$$

The predictive probability density function for X is expressed as:

$$f_X\left(x|x_1,x_2,\ldots x_n\right)=\frac{1}{\sqrt{2\pi}\sigma'''}\exp\left(-\frac{1}{2}\left(\frac{x-\mu''}{\sigma'''}\right)^2\right) \qquad \text{Eq. 5.49}$$

where σ''' is calculated from the relation below.

$$\sigma'''^2=\sigma''^2+\sigma_x^2 \qquad \text{Eq. 5.50}$$

6 THE DAM

6.1 Introduction

Many dams in Sweden are today more than 50 years old and for different reasons questions are raised about their structural integrity and safety. The structures are subjected to different deterioration mechanisms and there is a lack of information regarding the original design assumptions. All dams in Sweden where the consequence of failure is judged to be serious are subjected to an assessment every 15-year (RIDAS 1997) in which the structural integrity and safety of the dam are verified. In this chapter an existing dam is used as a case to investigate the possibility of applying reliability theory to safety assessment. A comparison will also be made between the results obtained from the probabilistic analysis and a deterministic analysis. Suggestions will be made regarding how to introduce results from ongoing monitoring programme of the uplift pressure into the reliability analysis for the purpose of predicting the future safety of the structure.

The safety of a concrete dam depends on several factors and one of them is the uplift pressure distribution under the dam body. In many cases, this constitutes a significant load on the structure and in order to reduce the uplift pressure a grout curtain is installed along the upstream edge of the dam. A grout curtain consists of cement-injected holes in the rock foundation on the upstream side of the dam, but since cement exposed to streaming water starts to leach, the efficiency of the grout curtain is reduced with time. This phenomenon is expected to take place in several dams in Sweden, and there are concerns about future dam safety. A leaching model coupled to linear regression is proposed as a tool for the incorporation of monitoring results into the reliability analysis.

6.2 General considerations

The dam investigated is a structure common in Sweden, located across the river Dalälven, in the central Sweden. The structure consists of a series of concrete monoliths or columns that are located in a line with jack-gates between them. The system is exemplified by a photograph of a similar dam (Figure 6.1).

Figure 6.1 View from the upstream side of a dam, taken when the water reservoir was empty.

6.2.1 Structural system

The dam that will be investigated was built in 1988 and plan of the dam is shown in Figure 6.2. From this dam one monolith or column was chosen for further investigations. This column was chosen since it was easy to gain access to it to mount of monitoring equipment used for uplift pressure measurements.

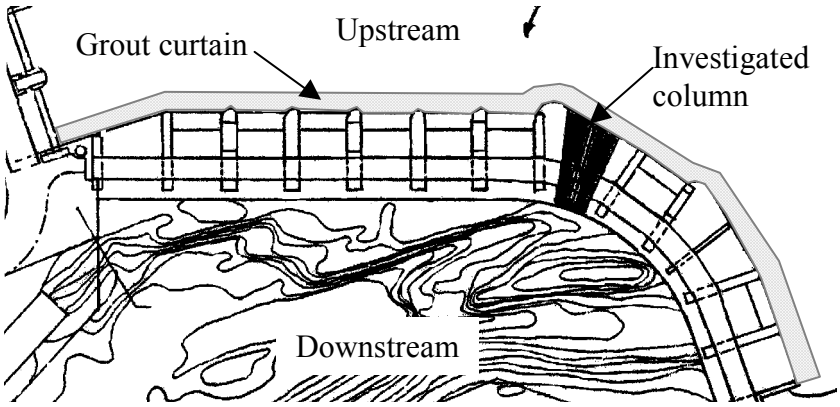

Figure 6.2 Elevation of entire dam structure.

The geometry of the investigated concrete column is shown in Figure 6.3 to Figure 6.5.

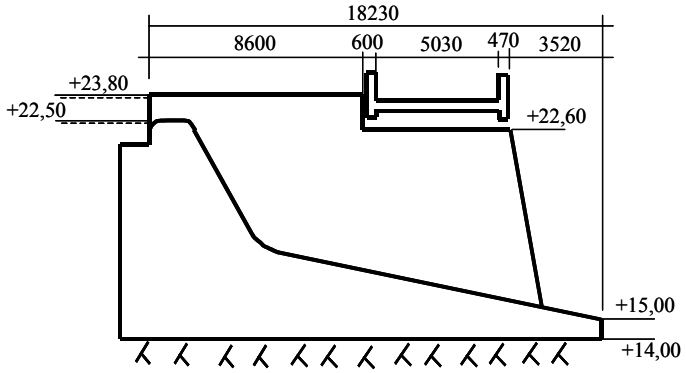

Figure 6.3 Section of dam column used in design (dimensions in mm).

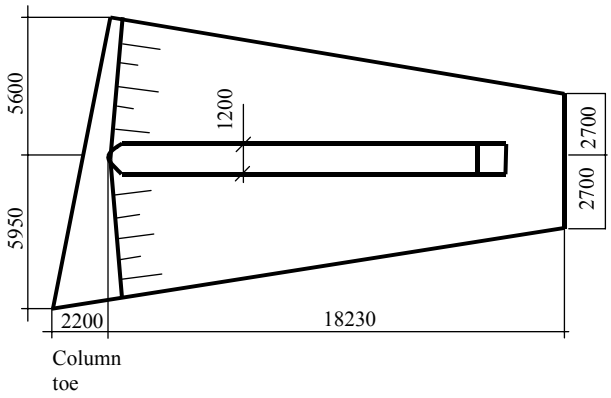

Figure 6.4 Geometry of bottom slab (dimensions in mm).

Different information exists regarding the inclination of the rock under the column. On drawings from the early phase of the project, no inclination of the rock surface is documented (Figure 6.3) but on drawings from the later phase of the project this has changed (Figure 6.5). The geometry according to Figure 6.5 was used. This geometry was verified in connection with the drilling of holes for monitoring the uplift pressure (see Section 6.6). To the author's knowledge there has been no redesign of the dam based on the difference in the rock profile, as seen in Figure 6.3 and Figure 6.5.

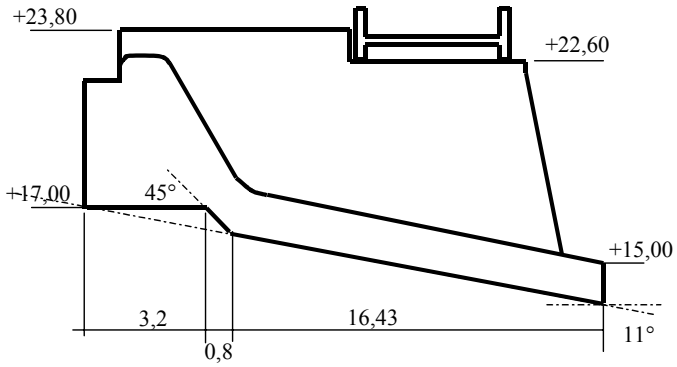

Figure 6.5 Section of dam column, note the inclined rock surface and compare with Figure 6.3 (dimensions in mm).

6.2.2 Codes

From the design drawings it cannot be established which code was used during the design process and sources within Vattenfall were unable to clarify the situation. Based on the author's knowledge it is reasonable to assume that the safety requirements are based on

praxis. The requirements shown in the existing design drawings are, however, stated and they are in compliance with RIDAS (2000), This is explained below.

6.2.3 Material

Concrete quality designated K300, with a water: cement ratio of maximum of 0.55 was used for the structure. It was also stated that the concrete should be watertight, with an air content of 5.5%. Reinforcement of type Ks40S was used. K300 is today referred to as K30, and this concrete has the characteristic and design strength given in Table 6.1, with ultimate limit state (ULS) values calculated according to Eq. 6.1. Characteristic values are used as design values in the serviceability limit state and accidental limit state.

$$f_{cd} = \frac{f_{ck}}{\gamma_m \gamma_n} \qquad \text{Eq. 6.1}$$

Here f_{cd} is the design value of concrete, f_{ck} is the characteristic value of concrete, γ_m is a partial factor taking variability in the material into consideration and γ_n is a partial factor related to the safety class of the structure. Safety classes are defined in Section 4.3, and for concrete γ_m is 1.5 and the different values of γ_n are shown in Table 6.2.

Table 6.1 Characteristic and design value of concrete, according to BBK 94 Band 1 (1995) for safety class 3.

Material property	Characteristic value [MPa]	ULS [MPa]
Compression	21.5	11.9
Tension	1.80	1.0

Table 6.2 Safety class and associated partial factor γ_n.

Safety class	γ_n
1	1.0
2	1.1
3	1.2

It is difficult to establish the mechanical properties of the underlying rock mass and no information is given in the available design drawings. Lack of information on the rock is regarded as a considerable problem for the assessment of the stability of this and other existing dams.

6.2.4 Damage

At the upstream edge of the row of monoliths or columns a grout curtain has been installed, as shown in Figure 6.2. Grout curtains are installed on all dams in Sweden as a precaution and for extra safety.

Proper functioning of the grout curtain is of great importance since the uplift pressure is often one of the dominating loads; see the schematic sketch in Figure 6.6. To the left a schematic uplift pressure distribution without grout curtain is shown and to the right reduced uplift pressure due to the grout curtain is shown.

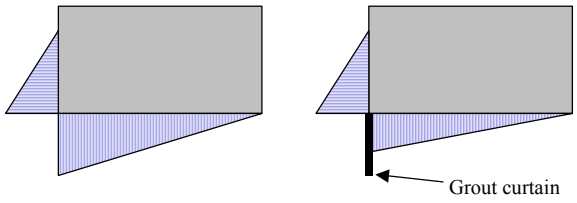

Figure 6.6 Schematic sketch indicating the difference in uplift pressure distribution with and without grout curtain.

After the dam is filled, it is believed that the function of the grout curtain will decay slowly due to leaching. It is impossible to verify the function of he grout curtain directly, but the uplift pressure beneath the column is an indirect measure of its functionality. Vattenfall Utveckling AB (VUAB), the owner's technical advisor and research company, has started continuous monitoring of the uplift pressure on the column. The current dam is designed for the uplift pressure of the type shown on the left in Figure 6.6, but this was not always the case with older dams.

6.3 Owner's requirements

6.3.1 Deterministic requirements

In recent years, Swedish dam owners have established a new design code for dams. It is called RIDAS (2000) and contains guidelines for dam safety. In this code, reference is made to BBK 94 Band 1 (1995) for the design of structural concrete, and special criteria are stated for the stability of different types of dams, i.e. concrete dams, earth-fill dams, etc.

For the current dam two load cases were applicable in the design.

- The normal load case, with water pressure corresponding to a water level of +22.5 m (Figure 6.3) and ice loads both parallel to the upstream surface and perpendicular to it. The water level corresponds to the mean water level, which is kept almost constant by use of a second dam, a few hundred metres upstream of the investigated dam. From the upstream edge to the downstream edge of the column, a linear reduction in the pressure is assumed leading to a triangular distribution of the uplifting water pressure, (see Figure 6.6). Full uplift pressure is assumed despite the fact that a grout curtain is used.
- The exceptional load case, with a water pressure corresponding to a water level of +23.80 m (Figure 6.3). In the exceptional load case there is no ice load. The water level used in this load case corresponds to an overflow of the dam.

The design requirements are summarised below. Different requirements are applied depending on the load case and the material in the foundations. Besides the two load cases used in the design of the dam, limits for an accidental load case are also given in RIDAS (2000) and these limits are reproduced below, although no calculations were performed for this load case.

Stability is verified by moment equilibrium around the downstream end of the column. For this stability check Eq. 6.2 is used, the ratio of the resisting moment (M_R) and the overturning moment (M_s) should be greater than the values given in Table 6.3.

$$M_R / M_S \geq s_{over} \qquad \text{Eq. 6.2}$$

Here s_{over} is the prescribed safety factor for overturning for the different load cases

Table 6.3 Ratio of resisting moment and overturning moment (RIDAS, 2000).

s_{over}	Load case		
	Normal	Exceptional	Accident
M_R/M_S	>1.5	>1.35	>1.1

The second design requirement is that the dam should slide. This is verified using the ratio between the resulting horizontal force (H) acting on the structure, and the vertical force (V). It is required that:

$$H / V \leq \mu_{till} \qquad \text{Eq. 6.3}$$

where μ_{till} is the allowable friction coefficient.

Table 6.4 reproduces the design values of μ_{till} according to RIDAS (2000).

Table 6.4 μ_{till} according to RIDAS (2000).

Foundation	Load case			tan δ_g
	Normal	Exceptional	Accident	
Rock	0.75	0.90	0.95	1.0
Moraine	0.50	0.55	0.60	0.75
Coarse silt	0.40	0.45	0.50	0.60

μ_{till} is related to the angle of friction for the ground material (δ_g) according to Eq. 6.4.

$$\mu_{till} = \frac{\tan \delta_g}{s_g} \qquad \text{Eq. 6.4}$$

The partial factor (s_g) is given in Table 6.5

Table 6.5 Partial factor s_g for calculation of μ_{till} (RIDAS 2000).

Foundation	Load case		
	Normal	Exceptional	Accident
Rock	1.35	1.10	1.05
Moraine	1.50	1.35	1.25
Coarse silt	1.50	1.35	1.25

Inserting values of $tan\ \delta_g$ from Table 6.4 and partial factors from Table 6.5 into Eq. 6.4 gives the permissible friction coefficients presented in Table 6.4.

Together with the requirement of no sliding, there is also a requirement stating that the resultant of all forces acting on the dam should fall in the middle third of the base area, both parallel to the column and perpendicular to it, for the normal load case. For the exceptional load case the resultant must fall within in the middle three fifths of the base area of the structure.

Besides the stability requirements stated above, it is also required that the strength of the concrete and the ground be greater than the stresses calculated using Navier's formula. (See Appendix A for details of this calculation.)

6.3.2 Reliability requirements

The concept of safety classes and partial factors is not used for the design of dams in Sweden. But since reference is made to BBK 94 Band 1 (1995) it would be logical to relate the safety system to BKR (2000). In BKR the target safety index is related to the safety class of the structure (see Section 4.3). The highest safety class, 3, is used when: the design and use of the buildings are such that many people are often present in or in the vicinity of the building, the element or structure is of such a nature that collapse would involve a high risk of personal injury, or when the element or structure has properties such that failure would cause immediate collapse.

The location of a dam has considerable influence on its classification, but since large economical values are at stake, both for the dam owner and for others downstream of the dam, the dam studied here is assumed to belong to safety class 3. The target safety index (β_{target}) for the ultimate limit state corresponding to safety class 3 is 4.8 (see BKR, 2000). RIDAS (2000) uses a system of consequence classes not correlated to the safety classes used in BKR (2000).

6.4 Critical failure modes

In order to establish the critical failure modes, a deterministic parameter study is usually performed. In this study the inclined rock surface as shown in Figure 6.5 was assumed. Since ice load was assumed to be the governing load, this parameter was varied.

In a recent study, Ekström (2002) pointed out that very high ice loads have been measured in Canada for spillway pillars. (A spillway pillar is used to keep the water at a specified level.) These ice loads were close to twice the force of 200 kN/m, which was used when designing

the present dam. In order to investigate the sensitivity of the dam's safety to high ice loads, the ice load was varied from 0 to 400 kN/m in the deterministic analysis.

6.4.1 Uplift pressure

In the first analysis a linear theoretical pressure distribution is assumed and due to the geometry of the underside of the bottom slab, the uplift pressure is divided into three sections (Figure 6.7), and the uplift force and overturning moment will be calculated for each part separately. According to Reinius (1968), this assumption is valid for dams where the concrete is impermeable compared with the underground, which can be assumed for this dam. Reinius also points out that it is praxis in Sweden to assume that the uplift pressure varies linearly from the upstream pressure to the downstream pressure.

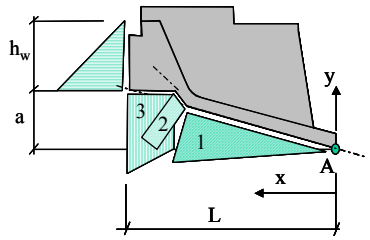

Figure 6.7 Schematic sketch of uplift pressure divided into three parts, labelled 1,2,3.

In order to calculate the forces related to the uplift pressure, expressions must be defined for the pressure variation along each segment of the bottom slab. It is assumed that the pressure varies linearly with the horizontal distance x, and with y, as defined in Figure 6.7.

$$p_{uplift}(x) = h_p(x)\rho_w \frac{x}{L} \qquad \text{Eq. 6.5}$$

h_p is the depth variation as a function of x, according to Eq. 6.6, and ρ_w is the water density, (expressed as unit force/volume).

$$h_p(x) = h_w + a - y \qquad \text{Eq. 6.6}$$

h_w is the water depth, and a is defined in Figure 6.7.

The next important expression is that for the variation of the bottom slab breadth (B) along the column, for $0 < x < 18.23$ m:

$$B(x) = 5.4 + \frac{11.2 - 5{,}4}{18.23} x \qquad \text{Eq. 6.7}$$

For $18.23 < x < 20.43$ the following expression applies

$$B(x) = 11.2\left(1 - \frac{x - 18.23}{2.2}\right) \qquad \text{Eq. 6.8}$$

Table 6.6 Rock inclination along the length of the column.

Section	x [m]	$\theta(x)$	y [m]
1	0< x < 16.43	11°	x tan 11
2	16.43 < x < 17.23	45°	16.43 tan 11+(x-16.43)tan 45
3	17.23 < x < 20.43	0°	16.43 tan 11+(17.23-16.43)tan 45

The overturning moment due to the uplift pressure is the sum of the vertical uplift ($\overline{M}_{w,v}$) and the horizontal uplift ($\overline{M}_{w,h}$) that are calculated from:

$$\overline{M}_{w,v} = \int_0^L x p_{uplift}(x) B(x) dx \qquad \text{Eq. 6.9}$$

and

$$\overline{M}_{w,h} = \int_0^L y(x) p_{uplift}(x) B(x) \tan\theta(x) dx \qquad \text{Eq. 6.10}$$

where $y(x)$ is the vertical position of the slab and $\theta(x)$ is the slab inclination, see Table 6.6. The total overturning moment ($\overline{M}_w$) resulting from the uplift pressure is:

$$\overline{M}_w = \overline{M}_{w,v} + \overline{M}_{w,h} \qquad \text{Eq. 6.11}$$

The resulting uplift force ($\overline{V}_w$) due to water pressure is given by:

$$\overline{V}_w = \int_0^L p_{uplift}(x) B(x) dx \qquad \text{Eq. 6.12}$$

The resulting horizontal force ($\overline{H}_w$) due to the uplift pressure is calculated in the same manner.

$$\overline{H}_w = \int_0^L p_{uplift}(x) B(x) \tan\theta(x) dx \qquad \text{Eq. 6.13}$$

In the limit state equations used below, the moment and resulting forces are normalised to the water density and the water depth upstream of the dam. This is done since the water depth is a random variable that is used in the limit state equations. (See Table 6.7 for new normalised variables and units.)

The results of calculations based on the above expressions are given in Table 6.8. These results were used as input in the deterministic analysis described in the next section.

Table 6.7 Normalised moment and resulting forces.

Variable	Normalised variable	Unit
$\overline{M}_w$	$M_w = \overline{M}_w / (\rho_w \cdot h_w)$	m^3
$\overline{V}_w$	$V_w = \overline{V}_w / (\rho_w \cdot h_w)$	m^2
$\overline{H}_w$	$H_w = \overline{H}_w / (\rho_w \cdot h_w)$	m^2

Table 6.8 Normalised results obtained using the theoretical pressure.

Variable	Normal load case h_w=5,5 m	Exceptional load case h_w=6,8 m
M_w	1391.5	1352.9
V_w	103.9	100.2
H_w	20.4	19.7

The methodology described above will also be used for the evaluation of the measured uplift pressure, which is described below.

6.4.2 Parameter study for normal load case and as-built geometry

The deterministic analysis was performed for two different load cases as defined above. The inclined rock surface shown in Figure 6.5 was used in the calculations. Results from the normal and exceptional load cases are presented in Table 6.9 and stresses in the concrete were evaluated according to Eq. A.2. In this study, the ice load is varied from the value of 200 kN/m required by RIDAS (2000) to 400 kN/m. 400 kN/m is used since it was shown by Ekström (2002) that ice loads of this magnitude may be possible.

The results in Table 6.9 regarding the normal load case indicate that sliding is the failure mode that is most sensitive to the increased ice load, while the overturning capacity is less sensitive to the change in ice load.

The position of the resultant becomes more favourable as the ice load is increased. This is related to the fact that the column is very heavy on the upstream side due to its broad, solid concrete wall, as can be seen in Figure 6.3 and Figure 6.5.

The utilisation of the concrete tension is very high as shown in Table 6.9. This would normally be a problem. However, for this dam, with the heavy upstream side, the highest tension stress occurs at the downstream edge of the column and at this downstream edge the water pressure is low and will not lead to crack propagation in the concrete.

Table 6.9 Results of the deterministic analysis with as-built assumptions regarding water depth and inclination of the rock surface.

Load case	Normal load case				Exceptional load case	
Failure mode	No ice load	200 kN/m	400 kN/m	Req.	No ice load	Req.
Overturning	3.24	2.59	2.16	≥1.5	2.35	≥1.35
Sliding	0.24	0.38	0.55	≤0.75	0.42	≤0.90
Position of resultant (x)	0.71	0.63	0.56	$0.33 \leq x \leq 0.67$	0.65	$0.20 \leq x \leq 0.80$
Concrete comp. [MPa]	1.84	1.19	0.55	≤ 11.9	1.2	≤ 21.5
Concrete tens. [MPa]	1.60	0.95	0.31	≤ 1.0	0.99	≤ 1.8

6.5 Time-invariant reliability analysis

Based on the deterministic analysis, limit state equations can be written for the different failure criteria that are used. The limit state equations of importance are overturning and sliding. No reliability analysis was performed regarding the stresses in the concrete or in the rock mass since the deterministic analysis showed that they were not critical. The position of the resultant is considered a serviceability limit state, even if a failure of this limit state can lead to higher uplift forces under the column. This could be the case if a crack were to propagate from the upstream edge of the column towards the downstream edge, but the column is heavy on the upstream edge, making this scenario less relevant in this case.

Due to the geometry of the dam, i.e. a long column with relatively low height, overturning is not expected to be decisive, as also indicated in the deterministic analysis. Sliding is expected to be critical and this is also the limit state with the most uncertain material parameters, i.e. the friction angle of the rock mass and the friction at the interface between the concrete and the rock.

Reliability analysis was performed on the basis of the principles given in NKB 55 (1987), and in the following section the limit state equations are derived. This section is then followed by sections in which the individual random variables are investigated and dealt with in detail.

6.5.1 Limit state equations

Based on the symbols in Figure 6.8 expressions can be derived for the resistance moment, the overturning moment, the sum of the vertical forces and the sum of the horizontal forces.

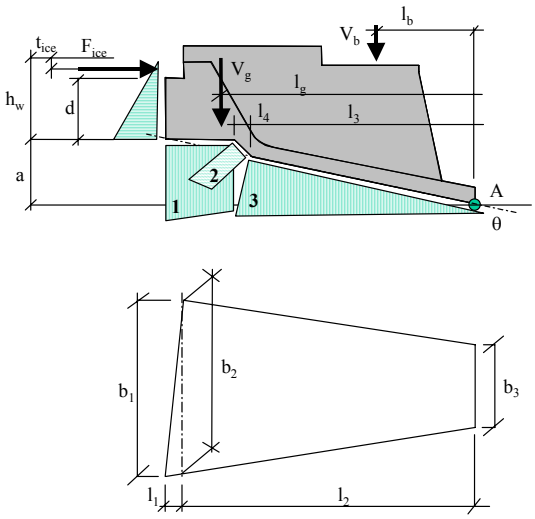

Figure 6.8 Explanation of symbols used in the limit state equations.

The resisting moment (M_R) is related to the dead weight of the column and the bridge and a small amount of water on top of the upstream edge of the column:

$$M_R = \rho_c \left(V_g l_g + V_b l_b\right) + \rho_w \left(h_w - d\right) \frac{l_1}{2} \left(\frac{b_1 + b_2}{2}\right) \left(\frac{l_1}{3} + l_2\right) \qquad \text{Eq. 6.14}$$

where ρ_c is the concrete density, V_g is the concrete volume, l_g is the lever arm from the rotation point A in Figure 6.8 to the centre of gravity of the concrete, V_b is the concrete volume of the bridge supported on the column, l_b is the lever arm from the rotation point A in Figure 6.8 to the centre of gravity of the bridge, and d, l_1, l_2, b_1, and b_2 are geometric parameters indicated in Figure 6.8.

The overturning moment (M_S) is related to the ice load, the horizontal water pressure and the uplift pressure underneath the column.

$$M_S = F_{ice} b_2 \left(a + h_w - t_{ice}\right) + \rho_w h_w \left(h_w \frac{b_2}{2} \left(a + \frac{h_w}{3}\right) + C M_w\right) \qquad \text{Eq. 6.15}$$

where F_{ice} is the ice load, a is a distance shown in Figure 6.8, t_{ice} is the ice thickness, C is the uncertainty related to the uplift pressure, and M_w is the overturning moment due to the uplift pressure normalised to the upstream water pressure (see Table 6.7).

The resulting vertical force is a combination of dead weight, vertical water weight and resulting vertical uplift pressure.

$$V = \rho_c \left(V_g + V_b\right) + \rho_w \left(h_w - d\right) \frac{l_1}{2} \left(\frac{b_1 + b_2}{2} \right) - \rho_w h_w C V_w \qquad \text{Eq. 6.16}$$

where V_w is the resulting uplift force from the water pressure normalised against the upstream water pressure, see Table 6.7.

The resulting horizontal force acting on the column is a combination of ice load and the horizontal water pressure, and is calculated from:

$$H = b_2 \left[F_{ice} + \rho_w \frac{h_w^2}{2} \right] + h_w \rho_w C H_w \qquad \text{Eq. 6.17}$$

where H_w is the horizontal force resulting from the uplift pressure normalised to the upstream water pressure (see Table 6.7).

Eq. 6.14 and Eq. 6.15 are combined into Eq. 6.18, to give the limit state function for overturning of the column.

$$M_R - M_s \geq 0 \qquad \text{Eq. 6.18}$$

Eq. 6.16 and Eq. 6.17 can be combined to give the limit state for sliding (Eq. 6.19) after transformation of the resulting forces along the inclined rock surface, where φ is the angle of the inclined rock surface (see Figure 6.8). This angle is assumed to be the mean angle of the inclined surface, and the notch at the middle of the column is neglected.

$$\tan \delta_g - \frac{V \sin \varphi + H \cos \varphi}{V \cos \varphi - H \sin \varphi} \geq 0 \qquad \text{Eq. 6.19}$$

6.5.2 Model uncertainty

Model uncertainty is a parameter used to take into consideration how well a theoretical model describes reality, see Section 4.6. For the current dam, rigid body motions are used to verify the stability, this is basic physics and for such a model it is reasonable to disregard the existence of any model uncertainty.

There is however an uncertainty associated with the uplift pressure, and this could also be treated as a model uncertainty in the load model. No information is available about this uncertainty and it was here assumed to be 15%. This is a rather high value, but in order to understand the behaviour of the dam with respect to this value a parameter study was performed on this uncertainty.

There are many factors that come into play when trying to evaluate the extent of this uncertainty. It has previous been assumed (see Section 6.4.1) that the uplift pressure varies linearly along the length of the surface exposed to the uplift water pressure. It is likely that there will be a deviation between the theoretical distribution and the assumed one. Reinius

(1946) claims that this deviation is insignificant, but nevertheless, in the present case the error arising from this assumption is regarded being a part of the load uncertainty (*C*), used in the limit state equations.

Reasons for the deviation may be cracks in the underlying rock mass, variation in the porosity of the rock mass etc. All these factors are very difficult to estimate, and when using results from monitoring a measuring error will also be included in this uncertainty. The measuring error resulting from the equipment can be evaluated, but this is likely to be small compared with other uncertainties. It is possible that one of the measuring points may be located in a crack in the rock mass, giving misleading pressure observation.

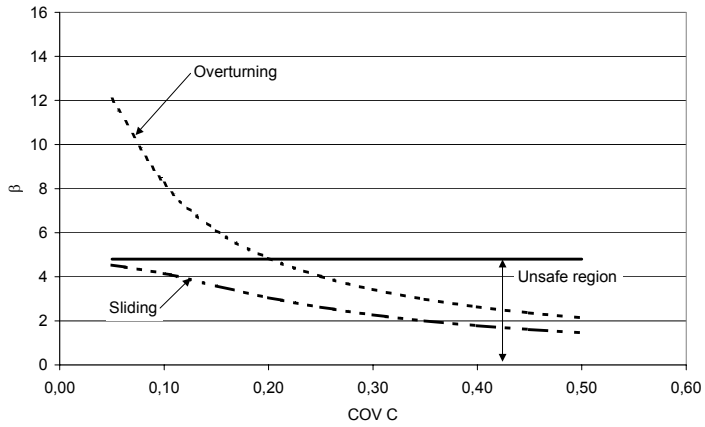

Figure 6.9 Normal load case, safety index as a function of the coefficient of variation for uplift pressure uncertainty with input according to Table 6.13.

Figure 6.9 show the safety index for overturning and sliding as a function of the coefficient of variation for the model uncertainty of uplift pressure distribution. It is clear that this uncertainty has a significant influence on the safety of the structure. For low uncertainties in the load due to the uplift pressure, overturning safety is sufficient, but if the uncertainty exceeds approximately 20% the safety index falls under the target safety index. With regard to sliding, the safety requirement is not fulfilled for any of the assumed uncertainties. The same investigation was carried out for the exceptional load case, see Figure 6.10.

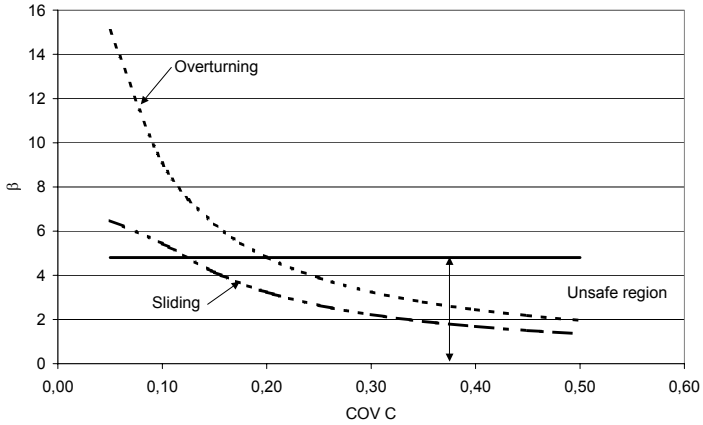

Figure 6.10 Exceptional load case, safety index as a function of the coefficient of variation for uplift pressure model with input according to Table 6.14.

In Figure 6.10 it can be seen that the exceptional load case behaves in the same manner as the normal load case with respect to uncertainties in the uplift pressure model, except that the safety is sufficient for sliding at small values of the coefficient of variation of *C*.

A limitation on the load uncertainty could be introduced based on physical arguments. There are upper limits for the moments and forces, which are related to the uplift pressure, since the worst possible scenario that can occur is if the uplift pressure is equally high both at the upstream and downstream edges of the dam. The physical limitations on the uplift pressure could be used to truncate the distribution function of *C*. No limitation was however applied since the base assumption with a 15 % coefficient of variation gives very small probabilities of *C* exceeding 2.0.

6.5.3 Water level

The water level of +22.5 m, (as seen in Figure 6.3), is kept as constant as possible in order to achieve a high energy output from the dam according to information from the dam owner. Based on this information the level is regarded as a mean value of the random variable (h_w) used to describe the water depth. +22.5 m corresponds to a water depth of 5.5 m, and the variable is truncated at 6.8 m, which is used as an upper limit of the water depth. The dam crest is located at this level and the water cannot be higher. In a situation where water overflows the dam crest, a certain water depth will arise on the dam crest. This situation was not taken into consideration in the following analysis. Neither was the possibility of an increase in water depth on the downstream side. This situation was deemed unlikely due to the steep bank at the downstream side of the dam.

At +22.5 m a variation of ± 1 cm may be expected under normal conditions. This very low value arises from the fact that a second dam is located a few hundred metres upstream of the

one under investigation. A higher variation, corresponding to a 10% coefficient of variation was used for the reliability analysis, which is described below.

Table 6.10 present values of the safety index for overturning and sliding for the cases when the water level was limited and unlimited, for coefficients of variation in the water depth of 1 and 10%.

Table 6.10 Values of the safety index for different assumptions regarding upstream water depth and the coefficient of variation of the water depth.

	Overturning		Sliding	
COV h_w	*Limited* h_w	*Unlimited* h_w	*Limited* h_w	*Unlimited* h_w
1%	6.9	6.9	4.3	4.3
10%	6.0	5.8	3.6	3.5

The results in Table 6.10 show that the safety of the dam is more sensitive to the coefficient of variation of the upstream water depth than the limitation of the water depth. A simple way of increasing the safety index would be to analyse data available for the upstream water depth and determine the actual coefficient of variation.

6.5.4 Ice load

According to RIDAS (2000) the recommended ice load is 200 kN/m, but this is not based on any available background information. Since compliance is claimed with BBK 94 Band 1 (1995), and since BKR (2000) is the governing document behind BBK 94 Band 1 the ice load is regarded as a natural load, and the value given in RIDAS is interpreted as a characteristic value.

In the safety system behind BKR, natural loads such as wind and snow are assumed to have normally distributed annual maximum values. A common value for their coefficient of variation is 40% and was the value used for the ice load in this case study. The ice load given in RIDAS is therefore assumed to be the 98 percentile of a normally distributed load. The relation between the characteristic value x, and the mean value μ is given by

$$x = \mu + \sigma k = \mu(1 + COV_{ice} \cdot k) \qquad \text{Eq. 6.20}$$

where σ is the standard deviation, COV_{ice} is the coefficient of variation and k is determined by the value of the 98th percentile of a normal distribution. k is defined as $\Phi^{-1}(0.98) = 2.05$.

Another interpretation is to assume that the value given, 200 kN/m is a mean value and estimate the coefficient of variation, see Table 6.11. In Table 6.11 the result of two different assumptions are showed. The *Characteristic assumption* assumes that the 200 kN/m ice load is a characteristic value, and the *Mean value assumption* assuming that the 200 kN/m ice load is a mean value.

Table 6.11 Mean value and standard deviation of the ice load for different assumptions and coefficients of variation.

COV_{ice}	Characteristic assumption		Mean value assumption	
	μ_{ice} [kN/m]	σ_{ice} [kN/m]	μ_{ice} [kN/m]	σ_{ice} [kN/m]
10%	166	16.6	200	20
20%	142	28.4	200	40
30%	124	37.2	200	60
40%	110	44.0	200	80
50%	99	49.4	200	100

The difference between the two assumptions is shown in Figure 6.11 for a 40% coefficient of variation. It can be seen in Figure 6.11 that the ice load based on these assumptions has values below zero, this is of course totally unrealistic and a truncation should be applied. This was however not done since the influence of truncation is negligible in the upper tail, which is the interesting part.

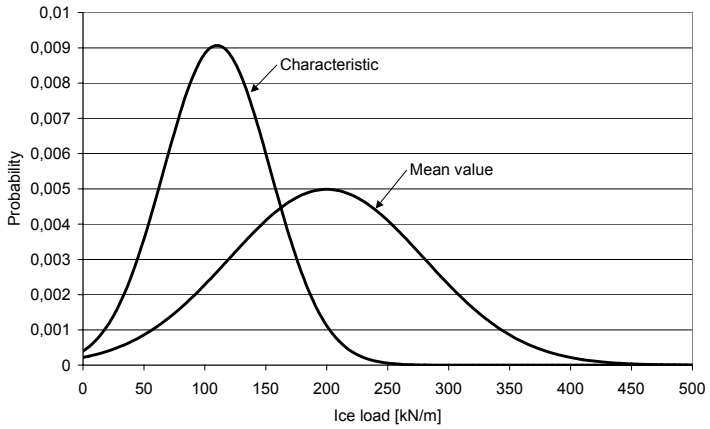

Figure 6.11 Density functions for ice load based on 40 % coefficient of variation and different assumption regarding the value given in RIDAS (2000).

Assuming that the characteristic value is constant, will cause the mean value to decrease with increasing COV_{ice}. This may lead to unexpected results in the reliability analysis since an increase in the COV_{ice} is expected to give a reduced safety index, see Figure 6.12. Both assumptions will be used in a parameter study.

From a historical perspective the value chosen on the ice load seems low. In a governmental report (Statens offentliga utredningar 1938:37, 1946) a design value of 300 kN/m was

suggested for an ice thickness of 1.0 m and 200 kN/m for ice thickness 0.75 m. In a later study (Statens offentliga utredningar 1961:12, 1961) values between 100 kN/m and 200 kN/m were suggested for structures over a certain length, and for extreme cases values of 300 kN/m or 400 kN/m were suggested.

A reduction in the ice load can, however, be expected if it is acting on the gates between the columns. These can be designed to fail before the prescribed ice load is reached. In order to protect these gates measures are taken to prevent ice growth in front of dams, the water can for example be kept in motion. These measures are, however, not 100% reliable and for the present dam with a full concrete upstream edge, a realistic value of the ice load must be used when verifying the stability.

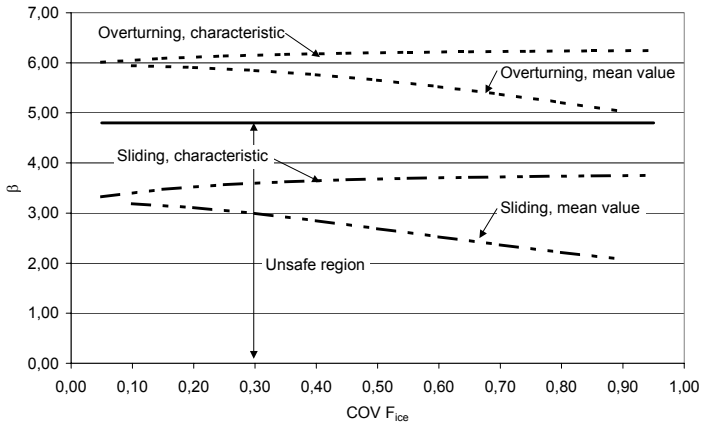

Figure 6.12 Normal load case; safety index as a function of coefficient of variation for the ice load. The solid line shows the required target safety index of 4.8.

Figure 6.12 shows that the structure not sensitive to the variability related to the ice load if the characteristic value is kept constant. The safety index is fairly constant even when high coefficients of variation are applied to the ice load, but the values of the safety indices are too low. Sliding falls below the required target safety index of 4.8.

In the case of a constant mean value and increasing standard deviation the structure is more sensitive to increased coefficients of variation. This exercise emphasises the importance of reliable background data for codes.

6.5.5 Friction coefficient

In Table 6.4 it can be seen that the friction coefficient (tan δ_g) is 1,0 for rock foundations according to RIDAS (2000). If RIDAS complies with BKR (2000), this friction coefficient corresponds to the 5 percentile. Assuming that this resistance variable is lognormally distributed the relation between the characteristic value ($tan\ \delta_g$) and the mean value ($\mu_{tan\delta}$) is given by:

$$\tan\delta_g = \mu_{\tan\delta} e^{-k \cdot COV_{\tan\delta}} \qquad \text{Eq. 6.21}$$

where $COV_{tan\delta}$ is the coefficient of variation of $tan\delta_g$, and k is given by $\Phi^{-1}(0.95)=1.65$.

Another assumption is also made, namely that the values given in RIDAS (2000) correspond to the mean value of the friction coefficient. Table 6.12 gives the mean values and standard deviation for the rock mass for different values of coefficient of variations under the assumptions described above. For the base case a 10% coefficient of variation was assumed. The mean value is then 1.18 and the standard deviation 0.12. The 10% coefficient of variation must be considered to be low since it is of the same order as the coefficient of variation for the compressive strength of concrete, and concrete is a manufactured material that is likely to be more homogeneous than rock.

Table 6.12 Characteristic values, mean values and standard deviations for the friction coefficient for different coefficients of variation under different assumptions.

	Characteristic assumption			*Mean value assumption*		
$COV_{tan\delta}$	*Char.*	$\mu_{tan\delta}$	$\sigma_{tan\delta}$	*Char.*	$\mu_{tan\delta}$	$\sigma_{tan\delta}$
5%	1.0	1.09	0.05	0.92	1.00	0.05
10%	1.0	1.18	0.12	0.85	1.00	0.10
15%	1.0	1.28	0.19	0.78	1.00	0.15
20%	1.0	1.39	0.28	0.72	1.00	0.20
25%	1.0	1.51	0.38	0.66	1.00	0.25
30%	1.0	1.64	0.49	0.61	1.00	0.30
40%	1.0	1.93	0.77	0.56	1.00	0.40
50%	1.0	2.28	1.14	0.52	1.00	0.50

In Handboken Bygg (1984) a short description is given of the evaluation of rock strength. Properties of natural materials are often uncertain and the friction coefficient of the rock is affected by the rock type and the plane of the cracks in the rock underlying the investigated structure. Handboken Bygg states that the properties of a rock mass are determined using empirical classifications. In one of these classification systems it is indicated that the best rock mass class can have a friction angle above 45°. In RIDAS (2000) a friction angel of 45° is used as the characteristic value for the rock mass, if full compliance can be assumed with BKR (2000). This means that properties corresponding to the best rock mass are assumed to be valid for all dams. This assumption should be investigated further, but is outside the scope of this thesis.

The sensitivity of the dam safety index for sliding to the statistical assumptions made for the rock friction given in Table 6.12 is demonstrated in Figure 6.13. The safety index is generally significantly lower than the required target safety index of 4.8; this is also the case for non-conservative assumptions.

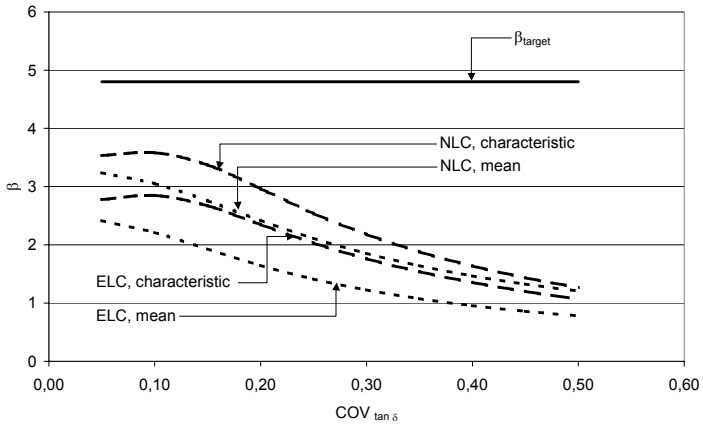

Figure 6.13 Safety index for sliding as a function of the coefficient of variation for the friction coefficient.

Assuming that value given in RIDAS (2000) is a characteristic value gives a higher safety index than using the value as a mean value; both for the normal load case (*NLC*) and the exceptional load case (*ELC*).

6.5.6 Summary of random variables

In Table 6.13 basic variables, their distribution, mean value and standard deviation for the normal load case of the dam are given. The values given below constitute the base case, and a parameter study will be described using different coefficients of variation of the same parameters.

Table 6.13 Basic variables for the normal load case interpreted from RIDAS (2000). Dimensions are defined in Figure 6.8.

Variable	Unit	Symbol	Distribution	Mean value	SD	COV [%]
Concrete density	kN/m^3	ρ_c	Lognormal	23	0.92	4[1]
Water density	KN/m^3	ρ_w	Deterministic	10	-	-
Concrete volume of dam	m^3	V_g	Deterministic	795.05	-	-
Volume of bridge	m^3	V_b	Deterministic	22.26	-	-
Lever arm for concrete	m	l_g	Deterministic	13.28	-	-
Lever arm for bridge	m	V_b	Deterministic	6.51	-	-
Width of dam upstream	m	b_1	Deterministic	11.55	-	-

[1] COV taken from JCSS (2002).

Variable	Unit	Symbol	Distribution	Mean value	SD	COV [%]
toe						
Width of dam at crest	m	b_2	Deterministic	11.20	-	-
Width of dam at downstream edge	m	b_3	Deterministic	5.4	-	-
Length of toe	m	l_1	Deterministic	2.2	-	-
Length of column	m	l_2	Deterministic	18.22	-	-
Geometric variable, see Figure 6.8	m	a	Deterministic	3.3	-	-
Height of toe	m	d	Deterministic	4.8	-	-
Water level	m	h_w	Normal (truncated)	5.5	0.55	10
Ice load	kN/m	F_{ice}	Normal	110	44	40
Ice thickness	m	t_{ice}	Deterministic	0.33	0.03	10
Friction angle of rock mass		$tan\delta_g$	Lognormal	1.18	0.12	10
Rock inclination angle	°	φ	Normal	11°	1.1°	10
Model uncertainty for uplift pressure		C	Lognormal	1	0.15	15

The ice thickness t_{ice}, given in RIDAS (2000) as 1/3 of the total ice thickness, and the ice thickness corresponding to an ice load of 200 kN/m is given as 1 m.

For the exceptional load case the situation is quite different. It is assumed that there is no ice load and the water level is constant at the crest of the dam; i.e. the variability of the loads applied to the dam is reduced significantly.

Table 6.14 Basic variables for exceptional load case according to RIDAS (2000). Parameters omitted have the same values as in Table 6.13.

Variable	Unit	Symbol	Distribution	Mean val.	SD	COV
Water level	m	h_w	Deterministic	6.8	-	-
Ice load	kN/m	F_{ice}	Deterministic	-	-	-
Ice thickness	m	t_{ice}	Deterministic	-	-	-

6.5.7 Results for the normal load case

As well as the studying the safety index, the sensitivity of the limit state to the basic variables can also be investigated, see Section 5.2.6. In the present analysis, the parameters given in Table 6.13 were used. Parameters used to describe the resistance have a positive α value and load variables have a negative value, i.e. it is possible to rank both resistance and load variables, as well as to see which parameters have the greatest influence on the safety of the structure. α values indicate how important the change in the mean value of the variable is for the safety, and values of α^2 indicate how important the standard deviation of the variable

is for the safety. Figure 6.14 shows how this sensitivity analysis is often presented, but henceforth this information will be presented in tables.

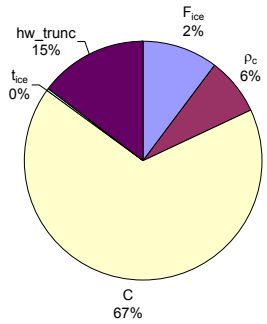

Figure 6.14 Representative values of α^2 for overturning limit state with input according to Table 6.13.

Table 6.15 Sensitivity values for overturning in the normal load case with input according to Table 6.13.

Stochastic variable	α	α^2
Ice load (F_{ice})	-0.322	0.103
Concrete density (ρ_c)	0.278	0.077
Uplift pressure uncertainty (C)	-0.819	0.671
Ice thickness (t_{ice})	0.004	0.000
Water depth (h_w)	-0.386	0.149
	$\Sigma\alpha^2$	1.000

Table 6.15 indicates which random variables are of the greatest importance for the reliability. It can be seen that the model uncertainty for the uplift pressure (C) is the most important variable for overturning and that the variation of the other variables investigated; i.e. the ice load (F_{ice}) is of little importance. In order to improve the reliability of the dam the uncertainties regarding the uplift pressure should be reduced, and monitoring of this pressure provides the means of achieving this. The same analysis was performed for sliding and the results are presented in Table 6.16.

As can be seen in Table 6.15 and Table 6.16, the representative value of a load variable has a negative value, and the uplift pressure uncertainty dominates both for sliding and overturning. For sliding, ice load and water depth are almost as important. In the case of unsatisfactory safety, this information can be used to decide which variable to investigated further. In this situation, the costs of investigating the different variables can be taken into consideration when deciding which one to investigate. In the current case, the water is already monitored and this data should be evaluated in a manner suited for reliability analysis and results used in a new calculation of the safety index. It is also obvious that the

ice thickness could have been assumed to be a deterministic variable since its influence on the safety index is very small.

Table 6.16 Sensitivity values for sliding in the normal load case with input according to Table 6.13.

Stochastic variable	α	α^2
Ice load (F_{ice})	-0.547	0.299
Concrete density (ρ_c)	0.251	0.063
Uplift pressure uncertainty (C)	-0.514	0.264
Ice thickness (t_{ice})	0.000	0.000
Water depth (h_w)	-0.444	0.197
Friction coefficient ($tan\ \delta_g$)	0.394	0.155
Rock inclination (θ)	-0.149	0.022
	$\Sigma\alpha^2$	1.000

6.5.8 Results for the exceptional load case

In Table 6.17 sensitivities are given for assumptions regarding the random variables given in Table 6.14, and it can be seen that the uncertainty for the uplift pressure governs the reliability with respect to overturning, while the friction coefficient and the slope of the rock surface governs the reliability with regard to sliding. These variables are also of significance in the normal load case, as was seen in Table 6.15 and Table 6.16.

Table 6.17 Sensitivity values exceptional load case with input according to Table 6.14.

	Overturning		*Sliding*	
Basic variable	α	α^2	α	α^2
Concrete density (ρ_c)	0.270	0.073	0.298	0.089
Uplift pressure uncertainty (C)	-0.963	0.927	-0.894	0.799
Friction coefficient ($tan\ \delta_g$)	-	-	0.313	0.098
Rock inclination (θ)	-	-	-0.119	0.014
	$\Sigma\alpha^2$	1.000	$\Sigma\alpha^2$	1.000

6.5.9 Summary of time-invariant reliability analysis

In the table below the safety indices are summarised for the basic variables given in Table 6.13 and Table 6.14. For both load cases there is sufficient safety with regard to overturning but not for sliding, comparing with the target safety index of 4.8 as stated in BKR (2000).

Table 6.18 Summary of safety indices.

Load case	Overturning	Sliding
Normal	5.6	2.6
Exceptional	6.2	3.8

There may be several reasons for the results shown above. Assumptions made concerning the uncertainties in the basic variables may be too much on the safe side. This problem can be addressed by further research providing more knowledge on the most important parameters. It has been shown that the uncertainty in the uplift pressure model is very important for both overturning and sliding. Based on the results of this study it was decided that monitoring of the uplift pressure should take place. This new information can be used to reduce the uncertainty with higher safety as a consequence.

With respect to sliding, the friction coefficient is the most important factor. In RIDAS (2000) this parameter is assumed to be rather high and yet the safety is not sufficient. This is just one single analysis but further work seems necessary in order to establish better values of the friction coefficient and its statistical properties.

New design guidelines are recommended for dam structures, both for the assessment of existing structures and for the design of new ones. By introducing suitable partial safety factors the target safety index can be achieved even if uncertain assumptions are made regarding the basic variables. This is not an economical approach but the safety requirements will be fulfilled.

6.6 Monitoring

The uplift pressure will be monitored using drilled open observation boreholes in the column. Monitoring is planned for the current dam and installation work is in progress. A new feature in this context is that the water level in these holes will be measured using the time domain reflectometry (TDR) method. This method makes possible to continuously monitor the water levels in the holes. Another advantage is that the measurements can be monitored from anywhere, site visits are not necessary.

TDR was developed in parallel with radar technology; the difference being that in TDR the electromagnetic pulse created does not leave the conductor as continuous radiation but as a pulse. The conventional use of TDR is in detecting and localising cable damage. The uplift pressure application is a further development of the method.

A steel wire inserted into the drilled holes, and an electric pulse is sent along the wire. When the water surface is reached, a part of the pulse is reflected since the difference in electric properties between air and water is large. The TDR instrument provides output on an amplitude graph that represents how the pulse is reflected along the sensor. The data are interpreted to give the liquid level.

The strength of the method is that installation in the structure is very simple, and requires no maintenance. Moreover, a single TDR instrument can serve a large number of observation boreholes that are spread geographically over a long distance, see Bernstone

(2000) for more information. Vattenfalls Utveckling AB monitoring via TDR has not yet started and there is no information about the error in the TDR measurements. This will be investigated when monitoring starts.

Since TDR monitoring has not been performed previously it is important that the predictive models be calibrated. To achieve this the maximum value of uplift pressure at each measuring position along with the maximum calculated uplift force and overturning moment should be collected on a daily, weekly, monthly and finally yearly basis. Since the evaluation will be based mainly on linear regressions using the least squares method, the amount of data is important since a large amount of test data reduces the uncertainty in the estimated parameters.

6.7 Incorporation of object-specific information

As yet, no object-specific information has been obtained from the TDR equipment that can be incorporated into the reliability analysis of this dam, but it has been decided that the uplift pressure will be measured at four points along the column. The pressure measured at these points should be incorporated into the analysis of the dam and the reliability will be calculated on a yearly basis in the future.

Figure 6.15 shows the position of the boreholes and the uplift pressure measured using a floating device. The floating device is lowered into the boreholes on a piece of wire, and when it starts to float, the length of the wire is measured. There is a considerable difference between the measured uplift pressure distribution and the theoretical one shown in Figure 6.7. Actual values are given in Table 6.19.

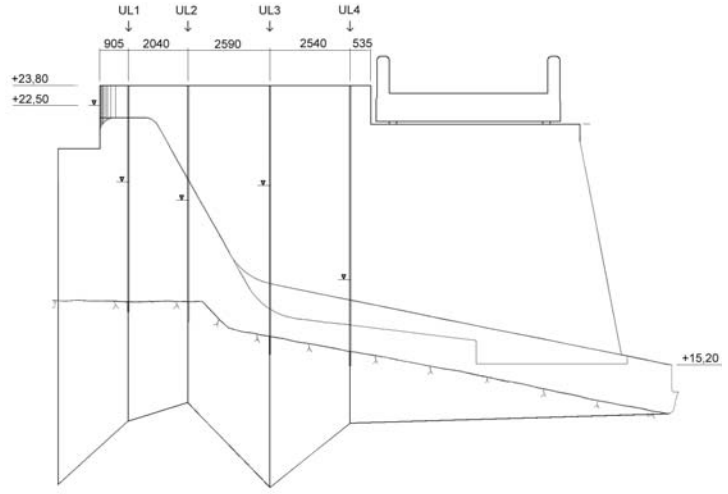

Figure 6.15 Measured uplift pressure in the boreholes drilled in the column.

In Table 6.19 the distance from the upstream edge is given. This has also been recalculated to give the value in the local x coordinate shown in Figure 6.7. The parameter measured, which is the distance from the top surface of the concrete to the water, is presented. The water pressure is calculated as the difference between this distance and the height of the concrete.

Table 6.19 Measurements of uplift pressure.

Distance from upstream edge [m]	x-coordinate [m]	Distance to water from concrete top surface [m]	Concrete height [m]	Water pressure [kPa]
0	-	-	-	55.0
0.905	17.325	3.03	6.8	37.7
2.945	15.285	3.65	6.8	31.5
5.535	12.695	3.17	7.9	47.3
8.075	10.155	6.22	8.4	21.8

It is assumed that the uplift pressure at the upstream edge of the column is equal to the hydrostatic water pressure, i.e. it corresponds to the current water depth multiplied by the density of water. This is not necessarily true, but since this drillhole is just above the grout curtain there is no way of measuring the pressure here. The assumption is on the safe side since this is the highest possible water pressure.

The uplift pressure distribution is assumed to be linear between the measured points. Using these assumptions it is now possible to calculate the overturning moment due to water (M_w) from Eq. 6.11, the resulting uplift force (V_w) from Eq. 6.12, and the resulting horizontal uplift force (H_w) from Eq. 6.13 to and normalise them to the upstream water pressure. The calculations gives M_w = 1070.7 m^2, V_w = 76.5 m and H_w = 14.5 m.

Table 6.20 Comparison of safety indices based on theoretical and measured pressure distribution.

β	Normal load case		Exceptional load case	
	Theoretical	*Measured*	*Theoretical*	*Measured*
Overturning	5.6	7.6	6.2	7.7
Sliding	2.6	5.0	3.8	5.5

The results given in Table 6.20 were calculated using the variables in Table 6.13 for the normal load case and in Table 6.14 for the exceptional load case. No effort was made to reduce the load model uncertainty of 15 %. This means that the values of the safety indices reflect a direct comparison of the different water pressures.

The results in Table 6.20 show that sliding now has a sufficient safety index. It is probable that it is the positive influence of the grout curtain on the uplift pressure distribution shown in Figure 6.15 and the reduction in the water pressure is achieved at the position on the

column where the bottom slab is wide. The uncertainties related to the friction coefficient are, however, still present and should be addressed.

6.8 Time-variant reliability analysis

No time-variant reliability analysis can be performed since the monitoring system is not yet in operation. In the following section a system that can be used for evaluation of time variant reliability analysis will be described.

The objective of the time-variant reliability analysis is to evaluate how the safety of the structure changes over time due to the deterioration of the grout curtain. Sensitivity analysis has shown that the uplift pressure is a dominating load on the structure, and this will be monitored. Results from this monitoring will be used to calculate the current status and will also form the basis of the input in a predictive model of the dam safety.

To achieve compliance with NKB 55 (1987) and NKB 36 (1978) a reference period of one year is to be used for the uplift pressure. This means that the annual maximal value is used for the calculation of the safety index. The annual maximum is also the value that will be used in the time variant leaching model described below.

In the field of robotics, recursive algorithms are often used to control different functions. It is often necessary to combine information about what has happened previously, together with new information of the current situation, in order to make sure that the object you are controlling is guided to a correct position in the future. For this purpose different recursive algorithms have been developed. In Johansson (2002) it can be seen that linear models, where the parameters can be evaluated with least squares regression are preferred.

With this information in mind, existing leaching models were reviewed (see Section 3.2.2) and found not to be suitable for recursive algorithms. Instead a model based on a simple physical relationship was used to create an indirect leaching model. The model is indirect in the sense that is does not take into consideration aspects related to the concrete and concrete chemistry but only the variation in uplift pressure.

6.8.1 The leaching model

The assumptions behind the proposed leaching model are the following.

- As leaching occurs in the grout curtain, the permeability increased progressively with increased leaching.
- The uplift pressure increases with increased permeability
- The uplift pressure at the upstream edge of the dam corresponds to the hydrostatic water pressure and the total uplift is proportional to this value.

Based on these assumptions the following differential equation (Eq. 6.22) can be established, stating that the change in uplift pressure behind the grout curtain (U) is proportional to the uplift pressure.

$$\frac{dU}{dt} \propto U \qquad \text{Eq. 6.22}$$

The proportionality can be expressed by the variable (κ), as in Eq. 6.23.

$$\frac{dU}{dt} = \kappa U \qquad \text{Eq. 6.23}$$

Reformulation and integration gives:

$$\int \frac{dU}{U} = \int \kappa dt \qquad \text{Eq. 6.24}$$

$$\ln U = \ln K + \kappa t \qquad \text{Eq. 6.25}$$

where K is a constant. Eq. 6.25 can be used in a recursive algorithm where the parameters κ and K are updated every time new data are available. Eq. 6.25 can also be written as below:

$$U = Ke^{\kappa t} \qquad \text{Eq. 6.26}$$

The information gained from monitoring the uplift pressure will be used to predict the future safety of the dam. This could be done by calculation of the uplift force and the overturning moment due to the uplift pressure. These two parameters are a combination of the results from the four measuring points. This means that if one of the sensors is giving spurious results this will be difficult to detect from the combined result. It is therefore suggested that the data from each monitoring point be evaluated separately, as well as the combined result in the form of uplift force and overturning moment.

When performing a linear regression using Eq. 6.25 it is also possible to evaluate the variance of the error related to the regression. If the variance is constant over time or decreases over time the assumed model is correct. If the variance increases over time the model should be revised.

From regression using least squares models it is possible to evaluate a mean and standard deviation for each regression variable, in this case κ and K. It is also possible to estimate an error between measured data and the regression model. This estimate gives an error that is normally distributed with zero mean and a standard deviation in for the logarithmic variables. The distribution of the error in the original variables is, however, unknown. According to Draper and Smith (1966) and Blom and Holmquist (1970), can the error not be transformed back to the original space. This indicates that simulation techniques must be used when calculating the future uplift pressure.

6.8.2 The recursive algorithm

The following procedure is recommended for the prediction of the future safety of the dam.

I. Evaluate annual the maximum vertical uplift pressure, since sliding is the most serious failure mode the vertical uplift force can serve as indicator of the maximum value. The corresponding horizontal force and overturning moment should be used in the reliability analysis. The vertical uplift force is used instead of a single pressure

measurement, since the value in one point under the dam is likely to be more uncertain than the resulting load effect from the uplift pressure.

II. As soon as data exist for more than one year, evaluate the parameters of Eq. 6.26 via linear regression.
III. Simulate the uplift pressure for the years of interest, i.e. what is the predicted uplift pressure on the dam at 10-year intervals and at the end of the residual service life of the dam?
IV. Calculate the safety indices for the simulated points in time.

As time progresses, the prediction of the expected uplift pressure will be more and more accurate.

6.9 Summary

A safety assessment of a concrete column in an existing dam has been made using both deterministic analysis and reliability theory. A discrepancy was found, showing that the rock surface under the column was inclined and not horizontal as assumed during the design. This deviation between assumptions during design and reality is probably not unique for this dam. It is suggested that during design of dams, the stability should be recalculated after the rock surface has been prepared. This approach is used on pile groups on bridges; i.e. they are all recalculated after they are hammered down. Discrepancies between theoretical assumptions and real life are then taken into account and measures can be taken if necessary.

Based on a deterministic assessment according to RIDAS (2000) the dam proved to fulfil the safety requirements, both for the assumptions made under the design phase and for the assumptions made for the as built situation.

The results of the reliability analysis show that the dam is safe regarding overturning but that it does not fulfil the safety requirements with regard to sliding. The fact that the dam column does not fulfil the safety requirements with respect to sliding is related to the modelling of the uplift pressure and the friction angle of the underlying rock mass. Further investigations of these parameters are necessary but this is outside the scope of this thesis.

All safety requirements are fulfilled when using the measured uplift pressure distribution. It is impossible to draw any conclusions on prediction of the dam's safety since the monitoring is not yet operation. The pproposed methodology for introducing new data into the reliability analysis is crude but is believed to be sufficient.

During the reliability analysis it was assumed that loads and material parameters in RIDAS (2000) could be evaluated in accordance with BKR (2000). This proved to give questionable results regarding mean values of, for instance, the friction coefficients for the rock material and for the ice load. Further investigations must be carried out to verify their compliance with BKR.

Even if reference is made in RIDAS (2000) to BBK 94 Band 1 (1995) the underlying safety philosophy in BKR (2000) that is the background document to BKK 94 is not fully taken into consideration. It seems that the strength and load values used in RIDAS are not evaluated so as to correspond to characteristic values according to suggestions made in BKR

(2000) and its background document NKB 55 (1987). Combination of the safety philosophies from RIDAS and BKR is not recommended and a probabilistic calibration of RIDAS is suggested.

7 THE RAILWAY BRIDGE

7.1 General considerations

The Swedish National Railroad Administration (SNRA) is the owner of a bridge that was built with cast-in-place concrete in 1955. It is a two span trough bridge with continuous girder designed as a frame, assuming interaction between the girder and the supports. A photograph of the bridge is shown in Figure 7.1 and an elevation is shown in Figure 7.2.

Figure 7.1 Photograph of the investigated bridge.

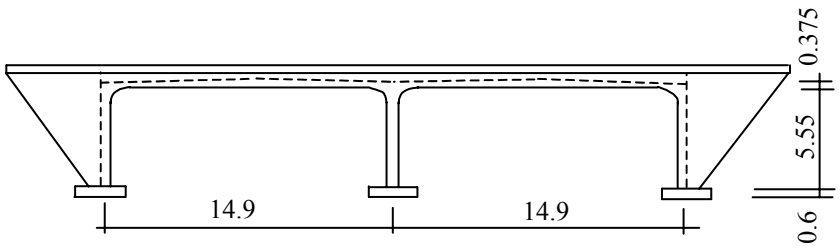

Figure 7.2 Elevation of the bridge (dimensions in m).

In Figure 7.3 the geometry of the trough is shown. Further information on dimensions of the trough can be found in Appendix B.

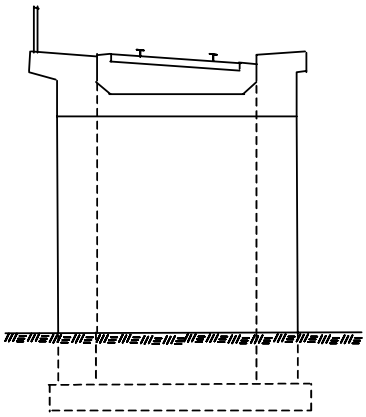

Figure 7.3 Bridge cross section.

7.1.1 Codes

According to the design drawings, the Swedish Concrete Code from 1934 (Statens offentliga utredningar 1934:17, 1934) and 1949 (Statens offentliga utredningar 1949:64, 1951) was used for the original design, together with the Cement Code from 1943 and the Reinforcement Code from 1938. It is also stated that train load type E46 was applied, see Figure 7.4 and Figure 7.5.

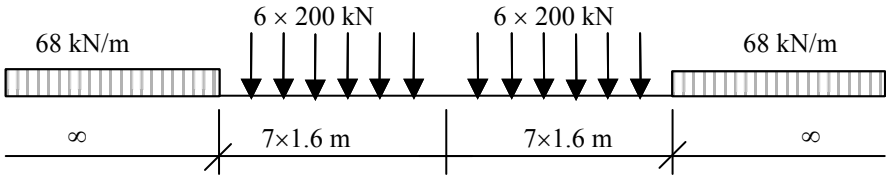

Figure 7.4 Load configuration E46 with two adjacent trains (Kungliga Järnvägsstyrelsen).

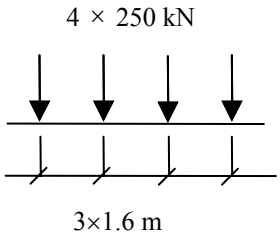

Figure 7.5 Load configuration E46 with a single train (Kungliga Järnvägsstyrelsen).

7.1.2 Materials

The concrete quality is specified as Btg I, Standard K400, group *A* watertight. Two different kinds of reinforcement steel were used: HJS 70 and Ks 60. The nominal strength of the concrete is 400 kp/cm^2 or 40 MPa. The nominal yield strength for the steel is 700 MPa for the HJS 70 and 600 MPa for the Ks 60 reinforcement.

Cores, 100 mm in diameter were taken from the bridge and the concrete properties were tested. The results of these tests are presented in Section 7.5.1. The parameters investigated were the cylinder compressive strength, the splitting tensile strength, and the modulus of elasticity.

The compressive strength was measured according to SS 13 72 30 on test specimens with a diameter of 100 mm and length of 200 mm. These values can be recalculated to correspond to test specimens with a length of 100 mm with Eq. 7.1. This was done since cylinders with a 100 mm diameter and length of 100 mm directly correspond to cube values with side length 150 mm which is the standard test object in Sweden.

$$f_{cc,l=100} = \frac{fcc,l=200}{0,82} \qquad \text{Eq. 7.1}$$

where $f_{cc,l=100}$ and $f_{cc,l=200}$ correspond to the compressive strengths of lengths the cylinders with lengths of 100 mm and 200 mm, respectively.

Splitting tensile strength values according to SS 13 72 13 must be converted into uniaxial tensile strength and calibrated for the discrepancy in size of the test object. Values used for design are based on Ø=150 mm, and for testing Ø=100 mm was used. In Betonghandboken Material (AB Svensk Byggtjänst, 1994) it is stated that the splitting tensile strength is 6-7 % stronger for a cylinder with Ø=100 mm and length 100 mm than for Ø=150 mm and length 300 mm used for design. The uniaxial tensile strength used for load carrying calculations is then calculated from:

$$f_{ct} = 0,8\frac{f_{ct,splitting}}{1,07} \qquad \text{Eq. 7.2}$$

where f_{ct} is the tensile strength of the concrete and $f_{ct,splitting}$ is the tensile splitting strength of 100 mm diameter concrete specimens.

The measured modulus of elasticity does not have any direct correspondence to the modulus of elasticity used in BBK 94 Band 1 (1995) for design purposes and the measured results will not be used in the calculation of the internal forces.

After conversion of the test results into values that can be used as input in capacity expressions in BBK 94 (1995), the results were evaluated, according to Banverket (2000), leading to strength classes as given in Table 7.1. These strength classes can now be used to calculate characteristic and design values. Design values were calculated according to:

$$f_{cd} = \frac{f_{cck}}{\eta\gamma_m\gamma_n} \qquad \text{Eq. 7.3}$$

where f_{cd} is the design value, f_{cck} is the characteristic value, $\eta\gamma_m$ is a factor taking uncertainties in the material strength into account and γ_n is a partial factor related to the safety class of the structure. $\eta\gamma_m$ is set to 1.5 and γ_n to 1.2. η takes into account the difference between the strength of test samples and the strength in the structure, and can, according to BBK 94 Band 1 (1995) be set to 1.2.

During the evaluation of the strength of concrete structure according to BBK 94 Band 1, it is implied that η is assumed to be 1.0. This assumption is based on the recommendations regarding the location of the testing. It is stated that cores should be taken from the position in the structure where the lowest strength can be found, or where the highest utilisation of the strengths is expected. In order to achieve this, it is recommended that cores be taken close to the upper surface of the structure. This requirement was not met during the testing of this bridge due to practical reasons. There was traffic present on the bridge during the testing period and cores were thus taken from the lower parts of the main girders at a convenient height on the substructure for a standing man. It is therefore likely that the evaluated strengths are overestimated.

Table 7.1 Strength classes and design values according to Banverket (2000).

	Tensile strength class	f_{ctd} [MPa]	Compressive strength class	f_{ccd} [MPa]
Superstructure	T3.0	$\frac{3.0}{1.5 \cdot 1.2} = 1.67$	- only two valid results	-
Substructure	T3.5	$\frac{3.5}{1.5 \cdot 1.2} = 1.94$	K80	$\frac{56.5}{1.5 \cdot 1.2} = 31.4$

No compressive strength class could be evaluated for the superstructure due to the requirement in Banverket (2000) and further cores are needed for this evaluation. Banverket (2000) also states that the mean tensile strength should be at least 7 % of the mean compressive strength, i.e. maximisation of the compressive strength might be needed. This is neglected in this case since the method described in Banverket (2000) and BBK 94 Band 2 (1994) will be compared to a direct statistical method later on.

prEN 13791:1999 is likely to replace BBK 94 Band 2 (1994) in the future when it comes to assessment of compressive concrete strength in structures; the used evaluation relationships are shown in Appendix B. In the same manner as for BBK 94 Band 2 there are two different criteria's that are used. When only 3 samples are available the strength class becomes C60/75 for the substructure. No assessment could be made for the superstructure due to only two valid results. The strength class gives the characteristic dry cylinder strength of 60 MPa and a characteristic dry cube strength of 75 MPa, if this value is converted to wet cylinder strength (see Eq. 7.36) a characteristic value of 55,6 MPa is obtained.

7.1.3 Damage

There are various indications that there could be problems with the structural integrity of the bridge. On the underside of the trough bottom, large pores are visible on the concrete surface, as well as exposed reinforcement bars. Photographs of the damage on the underside of the trough are shown in Appendix B. Corroding reinforcement is also visible on the sides of the girders, see Figure 7.6.

Figure 7.6 Corroding superficial reinforcement at the corner of a girder.

Concerns about the structural integrity have been raised since the exposed reinforcement visible on the sides of the girders is likely to be either shear reinforcement (3) or suspension reinforcement (1), see Figure 7.7. In both cases there is a significant risk of brittle failure if the reinforcement area becomes insufficient. Reinforcement quality, bar diameters and bar distances are given in Table 7.2.

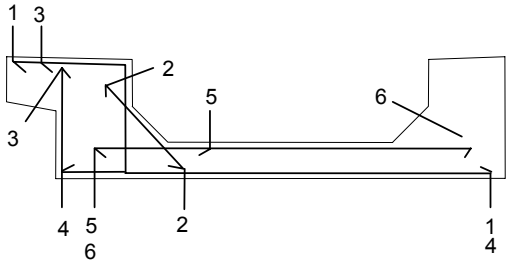

Figure 7.7 Reinforcement of trough section, numbers indicate beginning and end of individual bars.

Table 7.2 Diameter and separation between bars, reinforcement quality is Ks 60 for all bars. Bar numbers are related to Figure 7.7.

No.	Bar type	Diameter [mm]	Bar sep. mm]	No.	Bar type	Diameter [mm]	Bar sep. mm]
1	Suspension	12	300	4	Bending	16	300
2	Surface	12	300	5	Bending	12	300
3	Stirrup	12	300/150	6	Bending	10	300

The centre distance of the shear stirrups (bar no. 3 in Figure 7.7) is 150 mm over supports, and otherwise 300 mm.

Ocular inspection revealed that the suspension reinforcement, or the shear reinforcement, was visible at several positions along the inside of the west main girder. The ocular inspection also indicated that the reinforcement was corroded so much that the visible face of the bars had become flat. By measuring the length of the flat region ($2e_3$) see Figure 7.8, the amount of reinforcement that had been lost due to corrosion could be estimated.

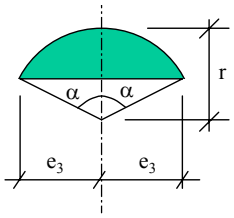

Figure 7.8 Symbols for calculation of area loss of reinforcement.

We intended to measure the length of the corroded steel region using digital sliding calliper, but due to the moisture in the air this failed. Instead of measuring at the site photographs were taken of the damaged reinforcement, after the surrounding concrete had been chiselled away and the reinforcement cleaned with hydochloric acid and brushed with a steel brush. The length of the flat region was then estimated from the digitalised images. The results are collected in Table 7.3, and the images shown in Appendix B, Figure B.11 to Figure B.20.

Table 7.3 Estimated flat lengths, based on Figure B.11 to Figure B.20.

Image	*$2e_3$ [mm]*	*Image*	*$2e_3$ [mm]*
1	9	*6*	-
2	11 11	*7*	12 9
3	10 11	*8*	9
4	10	*9*	9 11
5	9	*10*	8 10

Using Eq. 7.4 and Eq. 7.5 the area loss was calculated for each of the fourteen values in Table 7.3. The investigation resulted in a mean area loss of 21 mm^2 with a 12 mm^2 standard deviation. Using the symbols in Figure 7.8, the area loss can be expressed as:

$$\Delta A = r^2\left(\alpha - \frac{\sin 2\alpha}{2}\right) \qquad \text{Eq. 7.4}$$

where ΔA is the area loss, r is the nominal bar radius, and α is the angle according to Figure 7.8. The angle can be expressed as:

$$\alpha = \arcsin\left(\frac{e_3}{r}\right) \qquad \text{Eq. 7.5}$$

where e_3 is half of the measured flat length of the corroded bar, see Figure 7.8. The residual area ($A_{residual}$) was calculated as:

$$A_{residual} = A - \Delta A \qquad \text{Eq. 7.6}$$

where A is the nominal area of one bar and ΔA is calculated using Eq. 7.4. This calculation gave a mean residual area of 91.7 mm^2 and a standard deviation of the residual area of 12 mm^2.

The ocular inspection showed that only one of the main girders had visible damage, which could indicate that a mistake was made during construction. The question is how great is the damage if 14 of approximately 245 bars are corroded on one of the girders? The problem is unfortunately not limited to the bars with visible damage. At the time of inspection, the concrete cover was measured for all bars that could be detected with a cover meter in the vicinity of the north support of the bridge. A total of 32 covers were measured. The results are shown in Figure 7.9.

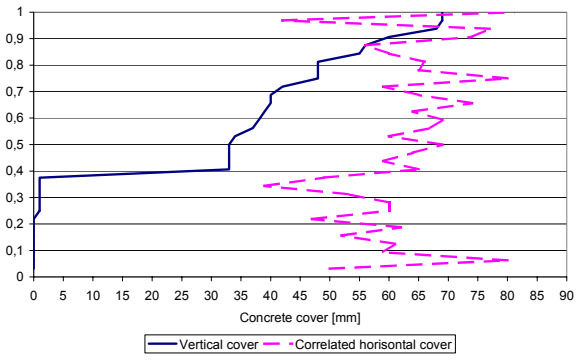

Figure 7.9 "Cumulative distribution for concrete cover" on damaged girder.

The cover for almost 40 % of the investigated bars is less than 5 mm. With a current carbonation depth of 2 mm, more bars than those visible can be expected to be corroded, or soon start to corrode. The critical vertical cover is the cover on the vertical surface of the main girder, and the correlated horizontal cover is the cover on the horizontal surface of the same bar.

7.2 Owner's requirements

7.2.1 Deterministic requirements

A railway-bridge-specific assessment code, Banverket (2000) has recently been issued. Load requirements are specified in this code for capacity calculations it refers to the Swedish

Concrete Design Code for structural design (BBK 94 Band 1, 1995) and to BBK 94 Band 2 (1994) for materials and verification at site. The assessment procedure used here was as follows.

- Establish the current load carrying capacity according to BBK 94 Band 1 (1995) based on as-built drawings.
- Calculate section forces for the structure using load intensities and load configurations from Banverket (2000). Compare these with the load carrying capacity and define the highest possible train load type.

Depending on the location of the bridge in the national railway network, different requirements are specified for train loads and velocities. The bridge investigated here is required to carry train load BV-4 (Figure 7.10). If this is not possible it should carry load UIC 71 (Figure 7.11) and as the next alternative it should carry BV-3 (Figure 7.12), all train loads are defined for a velocity of 100 km/h.

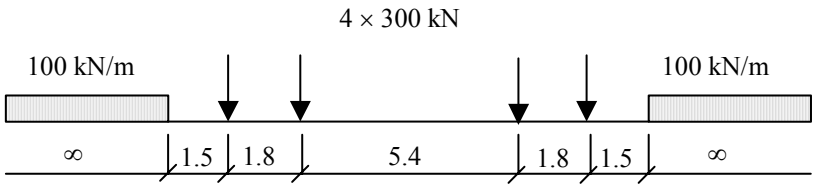

Figure 7.10 Train load BV-4 (Banverket, 2000), dimensions in metres.

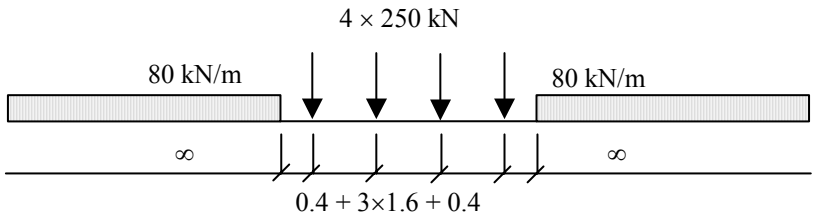

Figure 7.11 Train load UIC 71 (Banverket, 2000), dimensions in metres.

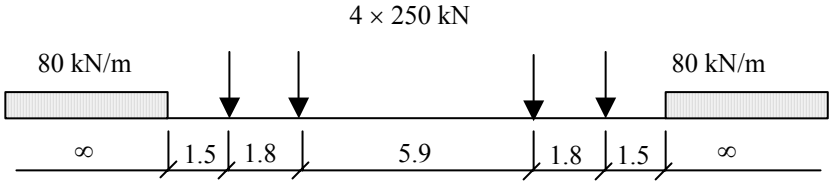

Figure 7.12 Train load BV-3 (Banverket, 2000), dimensions in metres.

Besides the load configuration there are also differences between the train loads described in Figure 7.10 to Figure 7.12 with regard to load distribution from the railway sleeper to the

bridge, and with regard to dynamic amplification factor. For calculation of the load effects the concentrated loads in train model UIC 71 can be replaced by a uniformly distributed load of 156 kN/m provided that the ballast thickness exceeds 0.6 m, as for the bridge in question.

The static loads, specified above, should be increased by a dynamic amplification factor. According to Sundquist (2000), the amplification factor is mainly related to the train velocity, the fundamental eigenfrequency of the bridge and the length of the bridge. An upper limit can be derived for the amplification factor and Sundquist concludes that the suggestions given in the current Swedish design codes are in agreement with this upper limit. No information is given about the statistical properties but it is believed that the suggested expressions contain an extra safety margin. The deterministic calculations behind the dynamic amplification factors given in Table 7.4 are presented in Appendix B. Since the dynamic amplification factor is strongly dependent on the member length, different calculations must be performed for the main girders and for the transversal direction of the trough slab.

Table 7.4 Dynamic amplification factors for structural elements of the bridge.

	Girder	*Slab*	
BV-4	1.30	1.52	(**Eq. B.13**)
UIC 71	1.18	1.33	(**Eq. B.18**)
BV-3	1.30	1.52	(**Eq. B.13**)

7.2.2 Reliability requirements

In Banverket (2000) it is stated that the assessment of an existing railway bridge should be performed in safety class 3, which may be interpreted such that the safety index should be 4.8 see Section **4.4**.

7.3 Deterministic analysis in the undamaged state

In order to establish the critical section for the bridge a full static analysis was performed according to the requirements of SNRA. The section forces shown in Figure 7.13 and Figure 7.14 were calculated for a specific load combination denoted *A* in Banverket (2000). Load combination *A* is used for ultimate limit state design and is defined in Table 7.5, where the loads that must be taken into consideration for the current bridge is shown

Table 7.5 Load combination A, Banverket (2000).

Permanent loads	Partial factor	Variable loads	Partial factor
Dead load	1.0	Train BV-4	0.7/1.3
Ballast	1.1	Train UIC 71	0.7/1.4
Earth pressure	1.0	Train BV-2, BV-3	0.7/1.3
		Braking and acceleration	0.4/1.2
		Overload	0.7/1.3
		Temperature change	0.6/1.3

The combined section forces according to load combination *A* was calculated for the three different train loads indicated in Table 7.5. In load combination *A*, a maximum of four variable loads was used according to Banverket (2000), and the main load was multiplied by the higher partial factor, while the remaining three variable loads were related to the lower partial factor. Section forces for the loads in Table 7.5 are given in Appendix B.

The load carrying capacity is then calculated according to BBK 94 Band 1 (1995). The capacities shown in Figure 7.13 to Figure 7.15 are based on tested concrete strengths, as given in Table 7.1, and the nominal steel yield strengths are assumed to correspond to characteristic values.

7.3.1 Main girders

When dealing with moving loads, it is common practice to evaluate two envelopes for the section force being investigated. When the load is moved over the structure, maximum and minimum values are recorded for every position, which results in the two curves shown in Figure 7.13. The capacity shown in Figure 7.13 is related to a specific train load since the bending moment capacity depends on the normal force acting on the beam. It can be seen that the bending capacity is sufficient for all positions along the girder. No adjustment was made to the bending moment capacity curves in this diagram with regard to anchorage lengths of the reinforcement.

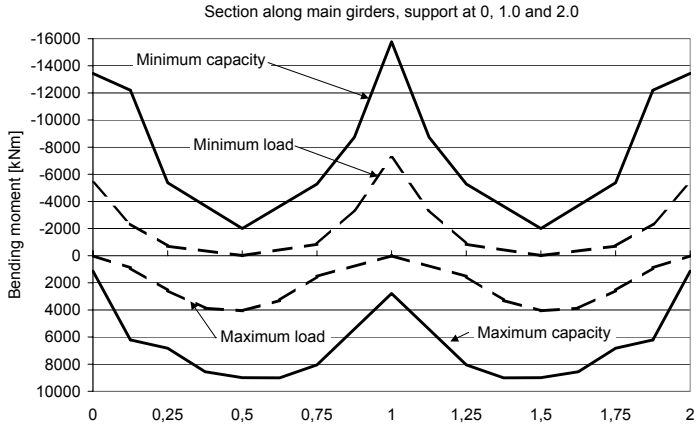

Figure 7.13 Bending moments for load combination A with train load BV-4 and bending moment capacities for main girders of the bridge.

Calculations of the shear forces indicate that train load BV-4 is decisive. In Figure 7.14 the maximum and minimum shear forces are shown together with the shear force capacity. In the first analysis, without any information on the measured tensile strength of the concrete, the shear capacity was found to be critical at mid-section of the girders, but after the

introduction of the concrete tensile strength based on test results shown in Table 7.1 the shear capacity was found to be sufficient.

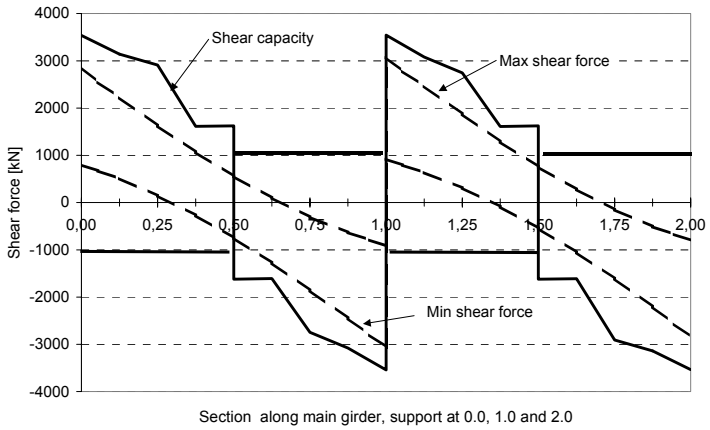

Figure 7.14 Shear forces and shear force capacities for main girders, load combination *A* with train load BV-4.

The total shear capacity for the girders is the result of different mechanisms. One component depends on the nominal shear stress (V_c), another on the stirrups ($V_{stirrup}$) and the third component depends on the bent-up longitudinal reinforcement ($V_{bend\ long}$). In Figure 7.15 the different components are shown together with the total shear capacity.

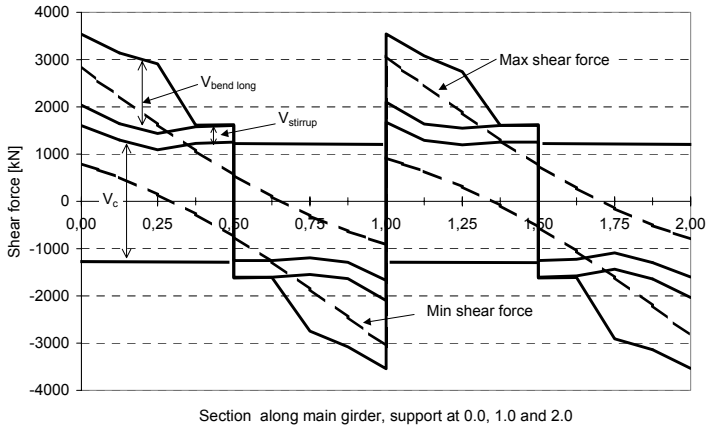

Figure 7.15 Shear forces for load combination *A* with train load BV-4 and shear force capacities for main girders according to the mechanisms acting.

Figure 7.13 and Figure 7.14 show that the load carrying capacity is sufficient with respect to bending and shear along the girders for the undamaged bridge.

7.3.2 The trough

The utilisation of the trough is often high and it is expected to be the critical part of the bridge. Besides the shear capacity and bending capacity of the trough, the suspension capacity of the trough must also be verified, since the load from the trough is transferred to the lower parts of the main girders. Verification of the suspension capacity ensures that this load does not cause shearing of the lower parts of the girders.

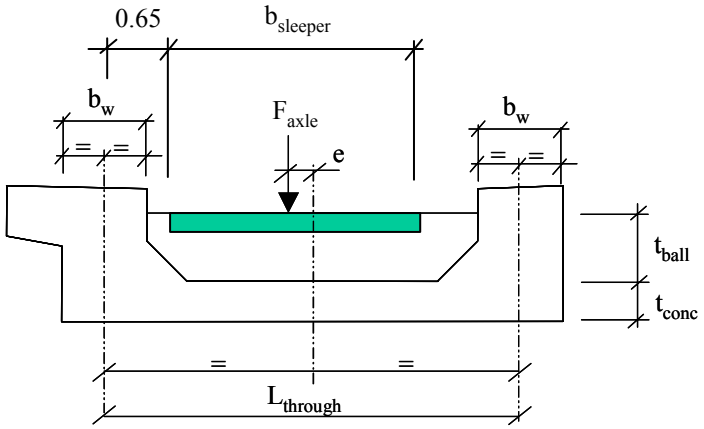

Figure 7.16 Trough section with explanation of parameters.

Figure 7.16 and Figure 7.17 show how the trough is loaded. The train load is placed with a small eccentricity (*e*) and there is ballast in the trough.

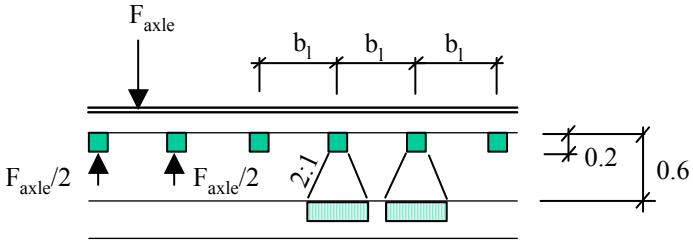

Figure 7.17 Load distribution between adjacent sleepers and from the sleepers to the concrete.

After the calculation of the load distribution, as suggested in Banverket (2000), it can be seen that the axle load can be assumed to be uniformly distributed. Calculations show that the load carrying capacity across the girders is critical with respect to bending and shear

capacity, see Figure 7.18 and Figure 7.19. The system lines during this analysis are placed at the centre of the main girders, see Figure 7.16.

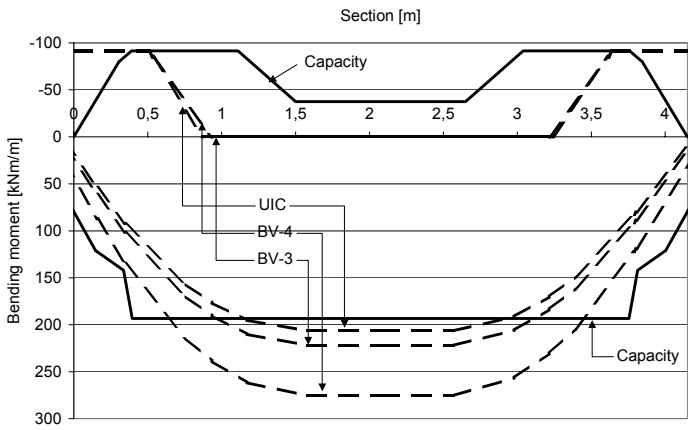

Figure 7.18 Transverse bending moment distribution for trough slab, load combination *A* for different train loads.

In the calculations on which Figure 7.18 is based, it is assumed that the top reinforcement in the slab is used to its maximum, i.e. the slab is assumed to behave plastic. This is not obvious from Figure 7.18 since the moment curves are displaced to assure that the bending reinforcement must be anchored beyond the expected shear crack. As indicated in the figure, there is not sufficient load carrying capacity for any of the train loads, and BV-3 and UIC have the lowest degree of utilisation.

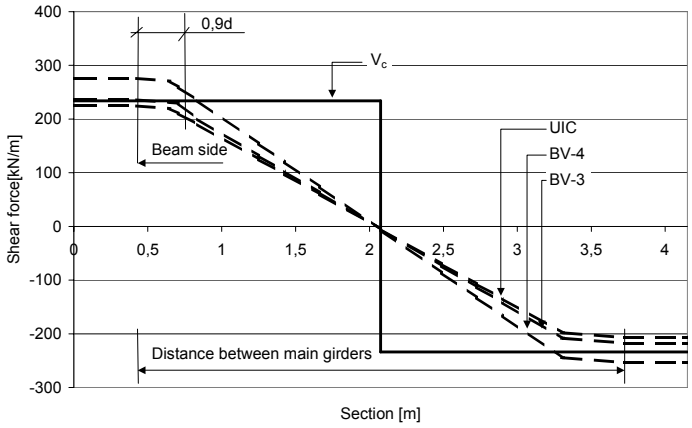

Figure 7.19 Shear force distribution for trough slab, load combination *A* for different train loads.

Due to the assumed 45° inclination of the shear crack in the ultimate limit state, the shear force capacity at a distance away, of 0.9 times the effective depth from the investigated position can be compared with the shear force at this position. It is shown in Figure 7.19 that sufficient shear capacity exists for load combination *A* with train load UIC and BV-3, but for BV-4 there is not enough shear capacity.

As mentioned above, the suspension capacity of the trough must also be verified, i.e. the suspension reinforcement (1) shown in Figure 7.7 must be checked regarding its load carrying capacity. This reinforcement alone was insufficient and the possibility of using the inclined surface reinforcement (2) in Figure 7.7 was investigated. Surface reinforcement is used here as a collective term for the required minimum reinforcement on the different faces of the concrete surfaces, employed mainly to counteract cracks during hardening of the concrete.

A linear elastic finite element analysis was performed to investigate the stress field in the trough cross section. In this analysis the nodes at the upper edge of the trough beams were assumed to be fixed in the vertical direction so that the trough is suspended. Circles in Figure 7.20 indicate areas where the concrete is in compression, showing that the main part of the structure is subjected to tension: especially the region close to the haunch is subjected to high tensile stresses. Based on this analysis, the idea of using the surface reinforcement as suspension reinforcement can be questioned since anchorage of reinforcement in concrete subjected to tensile stress is not reliable, its location can also be questioned. It is likely that a small displacement of the surface reinforcement would place its anchorage zone in concrete regions under tension. The location of the stirrups indicates poor craftsmanship (Figure 7.6) and it is suspected the location of all the reinforcement in the bridge can be questioned

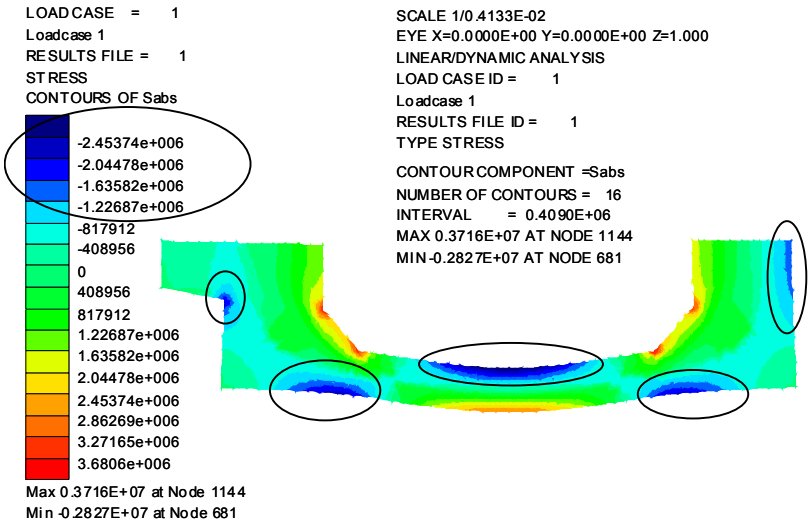

Figure 7.20 Trough cross section, showing the principle stresses when loaded according to load combination *A* and train load BV-4.

According to Betonghandboken Konstruktion (AB Svensk Byggtjänst, 1990), beams subjected to loads on the underside (F_s) as shown in Figure 7.21, should have additional reinforcement to transfer the load from the bottom of the beam to the top.

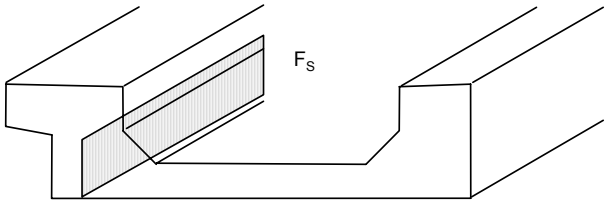

Figure 7.21 Load at the underside of a beam.

Since the surface reinforcement at the haunch could not be used as suspension reinforcement, this had to be found elsewhere. Bar no. 1 and no. 3 in Figure 7.7 are the only appropriate reinforcement types available. If the stirrups in the main girders (bar no. 3) are not fully utilises as shear reinforcement, they can be redistributed to function as suspension reinforcement. In order find a safe amount of stirrups that could be used in this purpose, the degree of utilisation of the stirrups was calculated at the position of the main girder with the highest degree of shear utilisation, i.e. position 0.625. At this position it was found that 103 mm^2 of the maximum 113 mm^2 shear stirrup area was available as suspension reinforcement. If this reinforcement area is used the suspension capacity will be 308 kN/m, and this is greater than the suspension forces for different train loads given in Table 7.6. The amount of available suspension reinforcement (103 mm^2) of the shear reinforcement will also be used in section 7.10.3 for extrapolation of safety indices.

Table 7.6 Suspension force, load combination *A*, different train loads.

Train loads	*Suspension force* [kN/m]
BV-4	276
UIC	224
BV-3	236

7.4 Time-variant deterministic analysis of the bridge

In Figure 7.6, corroding bars are show on the inside upper corner of the main girders. Since both the stirrups in the main girder (bar 3 in Figure 7.7) and the suspension reinforcement (bar 1 in Figure 7.7) have a 12 mm diameter it cannot be determined which one of the bar types is affected by corrosion. In order to investigate the influence of corrosion on both bar types, a simple corrosion model (Section 7.4.1) was applied to check the influence of corrosion on the load carrying capacity.

In Figure 7.14 it can be seen that positions 0.375 and 0.625 are most highly utilised positions with respect to shear capacity. At these positions the shear capacity is made up of two components: one related to the shear capacity of the concrete and one related to stirrups i.e. these positions are likely to be sensitive to corrosion of the stirrups. Due to symmetry this is also valid for positions 1.375 and 1.625.

The second failure mode of interest is the suspension of the trough, which is related to the shear capacity of the main girders, see Section 7.3.2. This failure mode is also highly sensitive to corrosion.

7.4.1 Extrapolation of area loss

In Section 3.2.1 it is suggested that the area loss of corroding reinforcement can be assumed to be linear with time after initiation of corrosion. If the time to initiation can be estimated it would be possible to estimate the future area loss by extrapolation based on the observed area loss at the time of inspection.

Since the age of the bridge is known, 46 years, the following relation is valid:

$$46 years = t_{initiation} + t_{corrosion} \qquad \text{Eq. 7.7}$$

where $t_{initiation}$ is the initiation time, and $t_{corrosion}$ is the time of corrosion

The initiation time is evaluated differently, depending on the reason for corrosion, i.e. whether it is initiated by chloride ion ingress or by carbonation. Based on measured chloride profiles (see Appendix B, Test results regarding chloride profiles), showing low chloride concentrations in the superstructure it is assumed that corrosion was initiated by carbonation. The measured carbonation depths of approximately 2 mm, as can be seen in Appendix B, support this assumption.

The carbonation depth must be compared with the actual cover of the reinforcement in order to see when the corrosion was initiated. However, since many of the bars had a cover of less than 5 mm, and several bars seemed to be covered only by cement slurry, it is assumed that $t_{initiation}$=0. It was assumed that corrosion started immediately after casting of the bridge, so $t_{corrosion}$ is set to 46 year. This assumption is not on the safe side since the future rate of corrosion is underestimated for a single bar. The importance of a correct estimate of the initiation time is shown in Figure 3.5.

The assumption that corrosion started immediately after the construction of the bridge must be justified. Figure 7.9 indicates that almost 60 % of the bars had a cover greater than 30 mm, and it is unlikely that these bars started to corrode at the same time as the other. Therefore, if all the bars are assumed to start corroding simultaneously and at the same rate in the following calculations, the assumption regarding the initiation time should be on the safe side.

At a first glance, these assumptions give a very uncertain prediction of the future area loss of the bars. However, the uncertainties in theoretical predictions should be compared with the variation in measurements. Luping (2002) compared commercially available equipment measuring corrosion currents (I_{corr}) and found that they can differ 5-50 times between different pieces of equipment. This large variability in I_{corr} can be compared with the difference in the slope for different values of $t_{corrosion}$. If the initiation time is increased from 0 to 10 years, the change in slope is 46/(46-10)≈1.28. This indicates that the method used for extrapolation of the residual reinforcement area is more robust than measuring I_{corr}.

Since extrapolation of the residual reinforcement area is uncertain, it is suggested that it be related to a management plan, i.e. the extrapolated values should be compared with real values at intervals of 5 to 10 years, and the new information should be used to improve the accuracy of new extrapolations. This situation is well suited for reliability theory and probability-based estimates.

Using data in Table 7.3 together with Eq. 7.4 and Eq. 7.5 gives a mean area loss for the reinforcement at the present time of 22 mm^2. This value is used for the extrapolation of the area loss of the reinforcement bars. The results of such extrapolation are given in Table 7.7.

Table 7.7 Corroded bar area as a function of time, based on the assumptions made above.

Year	*Residual area [mm^2]*	*Area loss [mm^2]*	*Comment*
1955	113	0	Nominal value
2001	91	22	Measured
2055	65	48	Extrapolated

7.4.2 The shear capacity of the girders

The shear capacity of the girders was calculated by superposition of various load carrying mechanisms according to BBK 94 Band 1 (1995):

$$V_R = V_c + V_{stirrup} + V_{bend\ long} \qquad \text{Eq. 7.8}$$

where V_R is the total shear capacity, V_c is a nominal shear capacity determined from Eq. 7.9, $V_{stirrup}$ is the shear capacity resulting from the stirrups see Eq. 7.10, $V_{bend\ long}$ is the shear capacity resulting from the bent up longitudinal reinforcement.

The first component of the capacity consists of a nominal shear capacity V_c, given by:

$$V_c = b_w d \xi \left(1 + 50 \frac{A_{s0}}{b_w d}\right) 0{,}30 f_{ct} \qquad \text{Eq. 7.9}$$

where ξ is a factor taking the size effect into account, for beams taller than 1,0 m which is the case for the investigated bridge, the value being 0.9. b_w is the width of the beam, d is the effective depth, A_{s0} is the amount of tensile reinforcement that is anchored one internal lever arm plus the anchorage length away from the critical position and f_{ct} is the tensile strength of the concrete.

The second component of the shear capacity is related to the shear reinforcement. In this case it consists of two different types: ordinary stirrups made of Ks 60 steel and bent up longitudinal reinforcement made of HJS 70 steel. The following relations are given in BBK 94 Band 1 (1995):

$$V_{stirrup} = A_{sv1} f_{sv1} \frac{0{,}9d}{s} \qquad \text{Eq. 7.10}$$

$$V_{bend\ long} = A_{sv2} f_{sv2} \sin \chi \qquad \text{Eq. 7.11}$$

where A_{sv1} is the area of the vertical stirrups, f_{sv1} is the yield strength of the vertical stirrups, s is the distance between the stirrups, A_{sv2} is the area of the bent up reinforcement crossing the shear crack, f_{sv2} is the yield strength of the bent up reinforcement and χ is the angle between the bent up reinforcement and the girder direction

Based on the assumption stated earlier, a linear reduction of the residual reinforcement area A_{sv1} is used in the predictions of the future load carrying capacity of the bridge, see Table 7.8. The bent up longitudinal bars are assumed to be unaffected by corrosion, i.e. A_{sv2} is constant over time. V_S was then calculated for load combination *A* and train load BV-4.

Table 7.8 Degree of utilisation of the shear capacity of the main girders, $V_S / V_R(t)$. V_S was calculated for load combination *A* and train load BV-4.

Year	*Position 0.375 / 1.625*	*Position 0.625 / 1.375*
1955	0.66	0.79
2001	0.69	0.83
2055	0.73	0.88

Both positions on the girder, 0.375 and 0.625 have sufficient shear capacity after 100 years at the estimated corrosion rate. The girders are not very sensitive to the corrosion of stirrups at the investigated positions. This can be explained by the fact that only approximately one fourth of the shear capacity is related to the vertical stirrups.

7.4.3 Suspension capacity

The influence of corrosion on the suspension reinforcement was studied under the same assumptions as for the shear reinforcement, i.e. a linear reduction of the residual area. Based on the assumptions presented in Section 7.3.2 on the suspension capacity, together with input regarding the residual reinforcement area from Table 7.8 the degrees of utilisation in Table 7.9 could be calculated.

Table 7.9 Degree of utilisation of suspension capacity, load combination *A* and BV-4 train load.

Year	$F_S(BV\text{-}4) / F_{S,cap}$
1955	0.86
2001	0.96
2055	1.12

The results Table 7.9 show that the suspension capacity is insufficient for train load BV-4 when the bridge is 100 years old, and that the degree of utilisation is quite high in the damaged state, as indicated for the year 2001.

7.5 Random modelling of concrete

Deterministic evaluation of concrete properties is a complex task, and the probabilistic approach is no simpler. In this section measured concrete properties are used to evaluate the properties of the random variables describing compressive strength and tensile strength.

Comparison is made with the deterministically evaluated values according to Banverket (2000), and prEN 13791:1999 in Section 7.1.2. Banverket (2000) refers to BBK 94 Band 2 (1994), which states that cores should be taken at locations where the lowest strength is expected to be found. If three samples are collected at positions where the concrete is poor the low value of strength obtained is assumed to represent the entire structure.

When investigating the deterministic evaluation of the cores (see Appendix B for details), it becomes apparent that this evaluation is based on the fact that one really works with the lowest strengths of concrete in the structure. Small variability is assumed when converting the measured mean value to strength classes, which in turn is converted to characteristic values as shown in Table B.3 and Table B.4.

The question that needs to be answered is what happens if one cannot take samples at locations where the lowest strength is expected? During testing it is often impossible to access positions where the concrete is poor. These positions may be highly utilised, and taking cores here could lead to damage to the structure. Needless to say, this must be avoided.

For the current railway bridge testing had to be made so that the train traffic was not interfered with. Cores were therefore taken at the outer side of the accessible main girder, close to the bottom. This is a position where good concrete quality is expected. As seen in Table 7.10 to Table 7.12 a small variability of high strength concrete is measured at these positions, even if the values from the superstructure is lower than the ones measured on the substructure. This information is now used to estimate a low concrete strength that should represent the whole bridge.

7.5.1 Measured concrete properties

It was decided that three test samples would be used for compressive strength, tensile strength and elastic modulus from both the substructure and the superstructure, i.e. the trough girders. The differentiation between different parts of the bridge is a consequence of the joint that is marked on the design drawings, which indicates that concrete from different mixes could have been used. Three samples from each structural element is a minimum requirement in Banverket (2000), fewer samples is regarded to give insufficient data for evaluation of the material properties.

In a comment from the Swedish National Testing and Research Institute (SP) where the testing of compressive strength (Table 7.11) and modulus of elasticity (Table 7.12) was performed. It is stated that there is a visible difference in ballast between the test objects labeled 1-3 and 4-6. Their interpretation is that the casting was performed with different batches of concretes. Splitting tensile testing (Table 7.10) was performed by a laboratory in Malmö owned by Vägverket (the Swedish National Road Administration).

Table 7.10 Measured tensile splitting strength, tested according to SS 13 72 13, and density according to SS 13 72 34.

	Test specimen	Density [kg/m^3]	Splitting tensile strength [MPa]
Superstructure	1	2350	3.7
	2	2350	3.6
	3	2350	4.9
		Mean value	***4.1***
		Standard deviation	***0.72***
Substructure	4	2400	5.1
	5	2400	5.3
	6	2400	5.0
		Mean value	***5.1***
		Standard deviation	***0.17***

Table 7.11 Measured compressive strength, tested according to SS 13 72 30.

	Test specimen	Density [kg/m^3]	Compressive strength [MPa]
Superstructure	1	2370	53.9
	2	2390	57.6
	3	-	-
		Mean value	***55.8***
		Standard deviation	***2.62***
Substructure	4	2410	62.7
	5	2420	59.3
	6	2440	72.2
		Mean value	***64.7***
		Standard deviation	***6.95***

Table 7.12 Measured modulus of elasticity, according to SS 13 72 32.

	Test specimen	Density [kg/m^3]	Modulus of elasticity [GPa]
Superstructure	1	-	-
	2	2390	30.5
	3	-	-
		Mean value	***30,5***
		Standard deviation	**-**
Substructure	4	2410	34.5
	5	2400	-
	6	2440	34.5
		Mean value	***34,5***
		Standard deviation	**-**

Results from the evaluation according to Banverket (2000) are shown in Table 7.1, and details of the evaluation can be found in Appendix B. The evaluated values are referred to as characteristic values but no information regarding their random distribution is given. In

Degerman (1981) data can be found that can be used as parameters to describe the compressive and tensile strength as random variables, as shown in Table 7.13.

Table 7.13 Random parameters for 28 days old K400 concrete from Degerman (1981).

	Compressive cube [MPa]	Tensile [MPa]
Mean value	50.2	2.62
SD	5.26	0.425
COV	10.5 %	16.2 %

7.5.2 Statistical evaluation of concrete properties

In this section a different approach to that described in Banverket (2000). The variability in the material properties will be taken into consideration, ultimately by Bayesian updating. When performing Bayesian updating based on new a sample, a priori information is needed. From the a priori information and the new data a predictive distribution can be calculated. The choice of a priori information is important, in this case information from Degerman (1981) will be used as a priori information for both compressive strength and tensile strength. This choice of a priori information is not without problems since Degerman's data are based on 28-day strength cube values and transformation of compressive cube values into tensile strength.

The statistical evaluation of the concrete strength consists of several steps the first of which is to investigate if the samples from the super- and substructure can regarded as one sample in order to increase the sample size. The next step is to transform the a priori information and the new information into comparable parameters. This series of conversions is schematically shown in Figure 7.22.

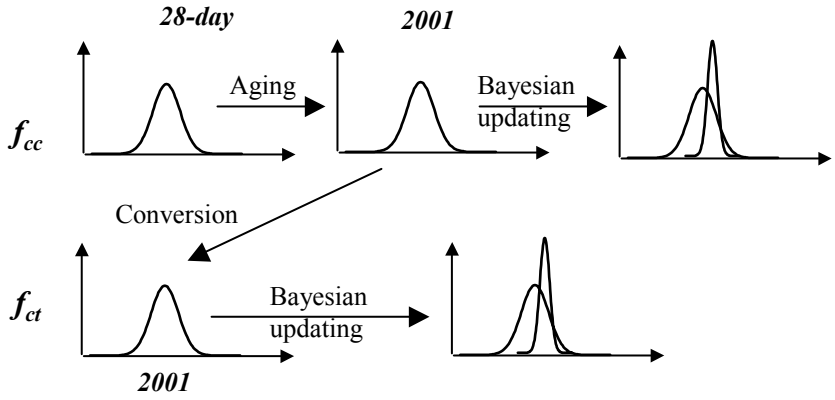

Figure 7.22 System of conversion and aging models required for Bayesian updating of the properties of concrete.

Based on a priori information on the compressive strength at 28 days, the concrete is aged to the year 2001. The compressive strength in 2001 is then converted to uniaxial tensile strength. These data are now used as a priori information and Bayesian updating is performed to obtain new statistical properties for the tensile strength.

Reliable aging models are available for prediction the compressive strength whereas knowledge about tensile strength development is uncertain. The tensile strength data presented by Degerman (1981) are based on conversion from compressive strength to tensile strength. It was therefore concluded that the procedure illustrated in Figure 7.22 was the most reliable way to include the information from the material testing.

Every time an aging model or conversion of strength parameters is introduced, uncertainties are also introduced. The uncertainties that must be included are related to the following transformations.

$$f_{28} \rightarrow f_{cc}(2001) \qquad \text{Eq. 7.12}$$

Here f_{28} is the 28-day compressive cube strength and $f_{cc}(2001)$ is the compressive cube strength in 2001. Conversion from compressive cube strength to cylinder strength ($f_{cc,cylinder}$) is carried out to obtain values that can be used in the design equations in BBK 94 Band 1 (1995).

$$f_{cc}(2001) \rightarrow f_{cc,cylinder}(2001) \qquad \text{Eq. 7.13}$$

Conversion from $f_{cc}(2001)$ to uniaxial tensile strength $f_{ct}(2001)$ is then performed

$$f_{cc}(2001) \rightarrow f_{ct}(2001) \qquad \text{Eq. 7.14}$$

This is followed by conversion of the measured tensile splitting strength to uniaxial tensile strength:

$$f_{ct,splitting}(2001) \rightarrow f_{ct}(2001) \qquad \text{Eq. 7.15}$$

where $f_{ct,splitting}$ is the tensile splitting strength

7.5.3 Sample size investigation

In Appendix B a statistical evaluation of the properties of concrete is presented. In order to investigate if the concrete in the superstructure and substructure can be considered to have the same properties a hypothesis test was performed for different strength parameters. In this case a two-sample *t*-test was used.

Assume that H_0 is the hypothesis that there is no difference in the mean values of the samples from the two structural parts (Eq. 7.16), and that H_1 is the hypothesis that there is a difference in the mean values (Eq. 7.17):

$$H_0 : \mu_1 = \mu_2 \qquad \text{Eq. 7.16}$$

$$H_1 : \mu_1 \neq \mu_2 \qquad \text{Eq. 7.17}$$

where μ_1 and μ_2 are the mean values of the three samples from the sub- and superstructure.

The hypothesis test with a 95% confidence interval shows that H_0 cannot be rejected, i.e. it cannot be concluded that there is a difference in mean strength between the superstructure and substructure. The same conclusion was obtained for both compressive strength and tensile splitting strength. The 95% confidence interval was chosen since it corresponds to the significance level of a characteristic value.

It is thus not unreasonable to treat the two samples as one sample, despite the fact that it is obvious from the test results and from the comments made at the laboratory that there is a difference between the two sampling sites. This, however, refers to an ocular difference in aggregate grading and aggregate type, not a difference in strength. In Table 7.10 to Table 7.12 it can be seen, even by an untrained eye, that there is a difference in strength between the two structural parts. This could be expected since the casting was probably performed on two different occasions.

In the following Bayesian updating exercise three situations will be tested. The sample is divided into super- and substructure and as a third alternative be regarded as one sample. Mean values and standard deviations are given in Table 7.14 for the parameters measured, under the assumption that all the results for each parameter belong to one group.

Table 7.14 Summary of the results of concrete testing for Ø 100 mm cylinders.

Parameter	*No. of samples*	*Mean value*	*SD.*	*Unit*
Splitting tensile strength	6	4.6	0.75	MPa
Compressive strength	5	74.5	8.5	MPa
Modulus of elasticity	3	33.2	2.31	GPa

The compressive strength values given in Table 7.11 were converted according to Eq. 7.1 to obtain values for use in the Bayesian updating procedure.

7.5.4 Strength development of concrete

A model for the development of the compressive strength development of concrete has been suggested by Fagerlund (1987), among others. Fagerlund proposes the relation:

$$f(t) = Af_0\left(\frac{\alpha(t)}{\alpha_{cr}} - 1\right) \qquad \text{Eq. 7.18}$$

where $f(t)$ is the strength, A is a coefficient described in Eq. 7.19, f_0 is the fictitious strength of a completely pore-free material, $\alpha(t)$ is the degree of hydration at time t described by Eq. 7.20, α_{cr} is a critical degree of hydration. Before α_{cr} is reached can the strength be regarded as zero.

The constant A is defined as:

$$A = \frac{1}{\frac{vct + L}{0.19\alpha_{cr}} - 1} \qquad \text{Eq. 7.19}$$

where *vct* is the water cement ratio and *L* is the air content.

The time dependency of the concrete strength is described via the time dependency of the hydration, given in Eq. 7.20:

$$\ln \alpha(t) = a(\ln t)^b \qquad \text{Eq. 7.20}$$

where *a* and *b* are material parameters and *t* is the time.

If *f* is related to the cube strength, then the strength development of a cube can be described via Eq. 7.18. To obtain a good fit of the parameters *a* and *b* in Eq. 7.20 the degree of hydration for concrete at 28 days was calculated. It is known beforehand that *a* and *b* for Standard Portland cement are approximately –10 and –2, respectively (Betonghandboken Material, AB Svensk Byggtjänst, 1994). Since it is only possible to solve for one of the parameters, *b* is set to –2.

f was set to the average 28-day strength of K400 concrete according to Degerman (1981), 50.2 MPa. According to Fagerlund (1987), f_0 is 186.1 MPa and α_{cr} is 0.09. The value of *vct* for bridges built according to Statens offentliga utredningar 1934:17 (1934) is required to be 0.44 for a plastic consistency and 0.49 for viscous consistency, and a mean value of 0.47 was assumed here. *L* for concrete without an air entraining agent is approximately 0,02 according to Betonghandboken Material (AB Svensk Byggtjänst, 1994). These data yield *A*=0.036.

$\alpha(t)$ is solved using Eq. 7.18 and Eq. 7.19 at an age of 28 days, and assuming that *b* is –2, the value of *a* obtained is –8.62. The degree of hydration can now be calculated with Eq. 7.20, and insertion of α into Eq. 7.18 gives the compressive cube strength.

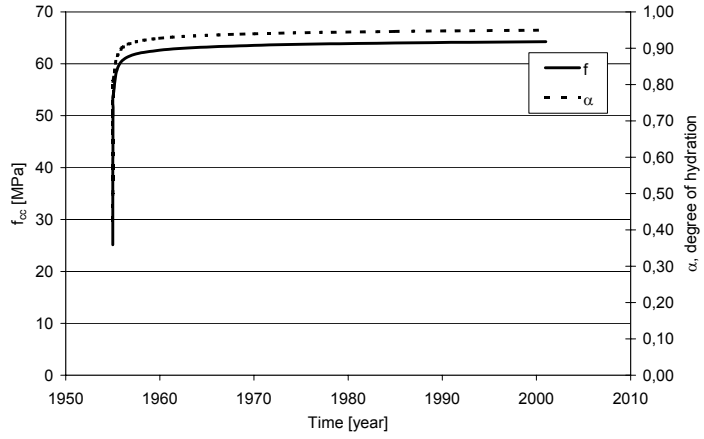

Figure 7.23 Compressive cube strength (f_{cc}) for K400 concrete and degree of hydration as a function of time.

Figure 7.23 shows the predicted development of the degree of hydration and compressive cube strength for a K400 concrete. There is rapid strength development during the first few

years, followed by a plateau. The model gives compressive cube strength of 62.5 MPa in 2001.

7.5.5 Uncertainties in the aging model

An additional uncertainty is introduced into the strength model suggested by Fagerlund (1987) as discussed in Section 7.5.1. In order to quantify the uncertainty the compressive strength is written as:

$$f_{cc}(t) = f_{28}(1+\psi(t)) = \lambda(t)\cdot f_{28} \qquad \text{Eq. 7.21}$$

where $f_{cc}(t)$ is the concrete strength at time t, f_{28} is the 28-day strength, and ψ is the relative increase in strength from 28 days until time t.

The expected value of ψ may be estimated from the strength development model presented in Section 7.5.4, to $(62.5-50.2)/50.2 = 0.245$. The coefficient of variation for ψ is not known, but it is likely to be quite high. It is reasonable to assume a value of 40%, which gives a standard deviation for ψ equal to $0.4 \cdot 0.245 \approx 0.1$. The standard deviation for λ $(1+\psi)$ can also be set to 0.1 so that the coefficient of variation for λ becomes

$$COV_{\lambda} \approx \frac{0.1}{1+0.245} \approx 0.08 \qquad \text{Eq. 7.22}$$

Now, assuming that both f_{28} and λ are lognormal distributed, the following relation is valid for the coefficient of variation for $f_{cc}(t)$:

$$COV_{f_{cc}(t)} = \sqrt{COV_{f_{28}}^2 + COV_{\lambda}^2} = \sqrt{0{,}105^2 + 0{,}08^2} = 0{,}132 \qquad \text{Eq. 7.23}$$

where $COV_{f_{28}}$ can be found in Table 7.13.

In the year 2001 the mean compressive strength is 62.5 MPa and with a coefficient of variation of 13.2 % the standard deviation is 8.25 MPa. This information will be used as a priori information for the compressive strength, see Section 7.5.8.

7.5.6 Transformation of compressive to tensile strength

Betonghandboken Material (AB Svensk Byggtjänst 1994) suggests the following relation between compressive strength and tensile strength:

$$f_{ct} = 0.24 f_{cc}^{2/3} \qquad \text{Eq. 7.24}$$

where f_{ct} is the tensile strength, and f_{cc} is the compressive strength.

JCSS (2002) suggests a conversion according to Eq. 7.25. Its probabilistic equivalent is shown in Eq. 4.17 with input from Table 4.8.

$$f_{ct} = 0.3 f_{cc}^{2/3} \qquad \text{Eq. 7.25}$$

Since the tensile strength is used as input in shear design, the approach that will be adopted below is same as that has been used by Hedman and Losberg (1975), in which they derived the shear design equation in BBK 94 Band 1 (1995), see Eq. 7.26:

$$f_{ct} = \xi\sqrt{f_{cc}} \qquad \text{Eq. 7.26}$$

where f_{ct} is the tensile strength and ξ is a conversion factor.

Degerman (1981) adopted the same approach as Hedman and Losberg (1975) and suggested a mean value of 0.37 and a coefficient of variation of 0.15 for the conversion factor ξ. The coefficient of variation for the tensile strength (COV_{fct}) can now be calculated with input regarding the $COV_{f_{cc}}$ from Section 7.5.6.

$$COV_{f_{ct}} = \sqrt{COV_{\xi}^2 + \left(\frac{1}{2}\right)^2 COV_{f_{cc}}^2} = \sqrt{0{,}15^2 + \frac{1}{4}0{,}132^2} = 0{,}164 \qquad \text{Eq. 7.27}$$

A 16.4% coefficient of variation for tensile strength may seem small, but since the tensile strength is to be used in an empirical design equation for shear capacity this value is acceptable. It is in of the same order as the coefficient of variation used when establishing the shear equations, which are discussed below.

7.5.7 Splitting tensile strength to tensile strength

The transformation from splitting tensile strength to tensile strength in this case also includes the difference in diameter of the test samples. BBK 94 Band 2 (1994) states that the tensile strength is based on Ø 150 mm cylinder values, but cores of Ø 100 mm were used for to determine the splitting tensile strength. The deterministic conversion is given in Eq. 7.2. This equation can be rewritten as:

$$f_{ct} = \rho_1 \frac{f_{ct,splitting}}{\rho_2} \qquad \text{Eq. 7.28}$$

where ρ_1 is a factor for converting splitting tensile strength to tensile strength, and ρ_2 is the conversion factor for the size difference. Both factors are assumed to be lognormally distributed and $f_{ct,splitting}$ is also assumed to be a lognormally distributed variable.

In Betonghandboken Material (AB Svensk Byggtjänst, 1994) a value between 0.7 and 1.0 is suggested for ρ_1. This implies that there is a large uncertainty involved in the conversion between splitting tensile strength and tensile strength. In BBK 94 Band 2 (1994) 0.8 is the value of ρ_1 used for the conversion. This value is assumed to be the mean value and different coefficients of variation are assumed in Table 7.15.

The size dependency seems to have a smaller uncertainty according to Betonghandboken Material (AB Svensk Byggtjänst, 1994). Based on six different test series with an unknown number of tests in each series, a mean value of 1.07, with a standard deviation of 0.017, was established i.e. a coefficient of variation $COV_{\rho_2} \approx 0{,}02$.

According to Table 7.14 the mean splitting tensile strength from all test results are 4.6 MPa and the standard deviation is 0.75, giving a coefficient of variation of 16.3%.

The mean value of the uniaxial tensile strength with the correct diameter as specified in BBK 94 Band 1 (1995) can be calculated from:

$$\mu_{f_{ct}} = \mu_{\rho_1} \frac{\mu_{f_{ct,splitting}}}{\mu_{\rho_2}} \qquad \text{Eq. 7.29}$$

where μ denotes the mean value of each parameter.

The coefficient of variation for the uniaxial tensile strength can be estimated as

$$COV_{f_{ct}} = \sqrt{COV_{\rho_1}^2 + COV_{\rho_2}^2 + COV_{f_{ct,splitting}}^2} \qquad \text{Eq. 7.30}$$

where COV is the coefficient of variation for each parameter.

Eq. 7.29 gives the mean value 3.44 MPa and Eq. 7.30 gives the results in Table 7.15 for different assumptions regarding COV_{ρ_1}. A 15% coefficient of variation was chosen for further studies.

Table 7.15 Variation of coefficient of variation regarding conversion from splitting tensile strength to tensile strength.

COV_{ρ_1}	$COV_{f_{ct}}$	$\sigma_{f_{ct}}$ *[MPa]*
0.05	0.171	0.59
0.10	0.192	0.66
0.15	**0.222**	**0.76**
0.20	0.259	0.88
0.25	0.299	1.02

7.5.8 Bayesian updating

Examples of reliability updating in the reassessment of structures are given in JCSS (2001), amongst others. The basic idea is to update prior probabilistic information, with new information, gained from for instance testing. This leads to an a posteriori probabilistic model, which in its turn can be used to derive a predictive probability distribution. The predictive probability distribution can then be used in reliability calculations. If closed solutions do not exist numerical calculations can be made based on conditional probability using Bayes' theorem. Background information about the updating used in the present case study can be found in section 5.4.1.

In the current situation, a priori information is taken from Degerman (1981) and new information is made available by testing. The a priori information gives us a general knowledge about the distribution of 28-day cubic compressive strength and 28-day tensile strength. This information is converted to correspond to concrete of the same age that tested, see Sections 7.5.4 and 7.5.5. This makes it possible to use the information as a priori when updating the strength model with information from testing.

Strength variables f_c, are assumed to be lognormal distributed i.e.

$$Y = \ln f_c \in N(\mu_Y, \sigma_Y) \qquad \textbf{Eq. 7.31}$$

where the parameters μ_Y and σ_Y are given by

$$\mu_Y = \ln m - \frac{\sigma_Y^2}{2} \qquad \textbf{Eq. 7.32}$$

$$\sigma^2 = \ln\left(1 + \left(\frac{s}{m}\right)^2\right) \qquad \textbf{Eq. 7.33}$$

and where m and s are mean and standard deviation of the strength f_c.

The Bayesian updating is here performed for the parameter μ_Y and the updated parameter are then transformed back to the updated mean and standard deviation for the basic variable f_c using Eq. 7.32 and Eq. 7.33.

It is assumed here that σ_Y is known, while μ_Y is treated as a random variable. σ_Y describes the variability for a general population of strengths, with m and s estimated from the data in Degerman (1981), see Table 7.26. This gives σ_Y=5.26 MPa. The random variable μ_Y describe the expected variation in mean value between different jobs and is assumed to be normal distributed with a prior distribution

$$\mu_Y \in N(\mu', \sigma') \qquad \textbf{Eq. 7.34}$$

where μ' and σ' are the parameters.

In absence of detailed information about the variance between different jobs, the different investigated years in Degermans (1981) is assumed to represent this variance between different jobs. Available information from Degerman (1981) is shown in Table 7.16. From these data the mean value m'_{28} = 50.2 MPa and s'_{28} = 0.68 MPa is estimated. The variability estimated in this manner is likely to be smaller than the real variability, but after taking aging into account, a reasonable variability is obtained.

In order to obtain a value of the concrete strength in 2001, the strength development is modelled in the same manner as in Section 7.5.4 above using Eq. 7.23 the coefficient of variation at year 2001 can be calculated as in Eq. 7.35 leading to s'=5.1 MPa with COV_λ from section 7.5.5.

$$\frac{s'_{2001}}{m'_{2001}} = \sqrt{\frac{s'_{28}}{m'_{28}} + COV_\lambda^2} = \sqrt{\left(\frac{0{,}68}{50{,}2}\right)^2 + 0{,}08^2} = 0{,}081 \qquad \textbf{Eq. 7.35}$$

Here m'_{28} and s'_{28} are shown in Table 7.16, from which the parameters μ' and σ' can be evaluated by use of Eq. 7.32 and Eq. 7.33.

Table 7.16 Mean and standard deviation for the compressive and tensile strength of K400 concrete, for the years 1965-1974, from Degerman (1981). The tensile strength values correspond to predicted values at year 2001 using Eq. 7.18.

		28 day compressive strength		Year 2001 tensile strength
Year	Series	Mean value [MPa]	SD [MPa]	Mean value [MPa]
1965	1532	50.4	5.5	2.971
1966	2289	50.8	5.3	2.965
1967	3619	51.3	5.7	2.997
1968	5196	51.1	5.4	2.991
1969	6771	50.1	5.4	2.962
1970	9478	50.0	5.3	2.959
1971	10041	49.7	5.3	2.950
1972	9991	50.3	5.1	2.968
1973	9701	50.4	5.1	2.971
1974	5267	48.9	5.0	2.926
Total	***63885***	***50.2***	***5.26***	***2.966***
		s'_{28} =***0.68***		s'_{2001} =***0.02***

In order to obtain s' for the tensile strength, the yearly mean compressive strengths in Table 7.16 are aged using Eq. 7.21 and transformed into tensile strength using Eq. 7.26. These values are used to calculate a mean tensile strength. The standard deviation of these values is 0,02 MPa. Eq. 7.23 is used to calculate s' for the tensile strength for in 2001. This gives a coefficient of variation of the same magnitude for the mean value of the tensile strength as for the compressive strength Eq. 7.35, since the uncertainty related to aging dominates.

Te Bayesian updating is performed both for the tensile strength and for the compressive strength using Eq. 5.43 to **Eq. 5.50** and the results of the calculations are given in Table 7.17 and in Table 7.18.

Table 7.17 A priori, a posteriori, and predictive probability parameters for compressive strength.

	m, s [MPa]	μ_Y, σ_Y	***m, s*** [MPa]	μ_Y, σ_Y	***m, s*** [MPa]	μ_Y, σ_Y	
	Total		***Superstructure***		***Substructure***		
m_{f_c} , μ_{f_c}	-	-	=		=		*A priori*
s_{f_c} , σ_{f_c}	8.25	0.13					
m' , μ'	62.5	4.14					
s' , σ'	5.1	0.08					

	m, s [MPa]	μ_Y, σ_Y	m, s [MPa]	μ_Y, σ_Y	m, s [MPa]	μ_Y, σ_Y	
$\bar{x}$	74.6	4.31	68.0	4.22	78.9	4.37	*A posteriori*
n	5	=	2	=	3	=	
n'	2.6	=	2.6	=	2.6	=	
m'' , μ''	70.3	4.25	64.9	4.17	70.9	4.26	
s'' , σ''	3.4	0.05	4.0	0.06	3.9	0.06	
m''' , μ'''	70.3	4.25	64.9	4.17	70.9	4.26	*Predictive*
s''' , σ'''	10.0	0.14	9.5	0.15	10.3	0.14	

Results from the calculations are also presented as in Figure 7.24 to Figure 7.26 together with the likelihood of the observations calculated with **Eq. 5.48**.

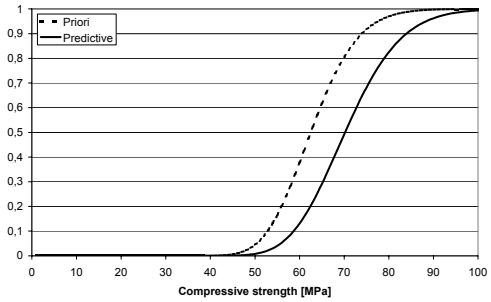

Figure 7.24 Cumulative distribution functions for compressive cube strength based on the total test sample.

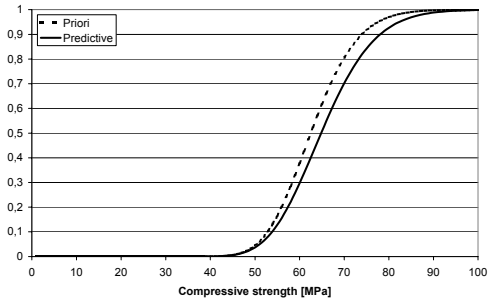

Figure 7.25 Cumulative distribution functions for compressive cube strength based on the test sample for the superstructure.

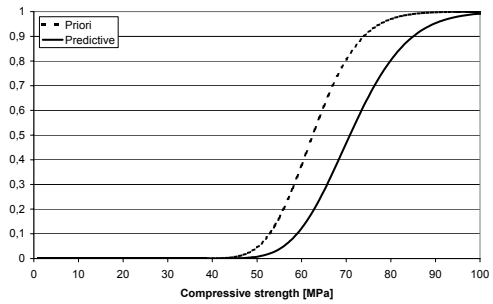

Figure 7.26 Cumulative distribution functions for compressive cube strength based on the sample for the substructure.

Figure 7.24 to Figure 7.26 shows that the largest difference between a priori and predictive distributions is found for the substructure (Figure 7.26).

Table 7.18 A priori, a posteriori, and predictive probability parameters for tensile strength.

	m, s [MPa]	μ_Y, σ_Y	m, s [MPa]	μ_Y, σ_Y	m, s [MPa]	μ_Y, σ_Y	
	Total		*Superstructure*		*Substructure*		
m_{f_c} , μ_{f_c}	-	-	=		=		*A priori*
s_{f_c} , σ_{f_c}	0.49	0.16					
m' , μ'	2.97	1.09					
s' , σ'	0.24	0.08					
$\overline{x}$	3.44	1.24	3.04	1.11	3.81	1.35	*A posteriori*
n	6	=	3	=	3	=	
n'	4.13	=	4.13	=	4.13	=	
m'' , μ''	3.24	1.17	3.00	1.10	3.31	1.20	
s'' , σ''	0.17	0.05	0.18	0.06	0.20	0.06	
m''' , μ'''	3.24	1.17	3.00	1.10	3.31	1.20	*Predictive*
s''' , σ'''	0.56	0.17	0.53	0.17	0.59	0.17	
f_{ctk}	2.45	-	2.25	-	2.48	-	*Deterministic*

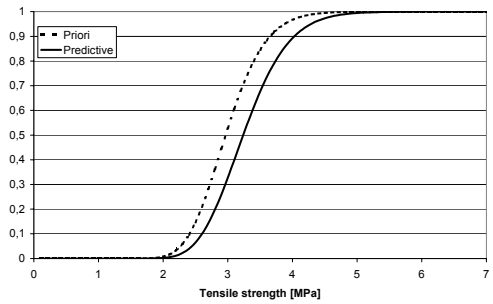

Figure 7.27 Cumulative distribution functions for tensile strength based on the total sample.

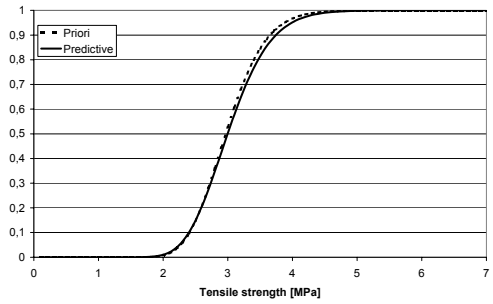

Figure 7.28 Cumulative distribution functions for tensile strength based on the sample for the superstructure.

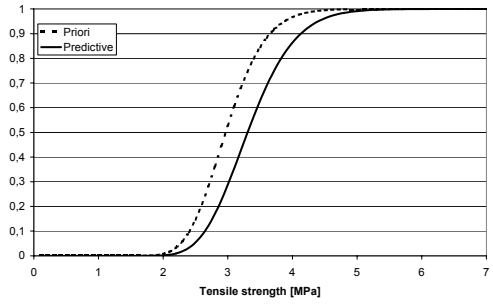

Figure 7.29 Cumulative distribution functions for tensile strength based on the sample for the substructure.

Figure 7.27 to Figure 7.29 show that the largest difference between the a priori and the predictive distribution is found for the substructure for the tensile strength, as was the case for the compressive strength.

7.5.9 Summary of the evaluation of concrete parameters

The cores taken from the bridge have been evaluated using different approaches. One approach follows strictly the recommendations in Banverket (2000) and the other is based on statistical evaluation of the test result.

The evaluation according to Banverket (2000) and BBK 94 Band 2 (1994) implies that a strength class is defined for the concrete in the structure. The characteristic value can then be determined from this strength class, but no information regarding the statistical distribution is obtained. The characteristic values obtained from this evaluation are given in Table 7.1. These values are valid only if the cores have been taken from parts of the structure where the concrete can be expected to have low strength, i.e. at the top of the section. Since this was not possible in the present case, the characteristic values given in Table 7.1 can be questioned. This approach and the objections are also valid for prEN 13791:1999.

The performed statistical evaluation is based on a priori information from Degerman (1981), and the core data are used to update this information. The results of this evaluation are given in Table 7.17 for compressive strength and in Table 7.18 for tensile strength. The results regarding the compressive strength in Table 7.17 must be converted to cylinder values before being used for design purposes. The values in Table 7.17 are related to the cube strength for dry specimens, while in BBK 94 Band 1 (1995) the cylinder strength for wet specimens is as a basis for design. Conversion is required between the cube strength ($f_{cc,cube}$) and the cylinder strength ($f_{cc,cylinder}$).

According to SS 13 72 07, Eq. 7.36 can be used for the conversion of dry 150 mm cubes to wet cylinders with Ø 150 mm and 300 mm length, under the assumption that the cylinder strength is between 8 and 50 MPa. This limitation is only valid for the strength of the superstructure, but since this is the strength that will be used below, Eq. 7.36 can be used.

$$f_{cc,cube} = 1.35 f_{cc,cylinder} \qquad \text{Eq. 7.36}$$

No information was found in SS 13 72 07 or Betonghandboken Material (AB Svensk Byggtjänst, 1994) with regard to the uncertainty of this conversion. It is, however, regarded as a well-known relation and a small uncertainty is assumed. It is also assumed that the conversion can be described by a lognormally distributed variable ρ with a mean value of 1.35 and a 5% coefficient of variation. These data were used in Eq. 7.37 and Eq. 7.38:

$$\mu_{f_{cc,cylinder}} = \frac{\mu_{f_{cc,cube}}}{\mu_\rho} \qquad \text{Eq. 7.37}$$

where μ denotes the mean values of each parameter.

The coefficient of variation for the cylinder compressive strength can be estimated from:

$$COV_{f_{cc,cylinder}} = \sqrt{COV_\rho^2 + COV_{f_{cc,cube}}^2} \qquad \text{Eq. 7.38}$$

where *COV* are the coefficient of variation for each parameter. Table 7.19 presents the results obtained with the two methods and it can be seen that the crude method suggested by Banverket (2000) is favourable in the sense that it gives high characteristic values.

Strengths evaluated for the superstructure with the statistical method will be used in the further analysis.

Table 7.19 Mean value, standard deviation and characteristic values, (all values in MPa except for the coefficient of variation).

	Compressive strength				*Tensile strength*			
	Banv.	*Total*	*Super.*	*Sub.*	*Banv.*	*Total.*	*Super.*	*Sub.*
Mean value	67.2	52.1	48.1	52.5	3.92	3.24	3.00	3.31
SD	7.0	7.8	7.5	8.0	0.63	0.56	0.53	0.59
COV [%]	10.5	15.0	15.5	15.3	16.2	17.2	17.7	17.8
Characteristic	56.5	40.7	37.2	40.8	3.0	2.45	2.25	2.48

The proposed conversion (Eq. 7.36) does not take into consideration the difference between strength of test specimen and *in situ* strength. The need for taking this difference into consideration at this moment can be discussed, since the values that has the largest influence on the outcome of the Bayesian updating is the measured data, and this data can be regarded as being representative for the *in situ* strength. Results presented in Table 7.19 is therefore used as *in situ* strength in the further calculations.

The large discrepancy between the characteristic strength evaluated according to Banverket (2000) and the values evaluated with Bayesian updating is interesting. The characteristic strengths evaluated according to Banverket (2000) are more than 30 % higher than the values evaluated with Bayesian updating. One should bear in mind that the values evaluated according to Banverket should be divided by $\eta\gamma_m$, where η is a factor that takes into account the difference between the strength in the real structure and in the sample. A value of 1.2 is used for η in BBK 94 Band 1 (1995). The characteristic values given in Banverket and BBK 94 is also said to correspond to 85% of the 5^{th} percentile; this reduction should take into account an expected strength decrease with time. The results in Table 7.19 have not been adjusted for long-term strength decrease.

It could be argued that the statistical method gives a more accurate value of the strength in the real structure and η could be given a smaller value if the strength evaluated in this way is used in a deterministic analysis. It is stated in BBK 94 Band 2 (1994), which is the code that Banverket (2000) refers to, that cores should be taken from the structure at positions with the highest utilisation or at positions where the strength is suspected to be low. These conditions were not fulfilled at the present case due to practical reasons, a situation that is probably very common. It is often impossible to test in positions with excepted low strength due to practical reasons, one could also be reluctant to drill cores a positions that are heavily reinforced but expected to have low strength. Therefore, the evaluation process described in BBK 94 Band 2 is not valid in this case, whereas the statistical method can be considered to be more reliable.

Another reason why one should not rely on the results based on Banverket (2000) is that the method used to related measured values to strength classes is not intended for use in an existing structure. It is primarily designed for concrete manufacturers to control if their

product is of sufficiently high quality. It is therefore questionable to apply the method for evaluation characteristic concrete strength in an existing structure. This is a fundamentally different situation and work is needed to design appropriate methods for evaluation of concrete strength based on *in situ* measurements. prEN 13791:1999 gives approximately the same result as BBK 94 Band 2 gives, see section 7.1.2. The same principal objections do apply to this method as for BBK 94 Band 2, see above.

When comparing conformity criteria in prEN 13791:1999 with he conformity criteria in EN-206:2000, a European code to be used for continuous concrete production, one can see that the same types of criteria are used in both cases. One difference between them are that are specified demands on how to evaluate the standard deviation in EN-206:2000. It is also stated here, that the criteria are meant to be used for quality control of continuous concrete manufacturing. Since this is not the case when assessing one single structure the difference between this code (EN-206:2000) and the two codes (BBK 94 Band 2 and prEN 13791:1999) is surprisingly small.

One should bear in mind that some of the uncertainties used for the statistical evaluation of the concrete strength can be reduced via further investigations. The aging model can be improved; uncertainties in the conversion from splitting tensile strength to tensile strength can be investigated.

7.6 Random modelling

Based on the deterministic analysis presented earlier it was decided that probabilistic analysis should be performed for three failure modes.

- The suspension capacity was analysed at position 0.625 and since the reinforcement used for the suspension capacity is corroding, a time variant analysis was performed.
- The shear capacity of the trough slab is critical, according to Figure 7.18, and was analysed with probabilistic methods.
- The bending capacity or the though slab is also critical, see Figure 7.19, and this was also analysed using probabilistic methods.

In a first step the undamaged bridge was analysed, and when required by the situation requires, a time-variant analysis was performed to take into account the corroding reinforcement.

7.7 Random modelling of the suspension capacity

As stated earlier, positions 0.625 and 1.375 have the highest degree of utilisation with respect to suspension capacity. It was shown in Table 7.9 that when the bridge is 100 years old the suspension capacity would be critical due to corrosion of the stirrups and the suspension reinforcement.

In the following sections a limit state equation will be presented, together with the statistical modelling for the random variables used in the limit state equation. The random variables

are summarised in Table 7.22, and the results of the reliability analysis are presented in Section 0.

7.7.1 The limit state equation

In general, resistance variables are assumed to be lognormally distributed and load variables are taken to be normally distributed, in accordance with NKB 55 (1987). The limit state equation for the suspension capacity can be written as:

$$F_R - F_S = 0 \qquad \text{Eq. 7.39}$$

where F_R is the suspension force, according to Eq. 7.40, and F_S is the suspension force according to Eq. 7.41.

$$F_R = Cf_{st}\left(\frac{A_{s1}}{s_1} + \frac{A_{s2}}{s_2}\right) \qquad \text{Eq. 7.40}$$

C is the model uncertainty, f_{st} is the yield strength of the reinforcement, A_{s1} is the suspension reinforcement, A_{s2} is the available stirrup reinforcement (see Section 7.3.2), s_1 is the distance between suspension reinforcement bars, and s_2 is the distance between stirrups.

$$F_S = (1+\varphi)\frac{F_{axle}}{2 \cdot b_l}\frac{(L_{trough}/2 + e)}{L_{trough}} + (\gamma_{conc}t_{conc} + \gamma_{ball}t_{ball})\frac{L_{trough} - b_w}{2} \qquad \text{Eq. 7.41}$$

The geometric properties are shown in Figure 7.16 and Figure 7.17, φ is the dynamic amplification factor, F_{axle} is the axle load, b_l is the load distribution width, L_{trough} is the trough span, γ_{conc} is the concrete density, t_{conc} is the thickness of concrete the though bottom, γ_{ball} is the ballast density, t_{ball} is the ballast thickness, b_w is the width of one of the main girders, and e is a prescribed eccentricity between the track and the centre of the bridge.

7.7.2 Loads

In NKB 55 (1987) it is assumed that the characteristic values for permanent loads corresponds to the mean value. Permanent loads are usually assumed to be normally distributed. A 5% coefficient of variation is assumed in NKB 55 for all permanent loads.

According to James (2001) the coefficient of variation for static train loads is approximately 10%. Based on personal communication (James 2002), a static mean axle load of 199 kN with a standard deviation of 19 kN is a valid description of the train load measured at Hallsberg, a large railway intersection in central of Sweden. The situation in Hallsberg is similar to that in Malmö, with a combination of both passenger and goods trains.

NKB 55 states that the characteristic value of variable loads corresponds to the 98th percentile of a normal distribution. Based on these assumptions, and with characteristic values for the loads given in Banverket (2000), mean values and standard deviations were calculated for the variable loads.

Train load BV-4 has a characteristic axle load of 300 kN, this gives a mean value of 249 kN and a standard deviation of 24.9 kN. UIC and BV-3 have a characteristic axle load of 250

kN, giving a mean value of 207 kN and a standard deviation 20.7 kN. It is also assumed that the model uncertainty for the train load is included in the uncertainty of the load, i.e. no extra uncertainty was applied to the load.

7.7.3 Dynamic amplification factor

Deterministic calculations of the dynamic amplification factor can be presented in Appendix B, and the results are shown in Table 7.4. Nilsson et al. (1999) divided the dynamic amplification factor (D), into two parts: a static part and an additional dynamic part (φ):

$$D = 1 + \varphi \qquad \text{Eq. 7.42}$$

where the dynamic part is assumed to be normally distributed with a 50% coefficient of variation.

It was further assumed by Nilsson et al. that the design value of the dynamic amplification factor from the codes is some kind of characteristic value or upper limit corresponding to the mean value (μ_φ) plus one standard deviation (σ_φ).

$$\varphi = \mu_\varphi + \sigma_\varphi \qquad \text{Eq. 7.43}$$

Based on these assumptions it is possible to calculate the mean value and standard deviation for the dynamic part of the dynamic amplification factor (see Table 7.20). When the dynamic amplification factors are used further on, they will be truncated at zero since negative dynamic amplification factors are not realistic.

Table 7.20 Statistical parameters for dynamic part, φ, of the dynamic amplification factor.

	Girder			*Slab*		
	φ	μ_φ	σ_φ	φ	μ_φ	σ_φ
BV-4	0.30	0.20	0.10	0.52	0.35	0.17
UIC 71	0.18	0.12	0.06	0.33	0.22	0.11
BV-3	0.30	0.20	0.10	0.52	0.35	0.17

7.7.4 Reinforcement steel

For random modelling of the suspension capacity, the yield strength of the reinforcement must be described as a random variable. Based on references given in the design drawing, information was sought about the reinforcement steel in contemporary codes.

No information could be found in Statens Offentliga Utredningar (SOU) 1934:17 (1934), SOU 1942:44 (1942) or SOU 1949:64 (1951) regarding yield strength of either the Ks 60 reinforcement or the HJS 70 reinforcement. It is however assumed that the Ks 60 does have the same properties as newer reinforcement steel of the same type. The statistical properties of Ks 60 are given by Degerman (1981), see Table 7.21. This assumption is perhaps questionable since the quality may have improved over the years; thus the assumption may be on the unsafe side. Information in SOU 1949:64 (1951) states however that Ks 40 reinforcement has a lower yield strength of 400 MPa for diameters less than 18 mm and 380

MPa for diameters between 18 and 30 mm and the tolerance for the lower yield strength is according to SOU 1942:44 (1942) 5%. The 5% tolerance corresponds according to personal communication with Lindgren (2002) to the 5th percentile. These values are in good agreement with data for newer Ks 40 reinforcement according to Degerman (1981) (see Table 7.21), and this information supports the decision to use newer information for the Ks 60 reinforcement.

In a brochure from a Swedish ironworks, Halmstads Järnverk AB (1960), information was found regarding HJS 70 stating a lower nominal yield strength of 700 MPa. No information could be found regarding the variability, but from Degerman (1981) it was found that the coefficient of variation for the different dimensions and steel qualities tested, varied according to Table 7.21. A slight trend towards smaller coefficients of variations can be seen for higher steel qualities. Based on this aggregated information, a conservative estimate of an 8% coefficient of variation was assumed for the HJS 70.

Table 7.21 Lower yield strength for reinforcement (Degerman, 1981).

Quality	No.	Mean value [MPa]	SD [MPa]	COV
Ks 40	19074	484,7	37.7	7.8 %
Ks 40S	8375	464,0	30.4	6.6 %
Ks 60	3537	682,8	38.7	5.7 %
Ks 60S	647	676,5	32.7	4.8 %

7.7.5 Model uncertainty

The model uncertainty for the suspension capacity is estimated according to the principles in NKB 36 (1978), see Section 4.9. The accuracy of the calculation model, which in this case is pure tension of the reinforcement, can be assumed to be *good*. Table 4.10 gives a coefficient of variation of V_{I_1} =0.04 and a correlation coefficient of ρ_1= -0.3 for the correlation between the model uncertainty and the coefficient of variation for the reinforcement.

The possible deviation from the strength of material properties in the structure involved compared with the strength in the test samples, is *small* in this case, see Table 4.11. This leads to a coefficient of variation of V_{I_2} =0.04 and a correlation coefficient of ρ_2= -0.3.

The final factor influencing the model uncertainty is the degree of control on site. Available information does not indicate that the control was anything but normal, giving a coefficient of variation of V_{I_3} =0.06 and a correlation coefficient ρ_3=0, see Table 4.12.

Degerman (1981) gives a coefficient of variation for Ks 60 reinforcement as 5.7%, see Table 7.21. Eq. 4.27 then gives a model uncertainty of 7.4 %. This model uncertainty is valid as long as the reinforcement is firmly anchored. Given the reinforcement layout as shown in Figure 7.7 the suspension reinforcement is assumed to have sufficient anchorage lengths.

7.7.6 Summary of the random variables

All random variables used in the limit state equation for the suspension capacity are given in Table 7.22. This section presents a summary of the previous sections where the background information is given for the statistical description of the variables.

Table 7.22 Random variables for verification of suspension reinforcement.

Variable	Unit	Symbol	Distribution	Mean value	SD	COV [%]
Suspension reinforcement	mm^2	A_{s1}	Lognormal	113	5.65	5
Stirrup reinforcement	mm^2	A_{s2}	Lognormal	103	5.15	5
Yield strength	MPa	f_{st}	Lognormal	679.9	37.8	5.7
Distance	m	s_1	Deterministic Lognormal	0.3 0.3	- 0.03	- 10
Distance	m	s_2	Deterministic Lognormal	0.3 0.3	- 0.03	- 10
Axle load train BV-4 UIC BV-3	kN	F_{axle}	Normal	249 207 207	24.9 20.7 20.7	10 10 10
Load distribution width	m	b_1	Deterministic	0.65	-	-
Trough span	m	L_{trough}	Deterministic	4.15	-	-
Eccentricity	m	E	Deterministic	0.10	-	-
Dyn. Amp. BV-4 UIC BV-3		φ	Normal, truncated	0.35 0.22 0.35	0.17 0.11 0.17	50 50 50
Girder width	m	b_w	Deterministic	0.85	-	-
Concrete density	kN/m^3	γ_{conc}	Normal	24	0.96	4
Thickness of concrete	m	t_{conc}	Deterministic	0.375	-	-
Ballast density	kN/m^3	γ_{ball}	Normal	20	1	5
Ballast thickness	m	t_{ball}	Deterministic	0.60	-	-
Model uncertainty for resistance		C	Lognormal	1	0.074	7.4

7.7.7 Results

Two different analyses were performed, one where the spacing between the reinforcement bars was assumed to be deterministic and one where the spacing between the bars was assumed to be a random variable.

Table 7.23 Safety indices for different assumptions regarding bar separation and train loads with related dynamic amplification factors.

Train load	*Deterministic s_1, s_2*	*Random s_1, s_2*
BV-4	7.0	6.3
UIC	9.5	8.4
BV-3	8.1	7.3

Train load BV-4 is decisive. For the case with deterministic distances between the bars, a safety index of 7.0 was obtained and for the assumption of random distances a safety index of 6,3 was obtained. The difference between the two cases can be explained by the fact that more uncertain variables are introduced into the limit state equation, leading to a higher probability of failure for the case with random bar separations than for the case with deterministic bar separation.

Sensitivity analysis was performed for both cases and, as can be seen in Table 7.24, the results are very similar. In both cases the dynamic amplification factor is the dominating load variable, and the model uncertainty dominates the resistance variables. It is interesting to note that the two dominating random variables in this failure mode are the two variables with the least available background information.

Table 7.24 Sensitivity analysis of suspension capacity with train load BV-4.

	Deterministic s_1, s_2		*Random s_1, s_2*	
Basic variable	α	α^2	α	α^2
Suspension reinforcement (A_{s1})	0.184	0.034	0.161	0.026
Stirrup reinforcement (A_{s2})	0.169	0.028	0.150	0.022
Model uncertainty (C)	0.522	0.272	0.460	0.211
Dynamic amplification (φ)	-0.536	0.287	-0.493	0.243
Axle load train (F_{axle})	-0.471	0.222	-0.429	0.184
Yield strength (f_{st})	0.394	0.155	0.347	0.120
Ballast density (γ_{ball})	-0.023	0.001	-0.023	0.001
Concrete density (γ_{conc})	-0.013	0.000	-0.013	0.000
Distance (s_1)	-	-	-0.322	0.103
Distance (s_2)	-	-	-0.299	0.089
	$\Sigma\alpha^2$	1.000	$\Sigma\alpha^2$	1.000

7.8 Random modelling of the shear capacity of the trough

The shear capacity of the trough slab close to the main girders is almost sufficient, as shown in Figure 7.19, but in a deterministic world the slab will be deemed unsafe.

7.8.1 The limit state equation

In the trough slab, there is only longitudinal reinforcement and the limit state equation can therefore be written as:

$$CV_c - V_S = 0 \qquad \text{Eq. 7.44}$$

where C is a shear factor, V_c is the shear capacity of a concrete slab (calculated as in Eq. 7.45 explained in the next section) and V_S is the shear force. The shear force is at the position where the main girder and the slab meet, identical to F_S as shown in Eq. 7.41.

7.8.2 Model uncertainties

Shear failures are regarded as brittle failure modes. Shear failure is also associated with a rather large uncertainty since the actual failure mechanism is not fully understood, or fully describable in mathematical terms. Available design equations are often based on empirical evaluation of large numbers of shear tests, which is also the case for BBK 94 Band 1 (1995). The investigations on which Eq. 7.9 to Eq. 7.11 were based were performed by Hedman and Losberg (1975).

To estimate C in Eq. 7.44 the guidelines in NKB 36 (1978) may be used (see Section 4.9). The properties of C can be calculated from Eq. 4.27. The accuracy of the calculation model, see Table 4.10 can be assumed, *good*, *normal* or *bad*. Since it is known that shear models for concrete have large uncertainties and do not describe reality very good, this property is assumed to be *bad*, i.e. V_{I_1} =0.09 and ρ_1=0.3. ρ_1 denotes the correlation between the model uncertainty and the coefficient of variation for the material in question.

The next step is to estimate the possible deviation between the strength of the material in the structure involved and the strength of test samples. Three suggested levels could be found in NKB 36, they are made, *small*, *medium* and *large*, see Table 4.11. For ordinary concrete *medium* deviation can be assumed giving a coefficient of variation of V_{I_2} =0.06 and a correlation coefficient of ρ_2=0.

The final factor influencing the model uncertainty is the degree of control on site. The degree of control is proposed to be categorised as *strict*, *normal* or *gentle,* see Table 4.12. Available information does not indicate that the control was anything but normal, giving a coefficient of variation of V_{I_3} =0.06 and a correlation coefficient of ρ_3=0.

Insertion of the coefficients of variation and correlation coefficients above, together with the coefficient of variation for the concrete, 16.2%, from Degerman (1981) into Eq. 4.27 gives a model uncertainty of 15.5 %. With the same assumptions as above, but taking into consideration the coefficient of variation for the reinforcement (8%) instead of that for the concrete, a model uncertainty of 14.0 % is obtained. The 8% coefficient of variation is assumed to give a high value for the model uncertainty.

When the uncertainties are estimated, one must also has to estimate the mean value of the model uncertainty. In JCSS (2002) (see Table 4.13), the model uncertainty for shear in

concrete is suggested to be lognormal distributed with a mean value of 1.4 and a 25% coefficient of variation. The reason for the high mean value is shown in Figure 7.30.

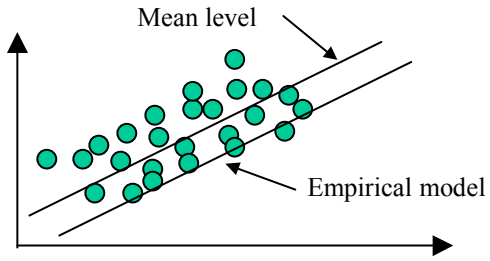

Figure 7.30 Schematic sketch of shear model uncertainty.

Investigations were made when evaluating the shear capacity equations presented in Section 7.4.2. Hedman and Losberg (1975) used their own experiments and results from international sources to establish the design equation for shear in BBK 94 Band 1 (1995), see Eq. 7.9. Two cases investigated by Hedman and Losberg (1975) are of interest here. They investigated the influence of longitudinal reinforcement and the influence of shear reinforcement when using the principle of superposition of shear capacity for beams with and without shear reinforcement, the so-called addition principle.

Hedman and Losberg (1975) expressed the "concrete" contribution V_c to shear capacity as:

$$V_c = (1{,}6 - d) b_w d f_v \qquad \text{Eq. 7.45}$$

where b_w is the beam or slab width, d is the effective depth and f_v is the nominal shear stress given by:

$$f_v = k_c \left(1 + 50 \frac{A_s}{b_w d} \right) \sqrt{f_{cc,cylinder}} \qquad \text{Eq. 7.46}$$

where k_c is a constant with mean value of 0.09 and a 15% coefficient of variation, A_s is the longitudinal reinforcement area and $f_{cc,cylinder}$ is the compressive cylinder strength. This is the mean level model as shown in Figure 7.30

When investigating the principle of addition Hedman and Losberg (1975) used linear regression fitting of results from 249 shear reinforced beams with Eq. 7.47. The coefficient of variation between the measured values and those given by Eq. 7.47 was estimated to be 18%.

$$\frac{V_u}{b_w d \sqrt{f_{cc,cylinder}}} = k_c + \frac{A_{sv} f_{sv} \dfrac{0{,}85d}{s}}{b_w d \sqrt{f_{cc,cylinder}}} \qquad \text{Eq. 7.47}$$

V_u is the total shear capacity, A_{sv} is the shear reinforcement area and f_{sv} is the yield stress of the shear reinforcement.

Comparison of the uncertainties based on the evaluation of the tested beams by Hedman and Losberg (1975) with the model uncertainties according to NKB 36 (1978) shows that they are of the same order of magnitude. For the shear capacity of the trough, Eq. 7.45 together with Eq. 7.46 will be used directly.

In the following analysis shear capacities without stirrups will be calculated, and in this analysis k_c will be assumed to correspond to the model uncertainty. The variable is assumed to be lognormally distributed with mean value of 0.09 and a 15% coefficient of variation, in accordance with data from Hedman and Losberg (1975).

7.8.3 Summary of random variables

Figure 7.7 shows the reinforcement of the trough, and it can be seen that two types of bars, no. 5 and 6, make up the longitudinal reinforcement area A_s. The total reinforcement area can be expressed as in Eq. 7.48:

$$A_s = \frac{A_{s5}}{s_5} + \frac{A_{s6}}{s_6} \qquad \text{Eq. 7.48}$$

where A_{si} and s_i are the bar areas and bar separations for bars i=5 and 6, as seen in Figure 7.7.

From the design drawings it can be seen that the slab thickness varies along the length between 0.3 m and 0.45 m in order to cater for water outflow from the slab. The analysis was performed for the mean thickness, the concrete cover is 30 mm, according to the design drawings and Ø 12 mm reinforcement is used. Eq. 7.49 gives the effective depth.

$$d = 375 - 30 - 12/2 = 339mm \qquad \text{Eq. 7.49}$$

The random variables used to for verification of the shear capacity is summarised in Table 7.25, the random modelling of several of the variables are shown in earlier sections. The concrete properties can be found in section 7.5.9, and the reinforcement properties can be found in section 7.7.4

Table 7.25 Random variables for verification of shear capacity.

Variable	Unit	Symbol	Distribution	Mean value	SD	COV [%]
Slab width	m	b_w	Deterministic	1	-	-
Effective depth of slab	m	d	Deterministic	0.339	-	-
Model uncertainty		k_c	Lognormal	0.09	0.0135	15
Longitudinal reinforcement	mm^2	A_{s5}	Lognormal	113	5.65	5
Bar distance	m	s_5	Deterministic Lognormal	0.3 0.3	- 0.03	- 10
Longitudinal reinforcement	mm^2	A_{s6}	Lognormal	78	3.9	5 5

Variable	Unit	Symbol	Distribution	Mean value	SD	COV [%]
Bar separation	m	s_6	Deterministic Lognormal	0.3 0.3	- 0.03	- 10
Compressive strength	MPa	$f_{cc,cylinder}$	Lognormal	48.1	7.5	15.6
Axle load train BV-4 UIC BV-3	kN	F_{axle}	Normal	249 207 207	24.9 20.7 20.7	10 10 10
Load distribution width	m	b_l	Deterministic	0.65	-	-
Trough span	m	L_{trough}	Deterministic	4.15	-	-
Eccentricity	m	e	Deterministic	0.10	-	-
Dyn. Amp. BV-4 UIC BV-3		φ	Normal, truncated	0.35 0.22 0.35	0.17 0.11 0.17	50 50 50
Girder width	m	b_w	Deterministic	0.85	-	-
Concrete density	kN/m^3	γ_{conc}	Normal	24	0.96	4
Thickness of concrete	m	t_{conc}	Deterministic	0.35	-	-
Ballast density	kN/m^3	γ_{ball}	Normal	20	1	5
Ballast thickness	m	t_{ball}	Deterministic	0.60	-	-

7.8.4 Results

Two different analyses were performed, one in which the separation between the reinforcement bars was assumed to be constant and the other in which the separation between the bars was assumed to be a random variable. The results in terms of safety indices for different load cases are given Table 7.26.

Table 7.26 Safety index for different assumptions regarding bar separation and train loads with related dynamic amplification factors.

Train load	*Deterministic s_1, s_2*	*Random s_1, s_2*
BV-4	2.5	2.5
UIC	3.9	3.9
BV-3	3.3	3.3

BV-4 is decisive and results in the lowest safety index. UIC however, exhibits the highest safety index and this is what desirable. When comparing the safety index for train load UIC with the target safety indices in Table 4.1 it can be seen that the shear capacity of the slab only fulfils the requirements for safety class 1. This result was surprising since the deterministic demand almost was fulfilled, see Figure 7.19. One reason for the discrepancy can depend on the different conversions between compressive strength and tensile strength used by Hedman and Losberg (1975) and used in BBK 94 Band 2 (1994).

Hedman and Losberg (1975) suggest that the nominal shear stress that was proportional to the mean compressive cylinder strength ($\sqrt{f_{ccm}}$) as shown in Eq. 7.46, should be replaced with 25% of the characteristic tensile strength ($0{,}25 f_{ctk}$). In BBK Band 2 (1994) is 30% of

the characteristic tensile strength used as seen in Eq. 7.9. This increase of 20% of the characteristic tensile strength does of course have a positive influence on the deterministic shear capacity, which is not taken into consideration in the reliability analysis.

Table 7.27 Sensitivity analysis of shear capacity with train load UIC.

	Deterministic s_1, s_2		*Random s_1, s_2*	
Basic variable	α	α^2	α	α^2
Longitudinal reinforcement (A_{s5})	0.013	0.000	0.013	0.000
Longitudinal reinforcement (A_{s6})	0.009	0.000	0.009	0.000
Dynamic amplification (φ)	-0.331	0.110	-0.331	0.110
Axle load train (F_{axle})	-0.360	0.130	-0.360	0.130
Compressive strength (f_{cd})	0.402	0.161	0.402	0.161
Ballast density (γ_{ball})	-0.032	0.001	-0.032	0.001
Concrete density (γ_{conc})	-0.018	0.000	-0.018	0.000
Model uncertainty (k_C)	0.773	0.598	0.773	0.597
Separation (s_5)	-	-	-0.026	0.001
Separation (s_6)	-	-	-0.018	0.000
	$\Sigma\alpha^2$	**1.000**	**$\Sigma\alpha^2$**	**1.000**

From the sensitivity analysis, the results of which are given in Table 7.24, it can be seen that the shear factor (k_C) is the dominating variable. If this uncertainty can be reduced the safety index would increase notably. It can also be seen that the bar separation can be assumed to be deterministic since this uncertainty has a negligible influence on the safety index.

7.9 Random modelling of trough bending capacity

The bending capacity of the trough slab is insufficient according to the deterministic analysis as presented earlier (Figure 7.18). A probabilistic analysis will be described in this section based on the same assumptions as those used for the deterministic analysis.

7.9.1 The limit state equation

The bending moment capacity at the middle of the trough is the sum of the capacity at the support based on the top reinforcement and the capacity at the mid section of the slab based on the reinforcement at the bottom of the slab. This value is compared with the bending moment at the middle of the slab. Despite the fact that the maximum moment is slightly eccentric, the difference is negligible.

$$C\left(M_R^{top} + M_R^{bottom}\right) - M_S \geq 0 \qquad \text{Eq. 7.50}$$

C is the model uncertainty, M_R is the bending moment capacity, and M_S is the bending moment at the middle of the trough, under the assumption that the trough is simply supported at the girders.

The bending moment capacity is calculated as follows:

$$M_R = f_{st} A_s (d - 0{,}4x) \qquad \text{Eq. 7.51}$$

where f_{st} is the yield stress, A_s is the reinforcement area of the position of interest, calculated according to Eq. 7.48, bar separation given in Table 7.2, d is the effective depth at the section of interest and x is the depth of the compressive zone in the section of interest, calculated according to Eq. 7.52. For M_R^{top} bars no. 5 and 6 in Table 7.2 were used, and for M_R^{bottom} bars no. 1 and 4 were used from the same table.

$$x = \frac{A_s f_{st}}{f_{cc} b \cdot 0.8} \qquad \text{Eq. 7.52}$$

Here f_{cc} is the cylinder compressive strength, b is the width, in this case set to 1 since both load and capacity are calculated per metre.

For the support section the effective depth is, d^{top} = 330 mm, see Eq. 7.49. With an assumed mean thickness of 375 mm and a 30 mm cover together with a 10 mm mounting reinforcement the effective depth in the mid section is given by Eq. 7.53. The reinforcement diameter was Ø 16 mm at the position of interest.

$$d^{bottom} = 375 - 30 - 10 - 16/2 = 327mm \qquad \text{Eq. 7.53}$$

The bending moment (M_S) disregarding the eccentricity is calculated as

$$M_S = M_{dead} + M_{ballast} + M_{train} \qquad \text{Eq. 7.54}$$

M_{dead} is the bending moment resulting from the dead load, $M_{ballast}$ is the bending moment from the ballast and M_{train} is the bending moment from the train load.

$$M_{dead} = \gamma_{conc} t_{conc} \left(\frac{L_{trough}}{2} \frac{\left(L_{trough} - b_w\right)}{2} - \frac{1}{2}\left(\frac{L_{trough}}{2} - \frac{b_w}{2} \right)^2 \right) \qquad \text{Eq. 7.55}$$

γ_{conc} is the concrete density, t_{conc} is the concrete thickness of the trough bottom, L_{trough} is the trough span and b_w is the width of the main girder. Geometric variables are shown in Figure 7.16.

$$M_{dead} = \gamma_{ball} t_{ball} \left(\frac{L_{trough}}{2} \frac{\left(L_{trough} - b_w\right)}{2} - \frac{1}{2}\left(\frac{L_{trough}}{2} - \frac{b_w}{2} \right)^2 \right) \qquad \text{Eq. 7.56}$$

γ_{ball} is the ballast density and t_{ball} is the ballast thickness.

$$M_{train} = (1 + \varphi) \frac{F_{axle}}{2 \cdot b_l} \left(\frac{L_{trough}}{2} + e - \frac{\left(L_{trough}/2 - 0{,}65 \right)^2}{b_{sleeper}} \right) \qquad \text{Eq. 7.57}$$

φ is the dynamic amplification factor, F_{axle} is the axle load, b_l is the lengthwise load distribution width, $b_{sleeper}$ is the sleeper width, L_{trough} is the trough span and e is the prescribed eccentricity between the track and the centre of the bridge.

7.9.2 Model uncertainties

The model uncertainty for the bending capacity was estimated according to the principles in NKB 36 (1978), see Section 4.9. The accuracy of the calculation model, which in this case is determined the by bending of the cross section, can be assumed to be *good*. Table 4.10 gives a coefficient of variation of V_{I_1} =0.04 and a correlation coefficient of ρ_1= -0.3 for the correlation between the model uncertainty and the coefficient of variation for the reinforcement. The possible deviation between the strength of the reinforcement in the structure compared to the strength from control specimens, can in this case be regarded as *small*, see Table 4.11. This gives a coefficient of variation of V_{I_2} =0.04 and a correlation coefficient of ρ_2= -0.3. Since the bending model is regarded as well established the bending capacity is related to the smaller variability of the reinforcement steel. The final factor influencing the model uncertainty is the degree of control on site. Available information does not indicate that the control was anything but normal, giving a coefficient of variation of V_{I_3} =0.06 and a correlation coefficient of ρ_3=0, see Table 4.12. The coefficient of variation for the reinforcement given by Degerman (1981) is 5.7%, see Table 7.21. Eq. 4.27 then gives a model uncertainty of 7.4 %.

7.9.3 Summary of random variables

The bending moment capacity was assessed for all train loads, in the same manner as previously. A summary of the random variables involved is given in Table 7.28.

Table 7.28 Random variables for verification trough bending capacity.

Variable	Unit	Symbol	Distribution	Mean value	SD	COV [%]
Top reinforcement	mm^2	A_{s5}	Lognormal	113	5.65	5
Top reinforcement	mm^2	A_{s6}	Lognormal	78	3.9	5
Yield strength	MPa	f_{st}	Lognormal	679.9	37.8	5.7
Compressive strength	MPa	f_{cc}	Lognormal	48.1	7.5	15.6
Separation top reinf.	m	s_5	Deterministic Lognormal	0.3 0.3	- 0.03	- 10
Separation top reinf.	m	s_6	Deterministic Lognormal	0.3 0.3	- 0.03	- 10
Effective depth	m	d^{top}	Deterministic	0.339	-	-
Bottom reinforcement	mm^2	A_{s1}	Lognormal	113	5.65	5
Bottom reinforcement	mm^2	A_{s4}	Lognormal	201	10	5

Variable	Unit	Symbol	Distribution	Mean value	SD	COV [%]
Separation bottom reinf.	m	s_1	Deterministic Lognormal	0.3 0.3	- 0.03	- 10
Separation bottom reinf.	m	s_4	Deterministic Lognormal	0.3 0.3	- 0.03	- 10
Effective depth	m	d^{bottom}	Deterministic	0.327	-	-
Axle load train BV-4 UIC BV-3	kN	F_{axle}	Normal	249 207 207	24.9 20.7 20.7	10 10 10
Load distribution width	m	b_l	Deterministic	0.65	-	-
Trough span	m	L_{trough}	Deterministic	4.15	-	-
Eccentricity	m	e	Deterministic	0.10	-	-
Dyn. Amp. BV-4 UIC BV-3		φ	Normal, truncated	0.35 0.22 0.35	0.17 0.11 0.17	50 50 50
Girder width	m	b_w	Deterministic	0.85	-	-
Sleeper width	m	b_{sleep}	Deterministic	2.65	-	-
Concrete density	kN/m^3	γ_{conc}	Normal	24	0.96	4
Thickness of concrete	m	t_{conc}	Deterministic	0.35	-	-
Ballast density	kN/m^3	γ_{ball}	Normal	20	1	5
Ballast thickness	m	t_{ball}	Deterministic	0.60	-	-
Bending model uncertainty		C	Lognormal	1	0.074	7.4

7.9.4 Results

Table 7.29 show that the bending moment capacity is insufficient for train loads BV-4 and BV-3 but sufficient for train load UIC. The results in Table 7.29 differ from the deterministic results in that the deterministic results indicated that the load carrying capacity was insufficient for all train loads. This analysis is performed with the same assumptions.

Table 7.29 Safety index for different assumptions regarding bar separation and train loads with related dynamic amplification factors.

Train load	*Deterministic s*	*Random s*
BV-4	3.2	3.1
UIC	5.3	5.0
BV-3	4.3	4.1

It can be seen from Table 7.30 that the axle load and the dynamic amplification factor are the dominating load variables, and that the model uncertainty together with the yield strength of the reinforcement are the dominating resistance variables.

Table 7.30 Sensitivity analysis of suspension capacity with train load UIC.

	Deterministic s		*Random s*	
Basic variable	α	α^2	α	α^2
Axle load train (F_{axle})	-0.500	0.250	-0,471	0,222
Reinforcement (A_{s1})	0.083	0.007	0,078	0,006
Reinforcement (A_{s4})	0.144	0.021	0,129	0,017
Reinforcement (A_{s5})	0.087	0.008	0,082	0,007
Reinforcement (A_{s6})	0.061	0.004	0,058	0,003
Model uncertainty (C)	0.564	0.318	0,522	0,273
Dynamic amplification (φ)	-0.465	0.217	-0,436	0,190
Compressive strength (f_{cc})	0.020	0.000	0,017	0,000
Yield strength (f_{st})	0.417	0.174	0,386	0,149
Ballast density (γ_{ball})	-0.037	0.001	-0,036	0,001
Concrete density (γ_{conc})	-0.022	0.000	-0,021	0,000
Separation (s_1)	-	-	-0,156	0,024
Separation (s_4)	-	-	-0,260	0,067
Separation (s_5)	-	-	-0,163	0,027
Separation (s_6)	-	-	-0,116	0,013
	$\Sigma\alpha^2$	1.000	$\Sigma\alpha^2$	1,000

7.10 Time-variant reliability analysis

Calculation of the safety as a function of time is done under the assumption that the reinforcement is continuously damaged due to corrosion. A time-variant expression for the residual area is developed and used for the purpose of predicting when the safety index becomes less than the required level. Loads and all other random variables are modelled in the same way as for the time-invariant analysis.

Based on measurements of the current reinforcement area, the safety index can be estimated both for the shear capacity of the girder and for the suspension reinforcement. Under the assumption that the decrease of the reinforcement area is linear with time it is possible to predict the future mean value and variance of the residual area using the following algorithms. The prediction of these parameters does not rely on any distributional assumptions.

Two different methods of prediction are suggested. They differ both in the amount of needed information and how available information is used. A common requirement for the methods is that the information regarding the residual area on different occasions in time must be linked to specific bars, i.e.

$$A_i = A_i(t) \qquad \text{Eq. 7.58}$$

where A_i is the residual area for bar i, and t is the time elapsed since initiation of corrosion.

7.10.1 Method A

This method is a simple linear extrapolation of both the mean value and the standard deviation obtained at time T_0. After Δt years into the future, i.e. at time $T_1 = T_0 + \Delta t$, the residual area is assumed to have decreased by a factor

$$K_1 = T_0 / T_1 \qquad \text{Eq. 7.59}$$

where T_0 is the elapsed time from initiation of corrosion to the time of the first observation (in this case equal to the age of the structure). This means that we make the following predictions for the values that we will obtain at time T_1:

$$\hat{x}_i(T_1) = K_1 x_i(T_0) \qquad \text{Eq. 7.60}$$

$$\hat{s}_{x(T_1)} = K_1 s_{x(T_0)} \qquad \text{Eq. 7.61}$$

7.10.2 Method B

Method A is a rather crude approach to the problem. Behind method B there are two new ideas. The first one is that the variation of the measurements shown in Table 7.3 consists of two parts: one is a measuring and evaluation error, and one comes from the variation in true residual area between bars. If the measuring error can be estimated from multiple measurements on the same sample, this part of the variance can be excluded in the extrapolation of the future state leading to a more realistic prediction of the variability of future values.

The second new idea is that when, at time T_1, we want to estimate the residual area, we have at our disposal not only the measurements obtained at time T_1 but those obtained at T_0 as well, and that also these provide information.

Assume a measuring error ε with zero expectation and standard deviation σ_ε. This makes it possible to write an observation x_i taken at time t as

$$x_i(t) = A_i(t) + \varepsilon_i(t) \qquad \text{Eq. 7.62}$$

where A_i is the residual area for an individual bar and ε_i is the measuring error. Thus it is now important to distinguish between the true residual area A_i and the measured value x_i of that residual area; in particular one should note the distinction between σ_A and σ_x.

Our model assumes that the true residual area at time $T_1 = T_0 + \Delta t$ will be

$$A_i(T_1) = K_1 A_i(T_0) \qquad \text{Eq. 7.63}$$

with the same K_1 as before; thus our prediction of what will be observed at time T_1 is

$$\hat{x}_i(T_1) = K_1 x_i(T_0) \qquad \text{Eq. 7.64}$$

just as in Method A. However, our prediction of the variability at time T_1 will be different: the observations at time T_1 will be given by

$$x_i(T_1) = A_i(T_1) + \varepsilon_i(T_1) \qquad \text{Eq. 7.65}$$

where the standard deviation of the first term is, according to our model,

$$\sigma_{A(T_1)} = K_1 \sigma_{A(T_0)} \qquad \text{Eq. 7.66}$$

but, and that is one of the points of Method B, the $\varepsilon_i(T_1)$ have the same standard deviations as the original $\varepsilon_i(T_0)$ that were active at time T_0. This means that our model gives

$$\sigma^2_{x(T_1)} = \sigma^2_{A(T_1)} + \sigma^2_{\varepsilon} = K_1^2 \sigma_{A(T_0)} + \sigma^2_{\varepsilon} \qquad \text{Eq. 7.67}$$

and since

$$\sigma^2_{x(T_0)} = \sigma^2_{A(T_0)} + \sigma^2_{\varepsilon} \qquad \text{Eq. 7.68}$$

the model tells us that

$$\sigma^2_{x(T_1)} = K_1^2 \left(\sigma^2_{x(T_0)} - \sigma^2_{\varepsilon}\right) + \sigma^2_{\varepsilon} = K_1^2 \sigma^2_{x(T_0)} - \left(K_1^2 - 1\right)\sigma^2_{\varepsilon} \qquad \text{Eq. 7.69}$$

Hence our prediction of the sample variance at time T_1 is

$$\hat{s}^2_{x(T_1)} = K_1^2 s^2_{x(T_0)} - \left(K_1^2 - 1\right)\sigma^2_{\varepsilon} \qquad \text{Eq. 7.70}$$

In particular one should note that the predicted variance is not equal to the variance among the predicted values.

Now we address the second new feature in Method B. When we have, at time T_1, the new observations $x_i(T_1)$ we can combine them with information from time T_0, the latter e.g. in the form $\hat{x}_i(T_1)$ $(= K_1 x_i(T_0))$. Clearly the same trust cannot be placed in both types of values and in order to minimise the impact of measurement errors a weight factor θ is introduced; the object is to minimise the variance of the measurement error part of

$$z_i = \theta x_i(T_1) + (1-\theta)\hat{x}_i(T_1) \qquad \text{Eq. 7.71}$$

Since the contribution of measurement errors to z_i is

$$\theta \varepsilon_i(T_1) + (1-\theta) K_1 \varepsilon_i(T_0) \qquad \text{Eq. 7.72}$$

the quantity to be minimised is

$$\left(\theta^2 + \left(1-\theta^2\right)K_1^2\right)\sigma^2_{\varepsilon} \qquad \text{Eq. 7.73}$$

and it is easy to see that the minimum is obtained when

$$\theta = \frac{K_1^2}{1+K_1^2} \qquad \text{Eq. 7.74}$$

With this choice of θ we have

$$\sigma_z^2 = K_1^2 \sigma^2_{A(T_0)} + \frac{K_1^2}{1+K_1^2}\sigma^2_{\varepsilon} \qquad \text{Eq. 7.75}$$

and, once again using Eq. 7.69, we find

$$\sigma_z^2 = K_1^2 \sigma^2_{x(T_0)} - \frac{K_1^4}{1+K_1^2}\sigma^2_{\varepsilon} \qquad \text{Eq. 7.76}$$

Thus at time T_0 our prediction of the sample variance among the z_i at time T_1 is

$$\hat{s}_z^2 = K_1^2 s_{x(T_0)}^2 - \frac{K_1^4}{1+K_1^2}\sigma_\varepsilon^2 \qquad \text{Eq. 7.77}$$

Clearly Method B assumes that we have independent information on σ_ε^2, obtained e.g. from multiple measurements on the same bar on the same occasion.

7.10.3 Extrapolated safety indices

In the original assumption regarding the area (A_0) of the stirrups it is assumed that the reinforcement has a 5% coefficient of variation. A_0 is lognormally distributed with a mean value o 113 mm^2 and standard deviation of 5.65 mm^2, for each leg of the stirrups. Calculations based on information in Table 7.3 and Eq. 7.4 and Eq. 7.5 give an residual reinforcement area in 2001 that is assumed to lognormally distributed with a mean value of 92 mm^2 and a standard deviation of 13.3 mm^2. This value will be introduced into the limit state equations for suspension reinforcement to calculate the safety index for year 2001.

Two types or bars are used for the suspension capacity; see section 7.3.2 and Figure 7.7. In a deterministic analysis it was checked how much of the stirrups (Bar 3 in Figure 7.7) that was available to be used as suspension reinforcement. The result was that 103 mm^2 could be used for this purpose, as seen in Table 7.31.

With the information concerning the residual area in 2001, Method A (see Section 7.10.1) was used to extrapolate the mean value and variance of the residual reinforcement area. The results are shown in Table 7.31. Intervals of six years were used since the Swedish National Railroad Administration uses this as the shortest time interval between two major inspections (Vägverket 1993a).

Table 7.31 Time-variant safety index for suspension capacity, mean and standard deviation for corroded reinforcement area. Load combination *A* and different train loads.

	Bar nr 1 (Figure 7.7)			Bar nr 3 (Figure 7.7)			*Safety indices*		
Year	μ_A [mm^2]	σ_A [mm^2]	COV [%]	μ_A [mm^2]	σ_A [mm^2]	COV [%]	β (BV-4)	β (UIC)	β (BV-3)
1946	113	5.65	5	103	5.15	5	6.3	8.4	7.3
2001	92.0	13.3	14	83.9	11.7	14	4.3	5.9	5.1
2007	89.3	14.7	16	81.4	13.0	16	4.0	5.4	4.8
2013	86.5	16.4	19	78.8	15.0	19	3.6	4.9	4.3

When comparing the results in Table 7.31 with the target safety indices given in Table 4.1 it can be seen that the suspension capacity of the bridge is insufficient in 2001 for train load BV-4. However, there is sufficient suspension capacity for train load UIC until year 2013.

In the deterministic analysis it was shown that the suspension capacity was almost sufficient for train load BV-4 in 2001 (Table 7.9) but this is not the case in the probabilistic analysis as can be seen in Table 7.31. The difference can be explained by the fact that the

uncertainty related to the residual reinforcement area is taken into account in the probabilistic analysis. This uncertainty is then increased as the residual reinforcement area is extrapolated, leading to a more rapid reduction in safety during the probabilistic analysis than in the deterministic analysis. The probabilistic approach is, however, more reliable than the deterministic one, since there is truly a large uncertainty and the prediction models also create extra uncertainties.

7.11 Summary

A two-span trough Railway Bridge in Malmö showed signs of corrosion upon ocular inspection. A detailed investigation of the load carrying capacity and residual service life was initiated with the purpose of finding the largest possible train load that could be allowed on the bridge. The train loads investigated are BV-4, UIC and BV-3, ranked in descending order after their axle loads, including dynamic amplification factor.

Concrete cores were removed from the bridge to measure the current material properties. The properties measured were splitting tensile strength, compressive strength and the modulus of elasticity. Both the splitting tensile strength and the compressive strength must to be converted in order to obtain the properties that are used in the design equations suggested in BBK 94 Band 1 (1995). Conversions were made for the size of the cores, from splitting tensile strength to tensile strength, as well as conversion from cube compressive strength to cylinder compressive strength. Three different evaluations were made of the measured properties, two deterministic ones, following Banverket (2000) and prEN 13791:1999, and another based on statistics. A discrepancy was found in the results between the deterministic methods and the statistical one.

A very important factor when evaluating the *in situ* strength is the position of the removed cores. If the cores are taken at positions as required in BBK 94 Band 2 (1994), i.e. where the strength is low or at positions where the structure is highly stressed the results from Banverket (2000) is easier to accept. But if practical reasons makes it impossible to remove cores from these positions, the evaluation method in Banverket results in high strength.

During the assessments of the bridge in accordance with Banverket it could be seen that the load carrying capacity for the main girders was sufficient in the undamaged state for all the investigated train loads. The slab between the two main girders was however highly utilised with respect to shear, bending and suspension capacity.

A deterministic time-variant analysis was performed based on the measured residual reinforcement area and the load carrying capacity in the damaged state was calculated. This indicated that the capacities related to the corroding bars were sufficient at present, but that the suspension capacity of the trough would be insufficient before the bridge reached its desired service life of 100 years.

Sections found to be critical in the deterministic analysis were analysed with reliability theory. Reliability analysis showed that the suspension capacity was sufficient in 2001 for train loads UIC and BV-3. BV-3 was the only train load that was safe with respect to the suspension capacity six years into the future. This result is based on extrapolation of both

mean value and variance of the measured residual area in 2001. The probabilistic analysis leads to an unsafe structure in a shorter time period than the deterministic analysis.

Calculations of the shear capacity of the trough were found less favourable with reliability theory than with deterministic analysis, while the opposite was found for the bending capacity. A higher bending capacity could be proved with reliability theory than with the deterministic analysis.

7.12 Conclusions

Evaluation of the material parameters investigated is crucial for the load carrying capacity or safety of the bridge since the strength of the concrete has a very large influence on the load carrying capacity. This is especially important with respect to the tensile strength of the concrete since this in many failure modes is directly proportional to the load carrying capacity. A comparison between the deterministic evaluation of the test results and the more direct statistical method shows that the deterministic evaluation according to Banverket (2000) results in higher characteristic values.

One reason for the high utilisation of strength in the structure, based on the measured concrete strengths can perhaps be found in the fact that the evaluation proposed in BBK 94 Band 2 (1994) is not intended to be used as suggested in Banverket (2000). The method in BBK 94 Band 2 is intended to be used by concrete manufacturers who by some reasons needs to verify that concrete of the correct strength is delivered from the plant after casting has taken place. This situation is very different from the situation in which one wants to prove that measured data can be used to increase the allowable stresses in the structure. The same objections seem to be relevant for prEN 13791:1999 that will replace the Swedish codes in the future.

Other very important parameters in reliability analysis are the model uncertainties related to different failure modes or failure mechanisms. The guidance given in NKB 55 (1987) is not sufficient; and reference should be made to NKB 36 (1978) if more specific information related to the actual failure modes cannot be given. From the sensitivity analysis it is obvious that the model uncertainties are the dominating variables in the reliability analysis.

From BKR (2000) reference is made to ISO 2394-1998, where it is stated that parameters that are of importance should be considered as random variables. This contradicts what is suggested in NKB 55 (1987) regarding geometric variables. In NKB 55 it is suggested that geometric variables be assumed to be deterministic variables. But, as shown by the sensitivity analysis and the various assumptions regarding bar separation, geometric properties can be of importance. The middle way suggested in JCSS (2002) is preferable. Here it is assumed that geometric variables consists of two parts, a deterministic part and a random error, see Section 4.8.

Sensitivity analysis indicates that the dynamic amplification factor is of considerable importance for the safety of the bridge. The size of the amplification factor is evaluated in a crude manner giving safe values on the safe side. This is good enough for design of new structures, but for the evaluation of load carrying capacities of existing bridges, the possible savings with refined descriptions of dynamic amplification factors could be large. If

reliability analysis is to be used, effort should also be devoted to find a statistical description of the dynamic amplification factor.

If reliability analysis is to be used when predicting future states of a structure, special consideration should be taken in estimating the measuring error of the test method. If this is done, this error can be excluded from the extrapolation of the future value of the parameter. This is important since a reduced uncertainty leads to a higher safety of the structure and for the same reason should be predictions more than 10 to 15 years into the future be avoided. Instead should a system be created that is open for new information, making it possible to refine the prediction when new information becomes available.

8 SUMMARY AND CONCLUSIONS

8.1 General considerations

Assessing the safety of existing structures is a difficult task and the economical consequences of the outcome are often significant. Structures can be judged inadequate for further use and expensive repair, or demolition and erection of a new structure, may be required. Due to the importance of this kind of assessment it may be of interest to perform in-depth analysis of the structural safety using reliability theory in order to utilise the structural capacity to its maximum.

The objective of assessing an existing structure which is subject to deterioration, without the intention of repairing it, is to answer the following two questions.

1. Is the structure safe to use now?
2. For how long will it continue to be safe to use?

8.2 Assessment procedure

For the purpose of creating a dialogue between the owner of the structure to be assessed and the engineer performing the assessment, a three-phase investigation process has been proposed by Schneider (1994). It consists of a Preliminary Evaluation, a Detailed Investigation and a phase called Finalising the Decision among a Team of Experts. After each step a discussion is held between the engineer and the owner, and decisions are made jointly regarding continued work. Finalising the decision amongst a team of experts is a situation similar to writing a structural design code and could therefore be regarded as defining an object specific code for the damaged structure.

To answer the first of the questions posed above, an approach suggested by Enevoldsen and Jensen (2000) was adopted, i.e. the safety requirements are stated based on the legal documents relevant for the structure. When the safety requirements have been identified, deterministic models are used to find critical failure modes and sections.

When trying to predict the residual service life it is important to have access to relevant deterioration models describing how the load carrying capacity will be affected by ongoing deterioration. It is the author's belief that it also is important to choose deterioration models based on parameters that can be monitored, since the prediction of the future behaviour is very uncertain. A good approach is to limit predictions of the future state to five to ten years, and after this period of time go to measure what has actually happened and compare the findings with the predicted results. Effort should be made to create recursive algorithms for this purpose from the beginning; hence the importance of choosing deterioration models with measurable parameters. A system should be ready and waiting for information from the latest inspection. After the incorporation of this information into the system the future status of the structure can be predicted with a higher degree of reliability.

8.3 Basis of design

Reliability analysis is allowed for Swedish structures, according to BKR (2000), which makes reference to NKB 55 (1987). To make reliability-based codes practically useful, the following cornerstones are required.

- Definitions regarding analysis methods
- Distribution functions for the stochastic variables
- Model uncertainties
- Target safety

Besides the distribution functions, model uncertainties are very important for the outcome of an analysis and recommendations are lacking in NKB 55. The information here is not sufficient. To achieve a useful reliability-based code, information is needed from its predecessor, NKB 36 (1978). The safety achieved is affected both by the actual value of the model uncertainty and also by the manner in which it is applied in the analysis. As an alternative to NKB 36, actual test data can be used to evaluate the discrepancy between measured values and values predicted using a design mode.

The main reason for choosing lognormally distributed resistance parameters and normally distributed loads, as suggested in NKB 55, is a lack of information. When working with loads for a one-year reference period extrapolated from measurements made over shorter time periods where the loads can be regarded as independent between periods, an extreme value distribution is the natural choice. Still NKB 55 prescribes that variable loads should be modelled normally distributed, and Swedish codes are calibrated under this assumption. For e.g. snow load, a normal distribution is as good as any distribution, since there is actually no information available about the tail. The annual maximum snow load is not the result of maximum of snow loads form shorter periods within one year, but rather an accumulated effect of snowfall during the year. For other loads, such as wind and traffic loads on bridges, however, an extreme value distribution would be more correct, since the annual maximum comes from maximum of loads which are more or less independent. Simulation techniques and extreme value theory, however, make it possible to evaluate the tails. In NKB 55 (1987) it is stated that parameters that can be shown to have a distribution other than normal or lognormal can be applied, and during analysis these distributions should be approximated by normal distributions at the design point.

Depending on which code is used, different suggestions are made regarding which parameters should be regarded as random and which are deterministic. NKB 55 refers to ISO2397-1998 and where it is stated “if the uncertainty of a random variable is judged to be important, either by experience of by sensitivity it shall be represented as a random variable”. This judgement can lead to large considerable differences in the calculated safety index, depending on who is doing the judging.

The choice of distribution function for the random variables are very important during calibration of codes in order to get a consistent level of safety. During assessment, more complex limit state functions are used, compared to the calibration situation. The complex limit state functions leads to arbitrary joint distribution functions independent of what distributions that are originally assumed for the basic random variables. This joint

distribution function is then used for the calculation of the failure probability. It is therefore not as important during assessment to use prescribed distributions as it is during calibration.

8.4 Test cases

8.4.1 The dam

A discrepancy was found regarding the geometry of the dam column, showing that the rock surface under the column was inclined, and not horizontal as assumed during design. This deviation between assumptions during design and in reality is probably not unique for this structure, and may be the case for many structures throughout the world. It is suggested that during the design of dams, the stability should be recalculated after the rock surface has been prepared, in the same manner that is done with pile groups for bridges. Discrepancies between theory and practice will then be taken into account and measures can be taken if problems arise.

During the reliability analysis much attention was placed on modelling the stochastic variables in accordance with the basis of design presented in Chapter 4. It was found that the ice load in RIDAS (2000) should be connected to a reference period or defined as a characteristic value. Investigations should be made to ensure that the load description employed follows the definitions in BKR (2000). Input for such an investigation could be found in the literature review by Ekström (2002).

A similar literature review should be carried out in order to establish the characteristics of the friction coefficient since it is decisive in failure due to sliding. During these investigations, finding methods of measuring of the parameters of interest for description of sliding resistance should be given high priority.

From the dam case it became apparent that the safety philosophy involving probabilistically calibrated partial factors, related to nominal predefined values of strength and load parameters, had not yet reached all parts of the construction industry. A full probabilistic calibration is suggested for RIDAS (2000) in order to fully adopt the safety philosophy into BKR (2000).

It is difficult to make any conclusive statements on the influence of monitoring the uplift pressure since the analysis presented is based on fictitious values. The method of introducing new data into the reliability analysis is crude, but will probably be sufficient.

8.4.2 The railway bridge

From the railway bridge case it became evident that access to old design codes, and background information for these codes, is of great importance for both deterministic and reliability analysis. Old codes are helpful when evaluating both material parameters and loads as stochastic variables, but not sufficient.

Evaluation of the stochastic properties of the material parameters demands a great deal of work. The nomenclature is not the same today as it was in 1955, so the available

information is not always easy to interpret. The reinforcement properties were evaluated based on information given by Degerman (1981), although these data were not old enough. Concrete properties were evaluated using both recommendations from Banverket (2000) and statistical methods, and it is obvious that Banverket allows for a higher utilisation of the strength in the structure based on the test cores.

During the statistical evaluation it became obvious that a model was needed to take into account the hardening of the concrete, otherwise there would be a large discrepancy between the a priori information and the tested data. This discrepancy overshadows the positive influence of Bayesian updating making the statistical evaluation useless.

A strength development model, see e.g. Fagerlund (1996) was used giving a deterministic hardening curve. Work is needed to describe the parameters involved as random variables. If this were done, it would be possible to compare concrete of a known age with test results. If a large discrepancy exists between the two, the possibility of ongoing concrete deterioration should be investigated. There is also a need to quantify the error related to the conversions between different geometries and sizes of the samples, i.e. cubes to cylinders etc.

Safety requirements were established for the bridge since it was clearly stated that safety class 3 was used. However, in order to perform reliability analysis model uncertainties are also needed and NKB 55 (1987) does not give enough information to determine these. Information was therefore taken from NKB 36 (1978) for this purpose.

Reliability does not always result in an increase in the permissible load, but the procedure of doing the assessment has the same positive influence as a risk analysis. It becomes evident which variables have the greatest influence on the safety, indicating where money is best spent in order to increase the permissible load.

Time-variant reliability analysis also highlights the importance of accurate deterioration models, since the uncertainties related to these model can overshadow the uncertainties related to the load carrying capacity, leading to insufficient safety indices. This test case shows that the problem of measuring the corrosion rate yet has to be solved if service life predictions are to be made for corroding concrete structures. The technique used in the present thesis involves to large measuring error.

8.5 Further work

Governmental agencies, such as the Swedish National Railroad Administration and the Swedish National Road Administration should, strive to compile a common database with all the design codes ever used in Sweden. At the same time, should efforts be made to recover as much background material as possible from universities and other institutions that have been involved in work with on these codes. This information could, to some extent be used to define suitable model uncertainties for the models used in modern Swedish design codes.

Further work should focus on creating guidelines for the practicing engineer. Guidance must be given regarding model uncertainties for the different failure mechanisms that are possible, such as bending, shear, anchorage, punching shear, localized loading, etc.

When tomorrow's engineers assess the structures designed today, the same recommendations will of course apply to our present code system. All background information should carefully preserved in order to help explain why things are the way they are.

If and when changes are to be made of the codes, they should be thoroughly documented, preferably by someone who has not been involved in the modification discussions in order to ensure objective documentation. At the same time as the background information is collected for the design codes, efforts should be made to describe traffic loads, both trains and road traffic, as random variables.

The National Railroad and Road Administrations should also give serious thought to suggestions made by Schneider about what he calls Finalising the Decision among a Team of Experts. This approach would give the authorities the means to assess and utilise structures that do not comply with the codes of today. If a group of experts can agree on the fact that a structure is safe to use, it probably is safe to use. There may be legislative problems associated with this approach but the possibility should at least be investigated.

A tool to evaluate the change in the strength of concrete over time should be developed if statistical evaluations are to be made of concrete properties since the only data for use, as a priori information is for 28-days-old concrete. With this tool, it would be possible to define a system based on Bayesian updating for the purpose of high utilisation of the concrete test results obtained during assessment. At the same time, uncertainties related to transformation from, for instance, cylinder to cube strength, or from splitting tensile strength to uniaxial tensile strength, should be quantified.

REFERENCES

AB Svensk Byggtjänst (1990). *Betonghandboken – Konstruktion, Utgåva 2 (Concrete Design Handbook, in Swedish).* ISBN 91-7332-533-3.

AB Svensk Byggtjänst (1994). *Betonghandboken – Material, Utgåva 2 (Concrete Material Handbook - Second Edition, in Swedish)*. ISBN 91-7332-709-3.

Banverket (2000). *Bärighetsberäkning av järnvägsbroar (Assessment of Railway Bridges, in Swedish).* Handbok BVH 583.11, Issued2000-03-11.

BBK 94 Band 2(1994). *Boverkets handbok om betongkonstruktioner, Band 2, Material, utförande, kontroll (Swedish Board of Housing, Design handbook for concrete, Volume 2, Material, Execution and Control, in Swedish).* ISBN 91-7332-687-9, Boverket 1994.

BBK 94 Band 1 (1995). *Boverkets handbok om betongkonstruktioner, Band 1, Konstruktion (Swedish Board of Housing, Design Handbook for Concrete, Volume 1, Design, in Swedish).* Boverket, Byggavdelningen, ISBN 91-7147-235-5, ISSN 1400-1012, Boverket 1995.

Bernstone, C (2000). *Instrumentering för kontinuerlig övervakning av betongdammar, litteraturgenomgång. (Instrumentation for Continuous Monitoring of Concrete Dams, the state of the art, in Swedish)*. VUAB-Report 20000-10-14.

Bickley, J A and Liscio, R. (1997). *Monitoring Parking Structure Repairs*. Concrete International, January 1997, pp 34-40.

BKR (1998). *Boverkets Konstruktionsregler, BFS 1993:58 med ändringar t.o.m. BFS 1993:39 (Design Regulations of Swedish Board of Housing, Building and Planning BKR, in Swedish),* November, 1998.

BKR (2000). *Design Regulations of the Swedish Board of Housing, Building and Planning BKR*. Swedish Board of Housing, Building and Planning, June 2000, ISBN: 91-7147-616-4, ISSN: 1100 0856

Blom, G (1984). *Sannolikhetsteori med tillämpningar, Andra Upplagan.* (*Probability Theory and Applications, Second Edition, in Swedish)*. Studentlitteratur, ISBN 91-44-04372-4

Blom, G and Holmquist, B. (1970). *Statistikteori med tillämpningar. Tredje Upplagan*. (*Statistical Theory and Applications, Third Edition, in Swedish*) Studentlitteratur, ISBN 91-44-00323-4

Bowles, D S and Anderson, L R. (2001). *Dam Safety Risk Assessment: What Can We Currently Use if For?* ICOLD – 69th Annual Meeting, Dresden. DTK Workshop, Vol. 1. pp 410-438

Broomfield, J P, Davies, K and Hladky, K. (2002). *The Use of Permanent Corrosion Monitoring System in New and Existing Reinforced Concrete Structures.* Cement & Concrete Composites 24. pp 27-34. Elsevier Science Ltd.

Calgaro, J-A (1998). *Loads on bridges*. Progress in structural engineering and materials, 1998, Vol. 1(4): 452-461

Carlsson F. (2002). *Reliability Based Assessment of Bridges with Short Spans.* Division of Structural Engineering, Lund Institute of Technology, Lund University. Report TVBK-1025, Lund 2002, ISSN 0349-4969

Chan, H Y and Melchers, R E. (1993). *Reliability of Time-dependent Structural Systems*. 12th International Conference on Offshore Mechanics and Artic Engineering, Glasgow, Scotland, June 20-24. 1993. pp 39-46

CIB W81. (1989). *Actions on Structures, Self-weight Loads*. First Edition, June 1989

CIB W81. (1996). *Actions on Structures, General Principles*. First Edition April 1996

CONTECVET (2001). *A Validated Users Manual for Assessing the Residual Service Life of Concrete Structures, Manual for Assessing Corrosion-affected Concrete Structures.* EC Innovation Programme, IN 30902I. Second Draft

Degerman, T. (1981). *Dimensionering av betongkonstruktioner enligt sannolikhetsteoretiska metoder (Design of Concrete Structures with Probabilistic Methods, in Swedish)*. Lund University, Lund Institute of Technology, Department of Building Technology. Report TVBK-1003, Lund, Sweden 1981

Ditlevsen, O and Madsen H O. (1996). *Structural Reliability Methods.* John Wiley & Sons. ISBN 0-471-96086-1

Draper and Smith. (1966). *Applied Regression Analysis.* John Wiley & Sons, Inc.

Dunker K F and Rabbat B G. (1993). *Why America's Bridges are Crumbling*. Scientific American, March, 1993, pp 18-24.

Duracrete (1997). *Design Framework. Probabilistic Performance based Durability Design of Concrete Structures.* Contract BRPR-CT95-0132, Project BE95-1347, Document BE95-1347/R1, March, 1997

Duracrete (1998). *Modelling of Degradationk. Probabilistic Performance based Durability Design of Concrete Structures.* Contract BRPR-CT95-0132, Project BE95-1347, Document BE95-1347/R4-5, December, 1998

Ekström T. (2001). *Leaching of Concrete, Experiments and Modeling*. Lund University Division of Building Materials. TVBM-3090. Lund

Ekström T. (2002). *Islaster mot hydrauliska konstruktioner (Ice Loads on Hydraulic Structures, in Swedish).* Elforsk Rapport 02:03

Ellingwood B and Naus D J. (1999). *Condition Assessment and Maintenance of Aging Structures in Critical Facilities – A Probabilistic Approach.* Case Studies in Optimal Design and Maintenance Planning of Civil Infrastructure Systems, Reston, VA, USA, 1999 pp 45-56

Ellingwood B and Tekie P B, (2001). *Fragility Analysis of Concrete Gravity Dams.* Journal of Infrastructure Systems, Vol. 7, No. 2, June, 2001, pp 41-48

EN 1990. *Eurocode – Basis of Design*. Final draft July 2001.

EN 206-1:2000. *Concrete - Part 1: Specification, performance, production and conformity*

Enevoldsen, I and Pup S. (2000). *Probabilistic-based Assessment of Swedish Road Bridges.* 4th International Conference on Bridge Management, University of Surrey, Guildford, Surrey, UK, 16-19 April, 2000

Enevoldsen, I and Jensen F.M. (2000). *Safety-based bridge Management for Extension of Service Lifetime.* 16th Congress of IABSE, Lucerne, 2000

Enevoldsen, I and Jensen F.M. (2001). *Safety-based bridge maintenance management.* Safety, Risk, Reliability – Trends in Engineering, Malta, 2001

Enevoldsen, I, (2000). *Probabilistic-Based Assessment of Bridges.* 16th Congress of IABSE, Lucerne, 2000

Enright, M P and Frangopol, D M. (1998a). *Probabilistic Analysis of Resistance Degradation of Reinforced Concrete Bridge Beams under Corrosion.* Engineering structures. Vol. 20. No. 11 pp. 960-971, 1998, Elsevier

Enright, M P and Frangopol, D M. (1998b). *Service-life Prediction of Deteriorating Concrete Bridges.* Journal of Structural Engineering, March 1998, pp 309-317

Estes A C, and Frangopol D M (1999). *Repair optimization of highway bridges using system reliability approach.* Journal of Structural Engineering, Vol 125. No.7 July 1999. pp 766-775.

Eurocode 2 (1991). *Design of concrete structures –Part1: General rules and rules for buildings.* European Prestandard ENV 1992-1-1:1991 E.

Faber M H. (2002). *Risk-Based Inspection: The framework.* Structural Engineering 3/2002. pp 186-194.

Fagerlund G. (1987). *Samband mellan porositet och hållfasthet hos cementbundna material (Relations between porosity and strength of cement bound materials, in Swedish).* Nordic Mini Seminar on Concrete Hydration, Copenhagen 1987.

Fagerlund G. (1996). *Livslängdsberäkningar för betongkonstruktioner, översikt med tillämpningsexempel (Servicelife calculations for concrete structures, in Swedish).* Lund University Division of Building Materials. TVBM-3070. Lund.

Fagerlund G. (2000). *Leaching of concrete, the leaching process, extrapolation of deterioration, effect on the structural stability.* Lund University Division of Building Materials. TVBM-3091. Lund.

Frangopol D M and Estes A C. (1997). *Lifetime Bridge Maintenance Strategies based on system reliability.* Structural Engineering International 3/97. pp 193-198.

Frangopol D M Lin K-Y and Estes A C. (1997). *Reliability of reinforced concrete girders under corrosion attack.* Journal of Structural Engineering. March 1997.

Getachew A (2000). *Trafiklaster på broar, Analys av insamlade och Monte Carlo generarde fordonsdata (Traffic loads on bridges, analysis of measured data and Monte Carlo generated traffic data, in Swedish).* Licentiate thesis, Kunliga Tekniska Högskolan, Institutionen för Byggkonstruktion. TRITA-BKN Bulletion 62, 2000, ISSN 1103-4270, ISRN KTH/BKN/B-62-SE

Goyet, Straub and Faber. (2002). *Risk-Based Inspection Planning of Offshore Installations.* Structural Engineering 3/2002. pp 200-208.

Hall W B. (1988). *Reliability of service proven structures.* Journal of Structural Engineering Vol 114, No 3 march 1988

Halmstads Järnverk AB (1960). *Halmstadstål HJS 70, kallsträckt armeringsstål med ankringsringar (HJS 70 cold stretched reinforcement with anchor plate, in Swedish)*. Press & Propaganda/Ivar Hæggströms Stockholm 1962.

Handboken Bygg (1984). *Geoteknik (Geotechnics, in Swedish).* LiberTryck, Stockholm 1984. ISBN 91-38-06077-9

Hasofer A M and Lind N C. (1973). *An exact and invariant First-Order Reliability Format.* Solid Mechanics Division, University of Waterloo, Waterloo, Ontario, Canada. Paper No 19, May 1973.

Hedman O and Losberg A. (1975). *Dimensionering av betongkonstruktioner med hänsyn till tvärkrafter (Shear design of concrete structures, in Swedish).* Nordisk Betong. 5-1975, pp 19-29

Hong H P and Zhou W. (1999). *Reliability Evaluation of RC columns.* Journal of Structural Engineering, Vol 125. No 7. July 1999

ICOLD (2000). *Twentieth Congress on large dams.* 19-22 September 2000, Beijing, China.

ISO 2394-1998. *General principles on reliability of structures.* ISO/FDIS 2394:1998(E).

ISO/CD 13822. (1997). *Bases for design of structures – Assessment of existing structures*

James G (2001). *Raising Allowable Axle Loads on Railway Bridges using Simulation and Field Data.* Royal Institute of Technology, Department of Structural Engineering, TRITA-BKN Bulletin 63, 2001. ISSN 1103-4270. ISRN KTH/BKN/B—63-SE. (Licentiate thesis)

James G, and Karoumi R. (2001). *Modelling and Reliability assessment of traffic loads on Railway bridges.* Safety, Risk, Reliability – Trends in Engineering, Malta 2001. pp 1001

James G. (2002). *Personal communication*.

JCSS (Diamantidis, D. editor), (2001). *Probabilistic Assessment of Existing Structures.* A publication of The Joint Committee on Structural Safety. RILEM Publications Sarl. ISBN: 2-912143-24-1

JCSS. (2002). *Probabilistic Model Code*. Internet print outs from http://www.jcss.ethz.ch/

Johansson R. (2002). *System modeling and Identification.* Prentice Hall, ISBN 0-13-482308-7. Prentice Hall, Englewood Cliffs, NJ 1993.

Kungliga Järnvägsstyrelsen. *Provisoriska belastningsbestämmelser för byggnadsverk .Hus och brobyggnader, (Temporary load regulations, in Swedish).* Vid Statens järnvägare, Kungliga Järnvägsstyrelsen, Bantekniska Byrån, Broavdelningen.

Lindbladh L. (Personal communication) (*The Bridge Management System of the Swedish National Road Administration, in Swedish).* Swedish National Road Administration, Head Office, Borlänge, Sweden

Lindgren G and Rootzén (1994). *Stationära stokastiska processer, fjärde utgåvan (Stationary stochastic processes, Fourth Edition, in Swedish).* Institutionen för matematisk statistik, Lunds Tekniska Högskola, Lunds Universitet.

Lindgren G. (2002). *Personal communication.*

Maage M et al. (1996). *Service life prediction of existing concrete structures exposed to Marin environment.* ACI Materials Journal November-December. pp 602-608.

Madsen H O, Krenk S and Lind N C. (1986) *Methods of Structural Safety.* Prentice-Hall Inc. ISBN 0-13-579475-7.

McClure S. (2002). *Public knowledge.* Bridge Design & Engineering. Issue No. 26, First Quarter 2002

Melchers R. (1999). *Structural Reliability Analysis and Prediction.* Second Edition. John Wiley & Sons.

Mirza S.A (1996). *Reliability based design of reinforced concrete columns.* Structural Safety Vol 18. No 2/3. pp179-194. 1996

Montgomery, D C. (2001). *Design and Analysis of Experiments, 5th Edition*. John Wiley & Sons. ISBN 0-471-31649-0.

Mori Y and Ellingwood B R. (1993). *Reliability-based Service-Life assessment of aging concrete structures.* Journal of Structural Engineering Vol 119, No 5 May 1993 pp1600-1621.

Mori Y and Nonaka M. (2001). *LRFD for assessment of deteriorating existing structures.* Structural Safety 32 pp 297-313. Elsevier Science Ltd.

Nilsson M, Ohlsson U and Elfgren L. (1999). *Partialkoefficienter för hållfasthet I betongbroar längs Malmbanan (Partial factors for strength in concrete bridges along Malmbanan, in Swedish).* Institutionen för Väg och Vattenbyggnad. Avdelningen för Konstruktionsteknik. 1999:03. ISSN: 1403-1536. ISRN: LTU-TR –1999/03--SE

NKB 36 (1978). *Recommendations for loading and safety regulations for structural design.* Publikation 36.

NKB 55 (1987). *Retningslinier for Last-og sikkerhedsbestemmelser for Bærende konstruktioner (Recommendations for loading and safety regulations for structural design, in Swedish).* NKB-skrift nr. 55. ISBN 87-509-6991-1. ISSN 0359-9981. Visoprint as, Köpenhamn.

Nowak A S and Saraf V K. (1996). *Target safety level for bridges.* Worldwide advances in structural concrete and masonry. 14th congress. 1996. Part 2. pp 696-703. ISSN 0-7844-0164-

Nowak, A S. (1995). *Calibration of LFRD Bridge Code.* Journal of Structural Engineering. Vol.121. No. 8. August 1995. pp 1245-1251. ASCE ISSN 0733-9445/95/0008-1245-1251.

prEN 13791:1999. *Assessment of concrete compressive strength in structures or structural elements.*

Rambøll (1999a). *Vägverket Sandsynlighedsbaseret klassificering Fase I, Baggrund for trafiklastmodeller (Swedish National Road Administraion's probability bases assessment, Phase I, in Danish)*. April 1999

Rambøll (1999b). *Vägverket Sandsynlighedsbaseret klassificering Fase A, Bro T531: Vägport under E18 ved Örebro (Swedish National Road Administraion's probability bases assessment, Phase A, Bridge T531, in Danish).* August 1999

Rambøll (1999c). *Vägverket Sandsynlighedsbaseret klassificering Fase B, Bro C295: Bro over Sävjaåen SO Berga å väg E4 Stockholm-Uppsala, Uppsala län (Swedish National Road Administraion's probability bases assessment, Phase B, Bridge TC295, in Danish).* August 1999

Rambøll (1999d). *Vägverket Sandsynlighedsbaseret klassificering Fase C, Bro E129: Bro over Motala ström N Skärblacka station å väg 1142. Kimstads Kyrka – Finspång, Östergötlands län (Swedish National Road Administraion's probability bases assessment, Phase C, Bridge E129, in Danish)*. August 1999

RCP Consult (1997). *STRUREL, A Structural Reliability Analysis Program System, COMREL & SYSREL Users Manual.* RCP GmbH Barer Strasse 50, 80799 München, Germany.

Reinius E, (1968). *Vattenbyggnader del 3, dammbyggnader, föreläsningar (Hydraulic structures, part 3, dams lectures, in Swedish)*. Stockholm 1968.

RIDAS (1997). *Kraftföretagens riktlinjer för dammsäkerhet (Hydropower companies guidelines for dam safety, in Swedish)*.

RIDAS (2000). *Kraftföretagens riktlinjer för dammsäkerhet, tillämpningsanvisnignar (Hydropower companies guidelines for dam safety, application instructions, in Swedish)*.

Sandberg P (1998). *Chloride initiated reinforcement corrosion in marine concrete.* Lund University, Lund Institute of Technology, Division of Building Materials, Report TVBM-1015, Lund, Sweden, 1998.

Schneider J. (1994). *Concepts and procedures in assessing existing structures.* Risk Analysis, proceedings of a symposium, 11-12 August 1994. Ann Arbor, Mich. USA University of Michigan 1994. pp 203-212

Schneider J. (2000). *Safety – a matter of risk, cost and consensus.* Structural Engineering International 4/2000. pp266-269

Schnieder J. (1992). *Some thoughts on the reliability assessment of existing structures.* Structural Engineering International 1/92. pp13-18

Soerensen and Faber. (2002). *Codified Risk-Based Inspection Planning.* Structural Engineering 3/2002. pp 195-199

Somerville G. (1992). *Service life Prediction – an overview.* Concrete International, Design & Construction November 1992, pp 45-49.

SS 13 72 07 *Concrete Testing - Hardened concrete - Compressive strength - Conversion factors (In Swedish)*

SS 13 72 30 *Concrete Testing - Hardened Concrete - Compressive strength of test specimens (In Swedish)*

SS 13 72 *32 Concrete Testing – Hardened concrete – Modulus of elasticity in compression (In Swedish)*

SS 13 72 34 *Concrete Testing - Hardened Concrete - Density for concrete containing aggregates of rock material (In Swedish)*

SS 17 72 13 *Concrete Testing - Hardened concrete - Strength in splitting (In Swedish)*

Statens offentliga utredningar 1934:17 (1934). *Statliga Cement och Betongbestämmelser av år 1934, Normalbestämmelser för leverans och provning av cement samt för byggnadsverka av betong och armerad betong (Swedish Cement and concrete regulations for 1934, in Swedish).* Sjunde upplagan, Nordiska Bokhandeln.

Statens offentliga utredningar 1938:37 (1946). *Normalbestämmelser för järnkonstruktioner till byggnadsverk. Nionde upplagan. (Iron regulations, in Swedish).* Nionde upplagan, Stockholm, K.L Beckmans boktryckeri

Statens offentliga utredningar 1942:44 (1942). *Tillägg Nr 1 till Statliga Cement och Betongbestämmelser av år 1934, Omfattande Tilläggsbestämmelser angående klassindelning av betong samt tillåtna påkänningar i armerad betong, Särskilda bestämmelser för användning av så kallat kamjärn av högvärdigt stål såsom armeringsjärn i byggnadsverk av armerad betong. (Additions to the Swedish Cement and concrete regulations for 1934, in Swedish).* Tredje upplagan, Nordiska Bokhandeln.

Statens offentliga utredningar 1949:64 (1951). *Statliga betongbestämmelser Del 1, Materialdelen Fastställ den 31 december 1949 (Concrete regulations for 1949, in Swedish).* Stockholm 1951.

Statens offentliga utredningar 1961:12 (1961). *Statliga bestämmelser av år 1960 för byggnadsverk, 1960 års belastningsbestämmelser (Load regulations, in Swedish).* Stockholm, 1961. Nordiska Bokhandeln

Stewart M G (1997). *Time-Dependent Reliability of Existing RC Structures.* Journal of Structural Engineering No 7 July 1997 pp 896-902

Stewart M G (1998). *Reliability-based bridge design and assessment.* Progress in Structural Engineering and Materials 1998 Vol 1(2) pp 214-222.

Stewart M G and Rosowsky D V (1998). *Structural Safety and serviceability of concrete bridges subjected to corrosion.* Journal of Infrastructure systems. December 1998 pp-146-155

Stewart M G och Attard M M. (1999). *Reliability and model accuracy for high-strength concrete column design.* Journal of Structural Engineering. March 1999. pp 290-300.

Stewart M G. (1996). *Serviceability reliability analysis of reinforced concrete structures.* Journal of Structural Engineering Vol 122 No 7 July 1996. pp794

Stewart, Rosowsky and Val (2002). *Reliability-based bridge assessment using risk-ranking decision analysis.* Structrual Safety 23 (2001). pp 397-405

Sundquist H. (2000). *Dimensionerande laster på järnvägsbroar och andra bankonstbyggander (Design loads on railway bridges).* Rapport utgiven i samband med doktorandkurs Upgradering av betongkonstruktioner hösten 1998. (Report from PhD course, Upgrading of concrete structures, fall 1998).

Tang L (2002). *Mätning av armeringskorrosion i betong (Measuring corrosion intensity in concrete, in Swedish)* Bygg & Teknik nr 7 Okt. 2002. pp 65-67.

Thoft-Christensen P and Baker M J. (1982) *Structural Reliability and Theory and its Applications.* Springer-Verlag. Berlin, Heidelberg, New York.

Thoft-Christensen P. (2000). *Modelling of the Deterioration of Reinforced Concrete Structures*. Proceedings of IFIP Conference on Reliability and Optimization of Structural System, Ann Arbor, Michigan, September 2000. pp15-26. ISSN 1395-7953 R0020

Thoft-Christensen P. (2001a). *Risk Analysis in Civil Engineering*. Risk and reliability in Civil Engineering, Short Course International Conference Malta, March 21, 2001.

Thoft-Christensen P. (2001b). *What happens with Reinforced Concrete Structures when the Reinforcement corrodes?* ISSN 1395-7953 R0116.

Thoft-Christensen P. (2002). *Deterioration of Concrete Structures*. First International Conference on Bridge Maintenace, Safety and Management. IABMAS 2002, Barcelona 14-17 July 2002. ISSN 1395-7953 R0130.

Tuutti, K. (1982). *Corrosion of steel in concrete.* CBI Research fo 4-82.

Vägverket (1993a). *Broinspektionshandbok (Handbook for bridge inspections, in Swedish).* Publ. 1993:34.

Vägverket (1993b). *Mätning och bedömning av broars tillstånd (Measurment and assessment of bridge conditions, in Swedish)*. Publ. 1993:35.

Vägverket (1996a). *SAFEBRO Kodförteckning för inspektioner (*SAFE*BRO code list for inspections, in Swedish)*. Publ. 1996:035

Vägverket (1996b). *SAFEBRO Kodförteckning för administrativa och tekniska uppgifter (SAFEBRO code list for administrative and technical information, in Swedish)*. Publ. 1996:041.

Vägverket (1998). *Allmän teknisk beskrivning för klassningsberäkning av vägbroar (Guidelines for assesssment of road bridges, in Swedish)*. Publikation 1998:78

Val D., Stewart M.G, Melchers R.E.. (1998). *Effect of reinforcement corrosion on reliability of highway bridges.* Engineering Structures Vol 20. No 11. pp. 1010-1019. 1998

Vrouwenvelder A. *Time variant processes in failure probability calculations.* TU-Delft/TNO, Netherlands

Vu K A T and Stewart M G. (2000). *Structural Reliability of concrete bridges including improved chloride-induced corrosion models.* Structural Safety 22, 2000, pp313-333

Xiutang F. et al. (2000). *Failure probability of gravity dams on rock foundation.* ICOLD. Twentieth Congress on large dams. 19-22 September 2000, Beijing, China.

APPENDIX A : THE DAM

Evaluation of σ_{tot}

When calculating the stress at the contact surface between the concrete and the rock (Table 6.9) Navier's formula is used:

$$\sigma_{tot} = \frac{V}{A} + \frac{M}{W} = \frac{N}{A} + \frac{N \cdot e}{W} \qquad \text{Eq. A.1}$$

where σ_{tot} is the resulting stress arising from all the actions applied to the structure without partial factors and A is the base area, W is the elastic section modulus, N is the sum of the vertical forces and e is the eccentricity calculated from the resulting overturning moment (M) and the resulting vertical force (N).

This requires knowledge of the size of the base area, and the elastic section modulus of the dam. The total stress is increased by using a partial factor γ_h set to 1.5 according to RIDAS (2000) before comparison with the design strength, Eq. A.2.

$$\gamma_h \sigma_{tot} \leq \frac{f_{ck}}{\gamma_m \gamma_n} \qquad \text{Eq. A.2}$$

In the deterministic parameter study described in Section 6.4.2, the following approximations were used.

- The column cross section was approximated by an inverted T-section.
- The minimum thickness of the bottom slab was used in the calculations (1.40 m), see Figure 6.3.
- The mean breadth of the bottom slab of the dam column was used (8.3 m), according to Figure 6.4.
- The mean height of the waas estimated as the mean value of the height at the upstream edge and the height at the downstream edge. The upstream height is +23.80-17.00 = 6.80 m, and the downstream height +22.6-15.00-1.40 = 9.00 m. See Figure 6.5.

Table A.1 Moment of inertia for the dam column (units in m, m^2 and m^4).

Part	Breadth	Height	Area, A	y_{top}	I	$A \cdot y^2$
Wall	1.2	6.5	7.8	3.25	27.5	43.6
Slab	8.3	1.4	11.6	7.2	1.9	29.2
		Σ	19.4	y_{tot} =5.6	29.4	72.8

The total moment of inertial is, 102.8 m^4, leading to an elastic section modulus of the contact surface of $102.8/(7.9-5.6)$ which is 44.7 m^3. The actual base area of the column, A, is used. According to measurements in Figure 6.4 this is 164 m^2.

APPENDIX B : THE RAILWAY BRIDGE

Geometry and geometrical properties of the bridge

For the purpose of showing the geometry of critical sections of the trough, a drawing has been copied from the original design drawings and is shown below.

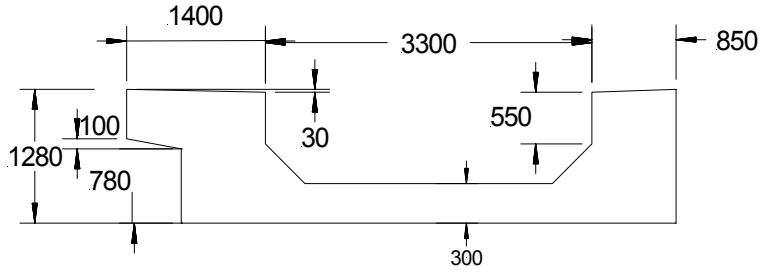

Figure B.1 Cross section of the trough (dimensions in mm).

In Table B.1 values of the concrete area and effective depth along the girder are shown.

Table B.1 Deterministic values for geometric variables along girder.

Section	A_c [m^2]	d [m]
0.000	4.95	1.486
0.125	3.64	1.199
0.250	3.64	1.196
0.375	3.64	1.212
0.500	3.64	1.213
0.625	3.64	1.213
0.750	3.64	1.214
0.875	3.64	1.193
1.000	3.64	1.465

Table B.2 shows how the reinforcement area changes along the girder.

Table B.2 Random geometric variables along the girder according to NKB 55 (1987), evaluated from design drawings.

Section	$\mu_{A_{s0}}$ [mm²]	$\sigma_{A_{s0}}$ [mm²]	$\mu_{A_{sv1}}$ [mm²]	$\sigma_{A_{sv1}}$ [mm²]	$\mu_{A_{sv2}}$ [mm²]	$\sigma_{A_{sv2}}$ [mm²]
0.000	20746	1037	226	11.3	3928	197
0.125	16819	841	226	11.3	3928	197
0.250	10385	519	226	11.3	3216	161
0.375	13270	664	226	11.3	-	-
0.500	14476	724	226	11.3	-	-
0.625	14476	724	226	11.3	-	-
0.750	10053	503	226	11.3	3216	161
0.875	16819	841	226	11.3	3928	197
1.000	24672	1234	226	11.3	3928	197

Evaluation of concrete strength

Banverket (2000)

In Banverket (2000) reference is made to BBK 94 Band 2 (1994) for the evaluation of test results to be used for calculations of the load carrying capacity. Based on the number of samples available, two different kinds of evaluations can be performed:

A) for a series of three samples from one structural part, or
B) for a series of six samples from one structural part.

For condition A the following equations are used to evaluate the compressive strength.

$$m_3 \geq f_{KK} + 4 \qquad \textbf{Eq. B.1}$$

$$x \geq \begin{cases} f_{KK} - 5 \\ 0.8 f_{KK} \end{cases} \qquad \textbf{Eq. B.2}$$

where m_3 is the mean value of at least three samples, f_{KK} is the characteristic compressive strength i.e. the demanded value, x is a single sample.

For condition A the following equations are used evaluating the tensile strength.

$$m_3 \geq f_{TK} + 0.5 \qquad \textbf{Eq. B.3}$$

$$x \geq \begin{cases} f_{TK} - 0.6 \\ 0.8 f_{TK} \end{cases} \qquad \textbf{Eq. B.4}$$

where f_{TK} is the characteristic tensile strength i.e. the outcome of the evaluation.

Based on the mean value, m_3, a required value is calculated. This value is then compared with those in Table B.3 and

Table B.4 and the nearest, lower values is the characteristic value in the assessment situation. Apart from the conditions in Eq. B.1 to Eq. B.4 there are in Banverket (2000) demands on the relation between compressive strength and splitting tensile strength. The mean splitting

tensile strength must be at least 7 % of the mean compressive strength. This implies that the mean compressive strength employed may be reduced. This demand is, however, neglected since a comparison will be made between this approach and a direct statistical approach.

Table B.3 Required values of compressive strength (f_{KK}) when testing concrete from existing structures (BBK 94 Band 2, 1994).

Strength class	f_{KK} [MPa]	Strength class	f_{KK} [MPa]
K8	7	K40	32
K12	10	K45	36
K16	13	K50	40
K20	17	K55	44
K25	21	K60	47
K30	25	K70	54
K35	28	K80	62

Table B.4 Required values of tensile strength (f_{TK}) when testing of concrete from existing structures (BBK 94 Band 2, 1994).

Strength class	f_{TK} [MPa]	Strength class	f_{TK} [MPa]
T1.0	0.9	T3.0	2.5
T1.5	1.3	T3.5	2.8
T2.0	1.7	T4.0	3.2
T2.5	2.1		

Results from the calculations described above are collected in Table 7.1.

Table 7.1 Strength classes and design values according to Banverket (2000)

	Tensile strength class	Compressive strength class
Superstructure	T3.0	- only two valid results
Substructure	T3.5	K80

No compressive strength class could be evaluated for the superstructure following the demands in Banverket (2000). Further cores are needed for this evaluation.

pr EN 13791:1999

Conformity of *in situ* compressive strength is assessed on cores using two different criteria's. Criteria *A* is used when 3 to 14 cores are available, and criteria *B* is used when at least 15 cores are available. The system is similar to the one suggested in BBK 94 Band 2 (1994), but different coefficients are used, and different numbers of tests *n*, are required. Compare Eq. B.1 to Eq. B.4 with Eq. B.5 to Eq. B.6. Criteria *A* uses the following relation for non-overlapping test result.

$$f_{m(n),is} \geq f_{ck,is} + k_1 \quad \text{Eq. B.5}$$

$$f_{is} \geq f_{ck,is} - 4 \quad \text{Eq. B.6}$$

Here $f_{m(n),is}$ is the mean *in situ strength*, $f_{ck,is}$ is the characteristic compressive strength according to Table B.5 and k_1 is a coefficient depending on the number of test results n as shown in Table B.6.

Table B.5 In situ compressive strength requirements for the strength classes according to EN 206-1.

Strength class	*Characteristic strength [N/mm²]*		*Ratio* in situ / *char.strength*	In situ *characteristic strength [N/mm²]*	
	$f_{ck,cyl}$	$f_{ck,,cube}$		$f_{ck,is,cyl}$	$f_{ck,is,cube}$
C8/10	8	10	0.85	7	9
C12/15	12	15	0.85	10	13
C16/20	16	20	0.85	14	17
C20/25	20	25	0.85	17	21
C25/30	25	30	0.85	21	26
C30/37	30	37	0.85	26	31
C35/45	35	45	0.85	30	38
C40/50	40	45	0.85	34	43
C45/55	45	55	0.85	38	47
C50/60	50	60	0.85	43	51
C55/67	55	67	0.85	47	57
C60/75	60	75	0.85	51	64
C70/85	70	85	0.85	60	72
C80/95	80	85	0.85	68	81
C90/105	90	105	0.85	77	89
C100/115	100	115	0.85	85	98

where $f_{ck,cyl}$ is the characteristic cylinder strength, $f_{ck,,cube}$ is the characteristic cube strength, $f_{ck,is,cyl}$ is the in-situ characteristic cylinder strength and $f_{ck,is,cube}$ is the in-site characteristic cube strength

Table B.6 k_1 coefficients dependence on the number of test results.

n	k_1
10-14	4
7-9	5
3-6	6

The following relations are used for criteria *B*.

$$f_{m(n),is} \geq f_{ck,is} + 1.48s \quad \text{Eq. B.7}$$

$$f_{is} \geq f_{ck,is} - 4 \quad \text{Eq. B.8}$$

where s is the standard deviation of the test result, but not less than 2 MPa.

Statistical evaluation

In order to investigate whether the concrete from the superstructure and substructure can be considered the same, hypothesis testing was performed for different strength parameters, in this case a two-sample *t*-test was used.

Assume that H_0 is the hypothesis saying that there is no difference in the mean values of the samples from the two structures (Eq. 7.16) and that H_1 is the hypothesis saying that there is a difference in the mean values from the two structures (Eq. 7.17).

$$H_0 : \mu_1 = \mu_2 \qquad \textbf{Eq. B.9}$$

$$H_1 : \mu_1 \neq \mu_2 \qquad \textbf{Eq. B.10}$$

where μ_1 and μ_2 are the mean values of the three samples from the sub- and superstructure.

The test is performed according to Eq. B.11 and Eq. B.12 below, for different measured material parameters, i.e. compressive strength, tensile strength and elastic modulus.

$$t_0 = \frac{\bar{y}_1 - \bar{y}_2}{S_p\sqrt{\frac{1}{n_1}+\frac{1}{n_2}}} \qquad \textbf{Eq. B.11}$$

Here $\bar{y}_1$ and $\bar{y}_2$ are the sample means, n_1 and n_2 are the number of samples, S_p^2 is an estimate of the common variance, $\sigma_1^2 = \sigma_2^2 = \sigma^2$, computed from Eq. B.12:

$$S_p^2 = \frac{(n_1-1)S_1^2 + (n_2-1)S_2^2}{n_1+n_2-2} \qquad \textbf{Eq. B.12}$$

where S_1^2 and S_2^2 are the two individual sample variances.

If $|t_0| > t_{\alpha/2,n_1+n_2-2}$ the H_0 hypothesis is rejected, and the two mean values are considered different. $\alpha/2$ is the upper percentage point of the *t*-distribution with n_1+n_2-2 degrees of freedom.

Using Eq. B.11 and Eq. B.12 t_0 was calculated for the splitting tensile strength and the compressive strength and the results are presented in Table B.7. (There was not enough information regarding the modulus of elasticity to do a hypothesis test for this property).

Table B.7 Results from hypothesis testing at the 95% significance level.

Parameter	$\alpha/2$	n_1+n_2-2	t-distr.	$\lvert t_0 \rvert$	Comment
Splitting tensile strength	2.5	4	2.78	1.61	H_0 is not rejected
Compressive strength	2.5	3	3.19	1.18	H_0 is not rejected

Based on Table B.7 it cannot be concluded that there is a difference in concrete strength between the super- and substructure. In the laboratory reports it was, however, stated that there was a visible difference in ballast type between the superstructure and the substructure.

This type of investigation raises an interesting question. Today it is said that concrete from different structural parts must be evaluated separately when using the methods in Banverket (2000). Here a minimum of three samples is required. But, as shown in this case, the number tests was less than three for one structural part due to practical problems. If this type of hypothesis testing were conducted the samples could be combined and the number of available test results increased.

Damage

Figure B.2 and Figure B.3 show the damage of the trough underside that was mentioned in Section 7.1.3.

Figure B.2 Underside of trough bottom, change of colour.

Figure B.3 Large pores and superficial reinforcement that is corroding on the underside of the trough.

Dynamic amplification factor

For the train loads BV-4 and BV-3 the following expressions were used to calculate the dynamic amplification factor, *D*:

$$D = 1 + \varphi = 1 + \varphi' + 0{,}5\varphi'' \qquad \text{Eq. B.13}$$

$$\varphi' = k/\left(1 - k + k^4\right) \qquad \text{Eq. B.14}$$

$$k = v/\left(2 \cdot L \cdot n_0\right) \qquad \text{Eq. B.15}$$

$$\varphi'' = 0.01\alpha\left[56e^{-(0.1 \cdot L)^2} + \left(0.625 \cdot L \cdot n_0 - 50\right)e^{-(0.05 \cdot L)^2}\right] \qquad \text{Eq. B.16}$$

$$n_0 = 94.76L^{-0.748} \qquad \text{Eq. B.17}$$

where v is the train speed, n_0 is the fundamental eigenfrequency for the unloaded bridge and L is the bridge length in metre, calculated according special rules. α is a coefficient related to the train speed, equal to 1 if the speed is greater than 22 m/s and v/22 if the speed is below 22 m/s.

In the structural analysis, the bridge was modelled as a frame. Specific assumptions were made for frames regarding the length (L) used for the calculation of the dynamic amplification factors in Banverket (2000). When calculating D for the girder, L is calculated as 1.4 times the arithmetic mean of the span length and the height of the support. This calculation gives L=14.84 m. The length used to calculate the dynamic amplification factor for the slab is 4.15 m and corresponds to the distance between the centrelines of the girders.

For train load UIC 71 the following expression for the dynamic amplification factor.

$$D = 1.0 + \frac{4}{8 + L} \qquad \text{Eq. B.18}$$

Concrete cover on substructure

Measurements were made in a grid pattern at three locations on the substructure and the results given in Table B.8 to Table B.10.

Table B.8 Concrete cover at mid support, south side in mm. Each square in the table represents a length of 100 mm.

63			39			32			38
62			39			34			63
55			35			35			50
55			34			33			67
53			40			28			79

Table B.9 Concrete cover at south support, west side in mm. * indicates visible bar. Each square in the table represents a length of 100 mm.

	97			70		40		28	
				78		40		28	
	97			55		40		28	
								*	
				55					
	97								
				55		28			
	97			45		45			

Table B.10 Concrete cover at south support, east side in mm. Each square in the table represents a length of 100 mm.

	38			34			54		93
	38			38			54		
	38			38			54		
									107
	38			38			54		
	41			38			54		
	38			49			54		111

The concrete cover was measured on the west longitudinal girder of the superstructure. Measurements were made of both vertical and horizontal cover on with low cover. This means that in practice, only the cover on bars adjacent to visible bars was measured.

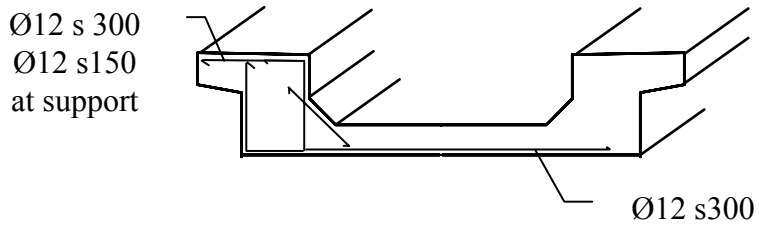

Figure B.4 Cross section of the trough girder showing the reinforcement subjected to corrosion.

Figure B.4 shows the layout of vertical bars in the girder. There are basically two types of reinforcement; stirrups to counteract the shear stresses in the girder, and mounting reinforcement connecting the bottom slab of the trough to the girders. Corrosion of either type of reinforcement is of course unacceptable in the long run.

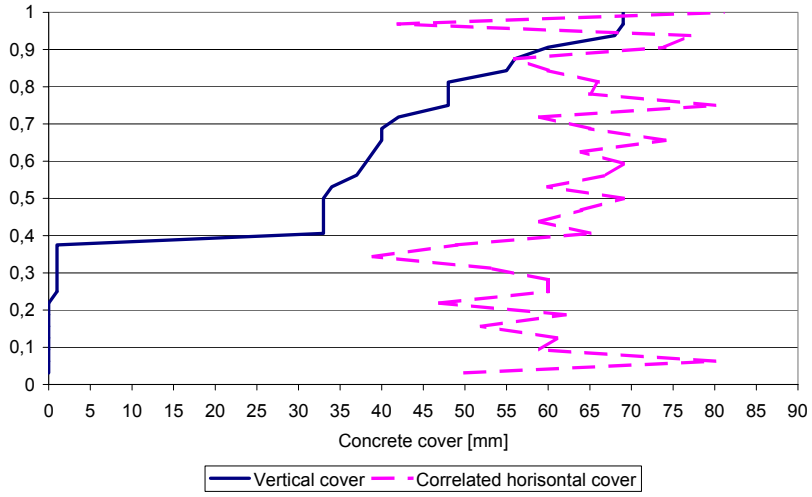

Figure B.5 Vertical concrete cover as cumulative distribution, the coupled horizontal concrete cover is also shown.

In Figure B.5 it is obvious that there has been some kind of mishap during the construction of the bridge. Almost 40 % of measured bars have a cover less than 5 mm. According to contemporary codes (Statens offentliga utredningar 1934:17, 1934) be at least 30 mm. The mean value of the measured vertical cover is 29 mm, but the standard deviation is 25 mm.

Test results regarding carbonation depth

Carbonation depths were measured using phenolphthalein solution in drilled holes. Based on the colour change, an estimated was made of the carbonation depth. Three measurements where made of the carbonation depth in the substructure and it was found to be 2 mm at each location.

Test results regarding chloride profiles

Six chloride profiles were investigated on the railway bridge, each of which had three measuring points. The chloride content was measured in concrete collected from drilling holes in the structure. The collection of concrete dust was done at intervals 0-10 mm, 20-30 mm and 30-40 mm. This implies that the results are mean values over each interval.

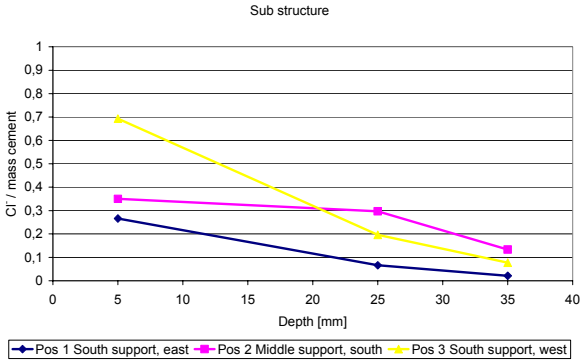

Figure B.6 Measured chloride profiles in the substructure.

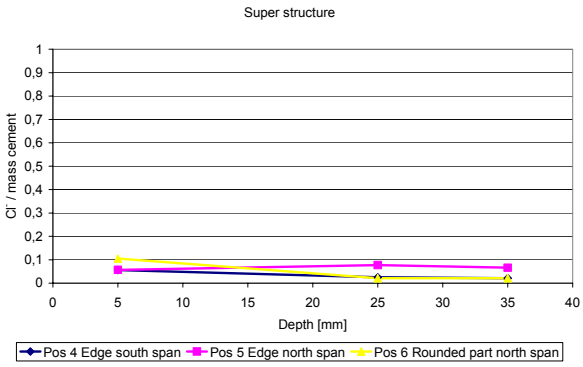

Figure B.7 Measured chloride profiles in the superstructure.

Figure B.6 shows the chloride profile measured in the substructure and Figure B.7 that in the superstructure. An approximate critical chloride concentration is 0.4 % chloride per kilogram cement and this level is not exceeded in more than one case in the substructure. Since it is the superstructure that is of interest with respect to safety, the focus is put on this structural part and, as can be seen, the chloride concentration is very low in this part.

In order to decide the initiation time for the concrete, a surface chloride concentration and diffusion constant were evaluated from the measured chloride profiles. This was done using a standard assumption regarding the chloride penetration model described below (see for instance Fagerlund, 1996).

The differential equation used requires a constant chloride level at the surface in order for ti to be valid. This is, of course, not the case for a bridge subjected to an outdoor climate and de-icing salt, but since this approach is commonly used it has also been used in this investigations. In order to solve the differential equation it must also be assumed that the

body penetrated by the chlorides is infinite. The evaluation was performed by fitting a curve to the solution of the differential equation described in Eq. B.19:

$$\frac{c_x}{c_s} = 1 - erf\left(\frac{x}{2\sqrt{Dt}}\right) \qquad \text{Eq. B.19}$$

where c_x is the concentration at depth x, c_s is the surface concentration, D is the diffusion constant for the material and t is time.

Table B.11 Chloride content as a function of depth (% Cl^-/(kg cement)).

	Depth [mm]	C_x				
Substructure		**0-10**	**20-30**	**30-40**	C_s	D
Pos 1	South support, east side	0.266	0.066	0.021	0.33	$1.3098 \cdot 10^{-13}$
Pos 2	Middle support, south side	0.350	0.297	0.133	0.41	$5.8594 \cdot 10^{-13}$
Pos 3	South support, west side	0.693	0.196	0.077	0.86	$1.4476 \cdot 10^{-13}$
Super structure						
Pos 4	Edge south span	0.056	0.025	0.021	0.07	$3.0331 \cdot 10^{-13}$
Pos 5	Edge north span	0.057	0.077	0.066	0.07	$3.4467 \cdot 10^{-11}$
Pos 6	Rounded part north span	0.105	0.021	0.021	0.12	$1.7923 \cdot 10^{-13}$

Table B.11 also presents values of the surface concentration of chlorides and the coefficient of diffusion. The result at position 5 is considered to be an outlier since this profile does not show a decrease in chloride concentration with depth in concrete as the other profiles do, see Figure B.10 (5).

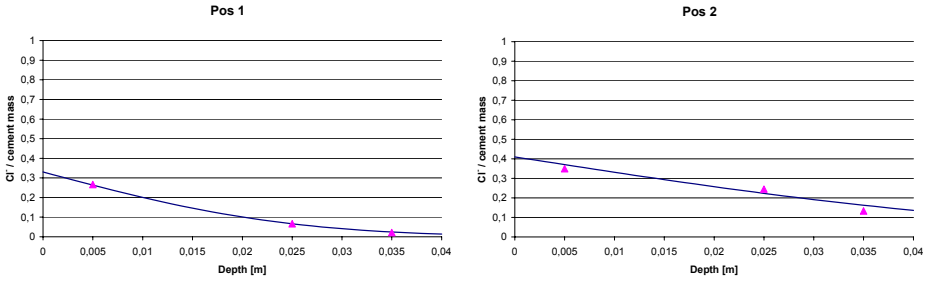

Figure B.8 Fitted chloride profiles for positions 1 and 2.

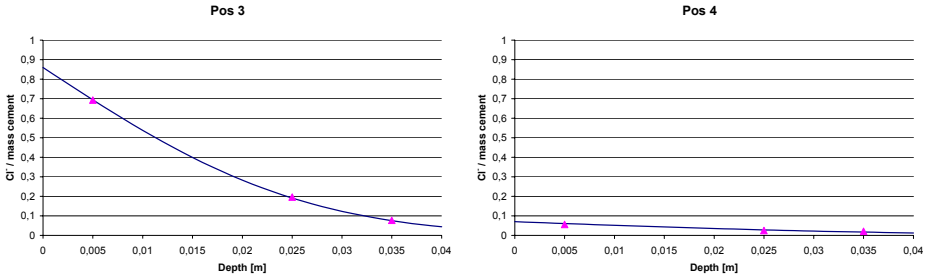

Figure B.9 Fitted chloride profiles for positions 3 and 4.

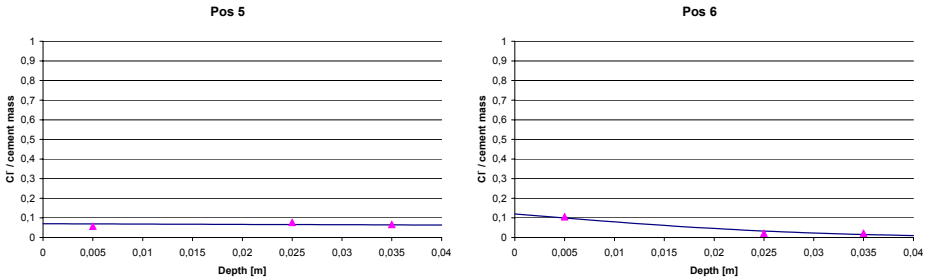

Figure B.10 Fitted chloride profiles for positions 5 and 6.

Measurement of current reinforcement area

An unusual method was chosen for the measurement of the residual reinforcement area. An ocular inspection revealed that the mounting reinforcement, or the shear reinforcement, was visible at several positions along the inside of the west girder of the trough. The inspection also indicated that the reinforcement was corroded so much that the bars visible side had become flat. Estimations of the flat length are shown in Figure B.11 to Figure B.20.

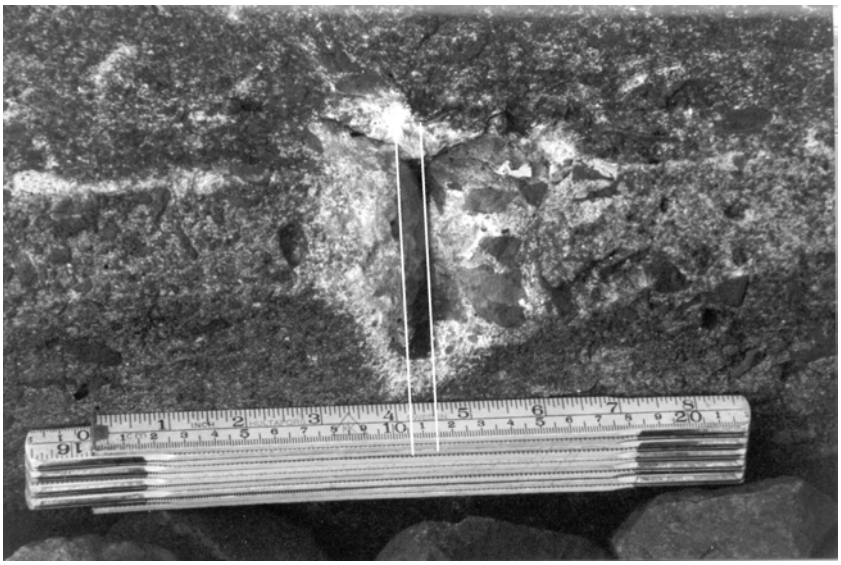

Figure B.11 Photography no.1

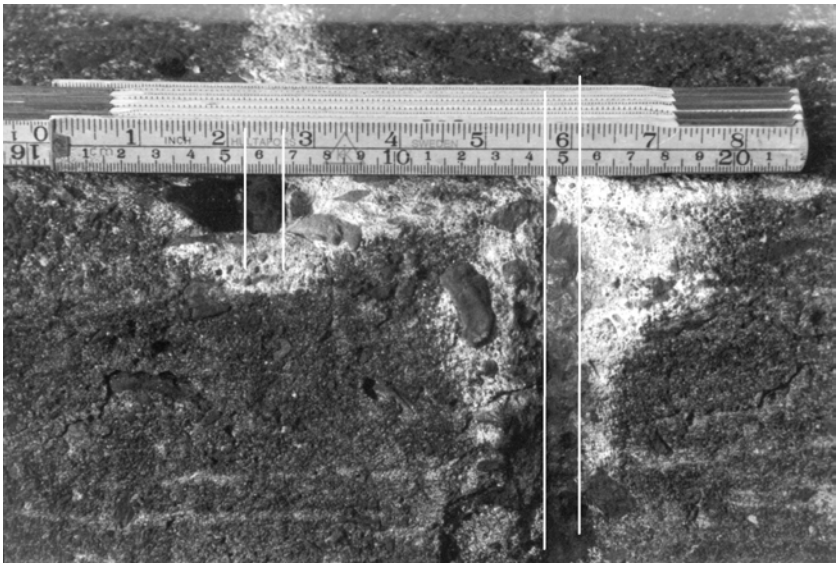

Figure B.12 Photography no. 2

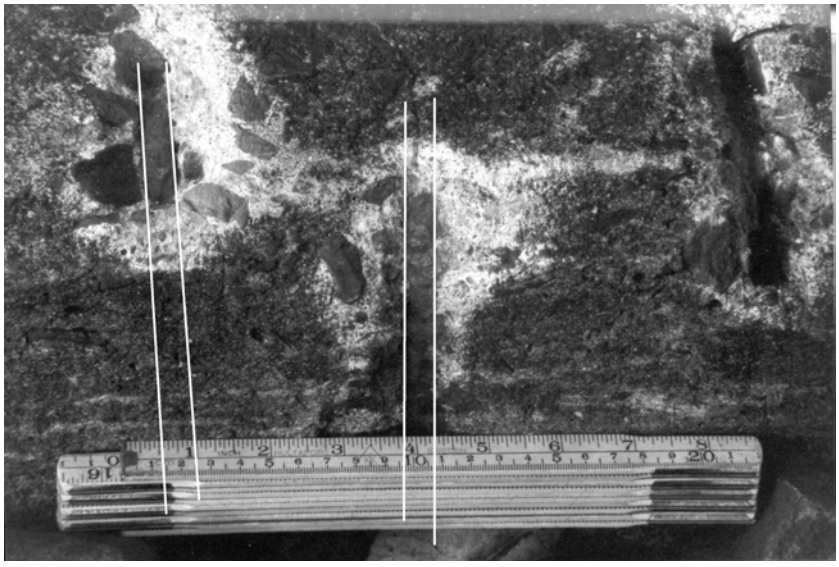

Figure B.13 Photography no. 3

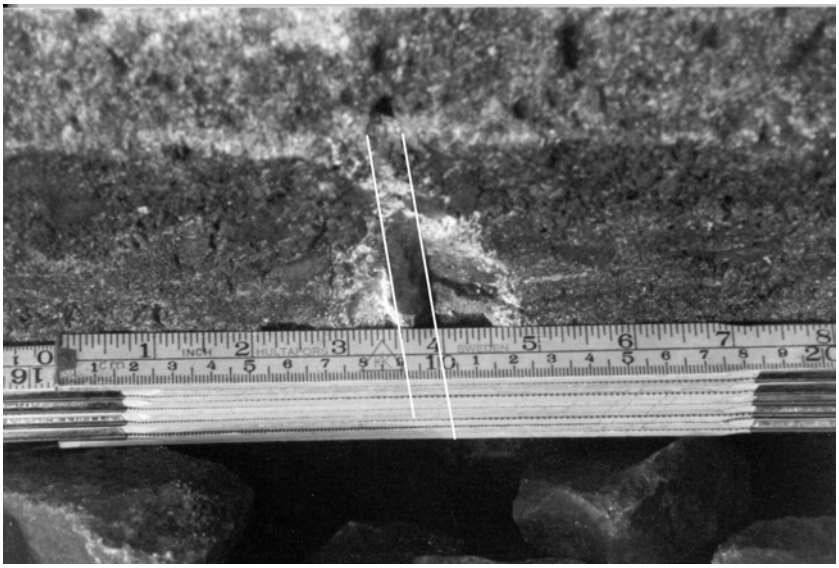

Figure B.14 Photography no. 4

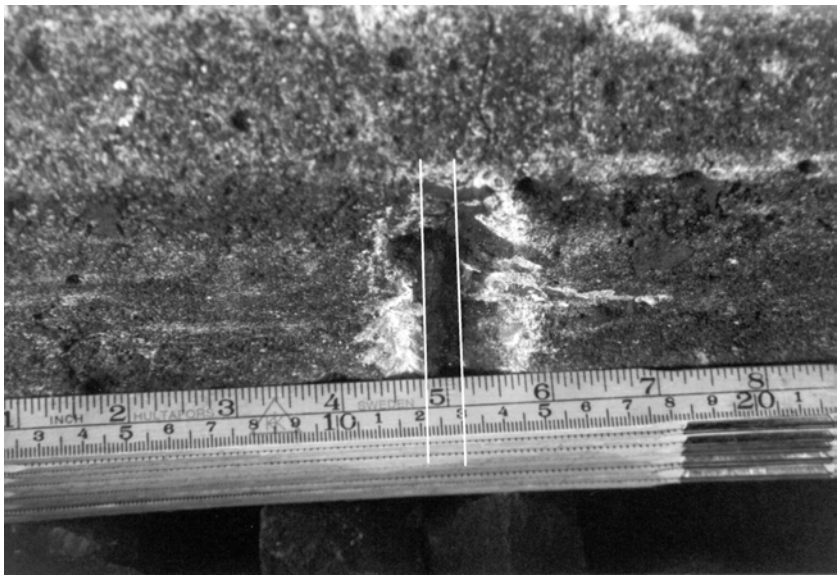

Figure B.15 Photography no. 5

Figure B.16 Photography no.6, not used for measuring purposes.

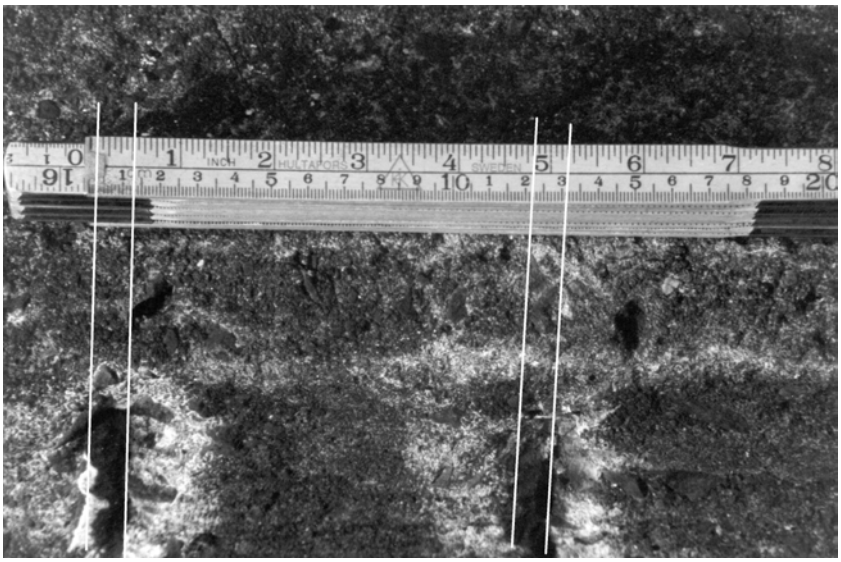

Figure B.17 Photography no. 7.

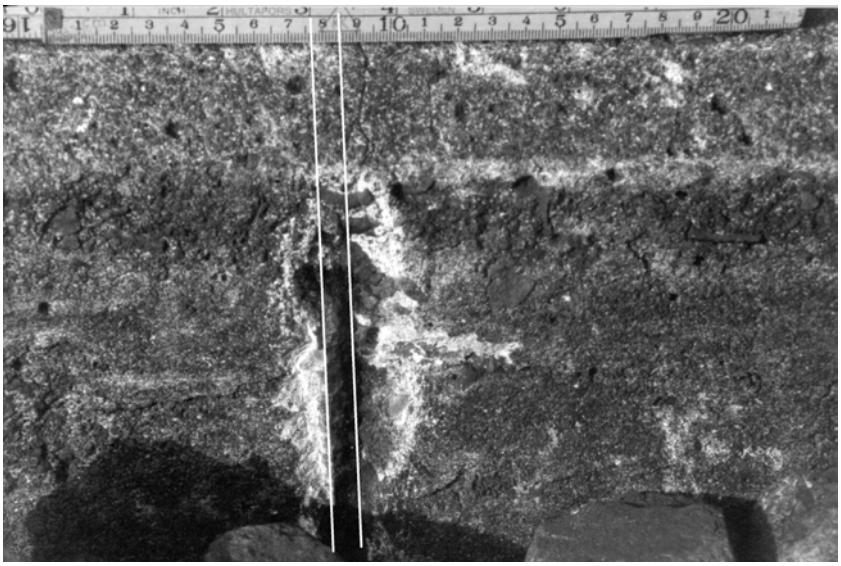

Figure B.18 Photography no. 8.

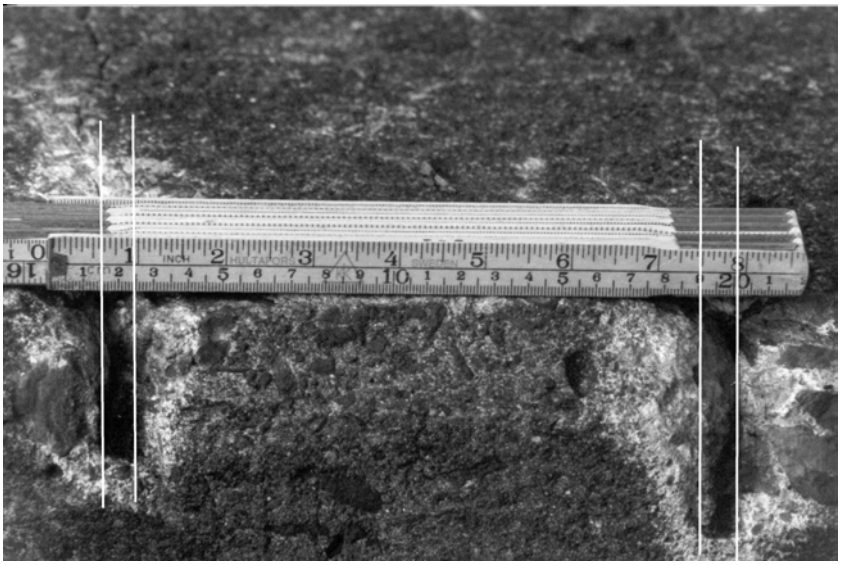

Figure B.19 Photography no. 9.

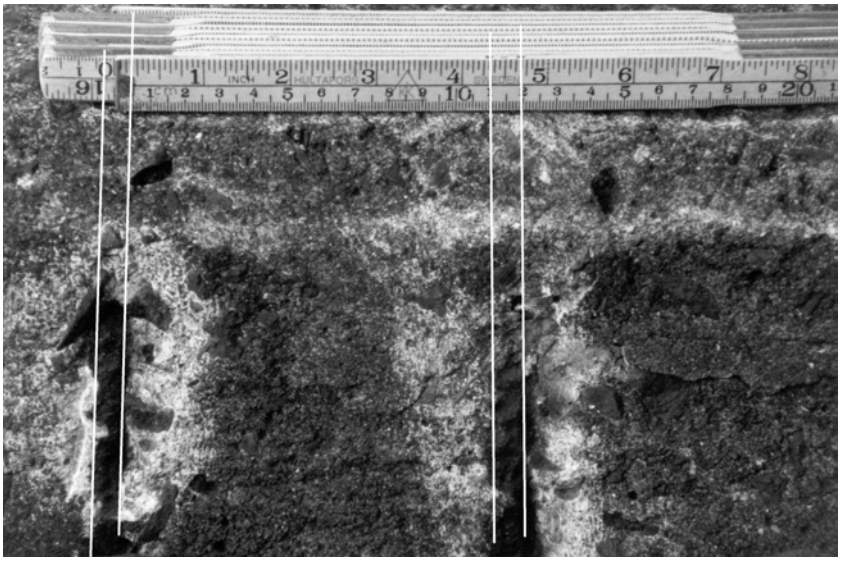

Figure B.20 Photography no. 10.

Section forces

A frame analysis was performed using Strip Step 2, a text-edited frame analysis program developed for large computers 1969. The program has survived the past 30 years due to its superb handling of load combinations and due to its capability to handle influence lines together with the combination of different load effects.

Table B.12 to Table B.14 gives section forces from permanent loads, the standard deviation is based on an assumed 5% coefficient of variation.

Table B.12 Section forces in main girder resulting from dead load.

Section	Moment [kNm]	σ [kNm]	Normal force [kN]	σ [kN]	Shear force [kN]	σ [kN]
0.000	-1329	-66	-70	-4	645	32
0.125	-334	-17	-70	-4	466	23
0.250	381	19	-70	-4	301	15
0.375	787	39	-70	-4	135	7
0.500	884	44	-70	-4	-31	-2
0.625	672	34	-70	-4	-197	-10
0.750	151	8	-70	-4	-362	-18
0.875	-678	-34	-70	-4	-528	-26
1.000	-1789	-89	-70	-4	-706	-35

Table B.13 Section forces in main girder resulting from ballast.

Section	Moment [kNm]	σ [kNm]	Normal force [kN]	σ [kN]	Shear force [kN]	σ [kN]
0.000	-518	-26	-84	-4	295	15
0.125	-81	-4	-84	-4	215	11
0.250	245	12	-84	-4	135	7
0.375	422	21	-84	-4	55	3
0.500	450	22	-84	-4	-25	-1
0.625	329	16	-84	-4	-105	-5
0.750	59	3	-84	-4	-185	-9
0.875	-360	-18	-84	-4	-265	-13
1.000	-890	-44	-84	-4	-345	-17

Table B.14 Section forces in main girder resulting from earth pressure.

Section	Moment [kNm]	σ [kNm]	Normal force [kN]	σ [kN]	Shear force [kN]	σ [kN]
0.000	-71	-4	-399	-20	25	1
0.125	-200	-10	-399	-20	25	1
0.250	-154	-8	-399	-20	25	1
0.375	-107	-5	-399	-20	25	1
0.500	-60	-3	-399	-20	25*	1*

Section	Moment [kNm]	σ [kNm]	Normal force [kN]	σ [kN]	Shear force [kN]	σ [kN]
0.625	-14	-1	-399	-20	25*	1*
0.750	33	2	-399	-20	25*	1*
0.875	79	4	-399	-20	25*	1*
1.000	302	15	-399	-20	25*	1*

All variable loads were assumed to have a characteristic value corresponding to the 98th percentile in a normal distribution, by assuming a 10% coefficient of variation for all loads, the mean and standard deviations where calculated and presented in Table B.15 to Table B.22.

Table B.15 Section forces in main girder resulting from overload; maximum shear force with associated moment and normal force.

Section	M_k [kNm]	μ_M [kNm]	σ_M [kNm]	N_k [kN]	μ_N [kN]	σ_N [kN]	V_k [kN]	μ_V [kN]	σ_V [kN]
0.000	-150	-124	-12	-190	-158	-16	25	21	2
0.125	-188	-156	-16	-190	-158	-16	25	21	2
0.250	-141	-117	-12	-190	-158	-16	25	21	2
0.375	-95	-79	-8	-190	-158	-16	25	21	2
0.500	-49	-40	-4	-190	-158	-16	25	21	2
0.625	-2	-2	-0.2	-190	-158	-16	25	21	2
0.750	44	37	43	-190	-158	-16	25	21	2
0.875	90	75	8	-190	-158	-16	25	21	2
1.000	221	183	18	-190	-158	-16	25	21	2

Table B.16 Section forces in main girder resulting from overload; minimum shear force with associated moment and normal force.

Section	M_k [kNm]	μ_M [kNm]	σ_M [kNm]	N_k [kN]	μ_N [kN]	σ_N [kN]	V_k [kN]	μ_V [kN]	σ_V [kN]
0.000	116	96	10	-216	-179	-18	-3	-3	-0,3
0.125	15	12	1	-216	-179	-18	-3	-3	-0,3
0.250	9	7	0,7	-216	-179	-18	-3	-3	-0,3
0.375	2	2	0,2	-216	-179	-18	-3	-3	-0,3
0.500	-4	-3	-0,3	-216	-179	-18	-3	-3	-0,3
0.625	-10	-9	-1	-216	-179	-18	-3	-3	-0,3
0.750	-17	-14	-1	-216	-179	-18	-3	-3	-0,3
0.875	-23	-19	-2	-216	-179	-18	-3	-3	-0,3
1.000	66	55	6	-216	-179	-18	-3	-3	-0,3

Table B.17 Section forces in main girder resulting from temperature loads; maximum shear force with associated moment and normal force.

Section	M_k [kNm]	μ_M [kNm]	σ_M [kNm]	N_k [kN]	μ_N [kN]	σ_N [kN]	V_k [kN]	μ_V [kN]	σ_V [kN]
0.000	-762	-632	-63	-234	-194	-19	87	72	7
0.125	-703	-584	-58	-234	-194	-19	87	72	7
0.250	-541	-449	-45	-234	-194	-19	87	72	7
0.375	-379	-315	-32	-234	-194	-19	87	72	7
0.500	-217	-180	-18	-234	-194	-19	87	72	7
0.625	-54	-46	-5	-234	-194	-19	87	72	7
0.750	107	89	9	-234	-194	-19	87	72	7
0.875	269	223	22	-234	-194	-19	87	72	7
1.000	535	444	44	-234	-194	-19	87	72	7

Table B.18 Section forces in main girder resulting from temperature loads; minimum shear force with associated moment and normal force.

Section	M_k [kNm]	μ_M [kNm]	σ_M [kNm]	N_k [kN]	μ_N [kN]	σ_N [kN]	V_k [kN]	μ_V [kN]	σ_V [kN]
0.000	1095	909	91	177	147	15	-118	-98	-10
0.125	954	792	79	177	147	15	-118	-98	-10
0.250	734	609	61	177	147	15	-118	-98	-10
0.375	514	427	43	177	147	15	-118	-98	-10
0.500	295	245	24	177	147	15	-118	-98	-10
0.625	75	62	6	177	147	15	-118	-98	-10
0.750	-145	-120	-12	177	147	15	-118	-98	-10
0.875	-364	-302	-30	177	147	15	-118	-98	-10
1.000	-662	-547	-55	177	147	15	-118	-98	-10

Table B.19 Section forces in main girder resulting from break loads; maximum shear force with associated moment and normal force.

Section	M_k [kNm]	μ_M [kNm]	σ_M [kNm]	N_k [kN]	μ_N [kN]	σ_N [kN]	V_k [kN]	μ_V [kN]	σ_V [kN]
0.000	-83	-69	-7	-13	-11	-1	9	8	1
0.125	-72	-59	-6	-13	-11	-1	9	8	1
0.250	-54	-45	-4	-13	-11	-1	9	8	1
0.375	-37	-31	-3	-13	-11	-1	9	8	1
0.500	-19	-16	-2	-13	-11	-1	9	8	1
0.625	-2	-2	-0,2	-13	-11	-1	9	8	1
0.750	15	13	1	-13	-11	-1	9	8	1
0.875	33	27	3	-13	-11	-1	9	8	1
1.000	56	47	5	-13	-11	-1	9	8	1

Table B.20 Section forces in main girder resulting from break loads; minimum shear force with associated moment and normal force.

Section	M_k [kNm]	μ_M [kNm]	σ_M [kNm]	N_k [kN]	μ_N [kN]	σ_N [kN]	V_k [kN]	μ_V [kN]	σ_V [kN]
0.000	71	59	6	-16	-13	-1	-8	-6	-1
0.125	49	41	4	-16	-13	-1	-8	-6	-1
0.250	35	29	3	-16	-13	-1	-8	-6	-1
0.375	20	17	2	-16	-13	-1	-8	-6	-1
0.500	6	5	0,5	-16	-13	-1	-8	-6	-1
0.625	-8	-7	-0,7	-16	-13	-1	-8	-6	-1
0.750	-23	-19	-2	-16	-13	-1	-8	-6	-1
0.875	-37	-31	-3	-16	-13	-1	-8	-6	-1
1.000	-45	-37	-4	-16	-13	-1	-8	-6	-1

Table B.21 Section forces in main girder resulting from train load BV-4; maximum shear force with associated moment and normal force.

Section	M_k [kNm]	μ_M [kNm]	σ_M [kNm]	N_k [kN]	μ_N [kN]	σ_N [kN]	V_k [kN]	μ_V [kN]	σ_V [kN]
0.000	-1628	-1116	-112	-263	-180	-18	1282	879	88
0.125	-40	-27	-3	-292	-200	-20	1016	697	70
0.250	1022	701	70	-279	-192	-19	771	529	53
0.375	1507	1034	103	-239	-164	-16	553	379	38
0.500	1506	1033	103	-188	-129	-13	369	253	25
0.625	1193	818	82	-132	-91	-9	222	153	15
0.750	712	488	49	-83	-57	-6	113	77	8
0.875	231	158	16	-42	-29	-3	39	27	3
1.000	-9	-6	-0,6	-29	-20	-2	11	8	0,8

Table B.22 Section forces in main girder resulting from train loads BV-4; minimum shear force with associated moment and normal force.

Section	M_k [kNm]	μ_M [kNm]	σ_M [kNm]	N_k [kN]	μ_N [kN]	σ_N [kN]	V_k [kN]	μ_V [kN]	σ_V [kN]
0.000	101	69	7	16	11	1	-55	-38	-4
0.125	365	250	25	-32	-22	-2	-90	-62	-6
0.250	845	580	58	-102	-70	-7	-181	-124	-12
0.375	1175	806	81	-154	-106	-11	-297	-204	-20
0.500	1345	923	92	-199	-137	-14	-455	-312	-31
0.625	1110	762	76	-228	-156	-16	-654	-448	-45
0.750	328	225	223	-238	-163	-16	-886	-608	-61
0.875	-968	-664	-66	-244	-167	-17	-1129	-774	-77
1.000	-2599	-1782	-178	-244	-167	-17	-1373	-942	-94

APPENDIX C : DISTRIBUTIONS FOR BAYESIAN UPDATING

In this appendix a posteriori and predictive distributions are given for different distributions and different a priori knowledge. All expressions are taken from JCSS (Diamantiedes 2001) and RCP Users Manual (1997).

Table C.1 Normal distribution with unknown mean.

Variable (density/distribution)	Unknown parameters
Normal $\varphi_x(x\|m,\sigma)=\frac{1}{\sqrt{2\pi}\sigma}\exp\left[-\frac{1}{2}\left(\frac{x-m}{\sigma}\right)^2\right]$ $\Phi_x(x\|m,\sigma)=\int_{-\infty}^{x}\varphi(t\|m,\sigma)dt$	m
A posteriori parameters	
$\xi''=\frac{\xi'\frac{\sigma^2}{n'}+\bar{x}\frac{\sigma^2}{n}}{\frac{\sigma^2}{n'}+\frac{\sigma^2}{n}}$ $\tau''=\sqrt{\frac{\left(\frac{\sigma^2}{n'}\right)\left(\frac{\sigma^2}{n}\right)}{\frac{\sigma^2}{n'}+\frac{\sigma^2}{n}}}$ $n''=n+n'$	
A priori/ a posteriori density/distributions of parameters	
Normal $\varphi_M(m)=\frac{1}{\sqrt{2\pi}\tau}\exp\left[-\frac{1}{2}\left(\frac{m-\xi}{\tau}\right)^2\right]$ $\Phi_M(m\|\xi,\tau)=\int_{-\infty}^{m}\varphi(\tau\|\xi,\tau)d\tau$	
Predictive density/distribution	
Normal $\varphi_Y(y)=\frac{\sqrt{\frac{n''}{n''+1}}}{\sqrt{2\pi}\tau''}\exp\left[-\frac{1}{2}\left(\frac{y-\xi''}{\tau''\sqrt{\frac{n''+1}{n''}}}\right)^2\right]$ $\Phi_Y(y\|\xi'',\tau'',n'')$	

Table C.2 Normal distribution with unknown standard deviation.

Variable (density/distribution)	Unknown parameters
Normal $\varphi_x(x\|m,\sigma)=\frac{1}{\sqrt{2\pi}\sigma}\exp\left[-\frac{1}{2}\left(\frac{x-m}{\sigma}\right)^2\right]$ $\Phi_x(x\|m,\sigma)=\int_{-\infty}^{x}\varphi(t\|m,\sigma)dt$	σ
A posteriori parameters	
$s''^2\upsilon''=s'^2\upsilon'^2 \qquad s^2=\frac{1}{\upsilon}\sum_i(x_i-m)^2 \quad \upsilon''=\upsilon'+\upsilon$	
A priori/a posteriori density/distributions of parameters	
Invers-Gamma-2 $f_\Sigma=\frac{\left(\frac{\nu}{2}\right)^{\upsilon/2}}{\Gamma\left(\frac{\upsilon}{2}\right)}\frac{2}{s}\left(\frac{s^2}{\sigma^2}\right)\exp\left(-\frac{\upsilon s^2}{2\sigma^2}\right) \qquad F_\Sigma(\sigma)=1-\frac{\Gamma\left(\frac{\upsilon}{s}\left(\frac{s}{\sigma}\right)^2,\frac{\upsilon}{2}\right)}{\Gamma\left(\frac{\upsilon}{2}\right)}$	
Predictive density/distribution	
Student $f_Y(t)=\frac{1}{s''}\frac{1}{B\left(\frac{1}{2},\frac{1}{2}\upsilon''\right)}\frac{1}{\sqrt{\upsilon''}}\left[1+\frac{t^2}{\upsilon''}\right]^{-\frac{\upsilon''+1}{2}} \qquad F_Y(y\|s'',\upsilon'')=\int_{-\infty}^{y}f_Y(t)dt \qquad t=\frac{y-m}{s''}$	